1996

Field study of energy savings in manufacturing facilities

Karen Louise Smith
Iowa State University

INFORMATION TO USERS

This manuscript has been reproduced from the microfilm master. UMI films the text directly from the original or copy submitted. Thus, some thesis and dissertation copies are in typewriter face, while others may be from any type of computer printer.

The quality of this reproduction is dependent upon the quality of the copy submitted. Broken or indistinct print, colored or poor quality illustrations and photographs, print bleedthrough, substandard margins, and improper alignment can adversely affect reproduction.

In the unlikely event that the author did not send UMI a complete manuscript and there are missing pages, these will be noted. Also, if unauthorized copyright material had to be removed, a note will indicate the deletion.

Oversize materials (e.g., maps, drawings, charts) are reproduced by sectioning the original, beginning at the upper left-hand corner and continuing from left to right in equal sections with small overlaps. Each original is also photographed in one exposure and is included in reduced form at the back of the book.

Photographs included in the original manuscript have been reproduced xerographically in this copy. Higher quality 6" x 9" black and white photographic prints are available for any photographs or illustrations appearing in this copy for an additional charge. Contact UMI directly to order.

UMI

A Bell & Howell Information Company
300 North Zeeb Road, Ann Arbor MI 48106-1346 USA
313/761-4700 800/521-0600

Field study of energy savings in manufacturing facilities

by

Karen Louise Smith

A dissertation submitted to the graduate faculty

in partial fulfillment of the requirements for the degree of

DOCTOR OF PHILOSOPHY

Department: Mechanical Engineering

Major: Mechanical Engineering

Major Professor: Howard N. Shapiro

Iowa State University

Ames, Iowa

1996

Graduate College
Iowa State University

This is to certify that the doctoral dissertation of

Karen Louise Smith

has met the dissertation requirements of Iowa State University

Signature was redacted for privacy.

Major Professor

Signature was redacted for privacy.

For the Major Department

Signature was redacted for privacy.

For the Graduate College

TABLE OF CONTENTS

LIST OF FIGURES

LIST OF TABLES

NOMENCLATURE

A	area
c	constant
C	clearance
C_f	empirical factor
C_p	specific heat
C4	conversion factor
D	diameter
dp	differential pressure
ES	energy savings
h	enthalpy
HHV	higher heating value
I	amps
k	specific heat ratio
L	length
N_{id}	empirical factor
M	molecular weight
m	mass
$\dot{m}$	mass flow rate
n	polytropic exponent, number of compressor stages
p	pressure

PF	power factor
Pr	fuel usage at proposed efficiency
P_T	compressor power
$q, \dot{Q}$	heat transfer rate
r	pressure ratio
RF	theoretical fraction of input energy that is recoverable
RTS	run time savings
R_u	universal gas constant
T	temperature
t	time
U	current energy usage
V	velocity
v	volume
V_o	volts
V_p	inlet volume per minute calculated on a perfect gas basis
V_{rl}	actual inlet volume per minute
$\dot{W}$	power
WR	fractional reduction in compressor work
wr	compressor work fraction reduction
Z	compressibility factor
δ	partial derivative
Δ	uncertainty, change

η	efficiency
ρ	density
υ	specific volume

ACKNOWLEDGMENTS

This project was funded as Iowa Energy Center contract number 9301a-12. I would like to thank my program of study committee: Ron Nelson, Michael Pate, Alison Flatau, and Marcus Kehrli, for their help and support. A special thank you goes to my major professor, Dr. Howard Shapiro, without whom I would never have finished this dissertation. I would also like to thank my family, especially my husband, Brad. Thank you for your patience.

CHAPTER 1. INTRODUCTION

According to the Energy Information Administration, manufacturing facilities used 20,257 trillion Btus in 1991 to generate heat, power and electricity, and as feedstocks and raw material inputs (Energy Information Administration, 1991). Experience shows that facilities do not efficiently use all the energy that is purchased. The problem is deciding where and how energy can be used more efficiently. In order to make this decision, an energy audit is completed. An energy audit is a study of how the facility is currently using energy. Calculations are then performed to estimate how much energy could be saved. The potential money that can be saved by conserving energy is then compared to the cost of the retrofit. If the cost of the improvement over its lifetime meets the company's criteria, the modification may be made. The company's criteria can be in terms of a minimum acceptable rate of return, life cycle cost, simple payback, etc.

The goal of this project was to determine the actual energy savings achieved when making certain modifications to compressors and boilers, and when reducing heating and cooling loads, and to compare the predicted energy savings with the actual energy savings. In order to determine the actual energy savings, in-situ data must be collected. A literature search revealed that virtually no actual experimental data are available for the energy used by the equipment operating in factories. Graphical and mathematical models are available that are used to predict the energy savings of an energy conservation improvement. This project compared the available models to determine which models best predict the actual energy

savings. This project investigated whether certain retrofits relating to boilers, compressors, and reducing heating and cooling loads are saving the energy that was expected.

Many energy conservation projects have been implemented in industry, and a great deal of investment is to be made in the future. Yet little data are available showing the actual savings achieved in practice or the net economic benefits. This project evaluated actual energy conservation projects through monitoring at six industrial facilities and on-campus facilities. This monitoring consisted of collecting energy use data and determining the energy savings of each conservation project. It is hoped that increased knowledge of the actual energy savings will stimulate greater interest in implementing the energy conservation projects that save the most energy and money. Currently, when an opportunity to save energy is being evaluated, calculations are performed to determine if the possible savings are worth the cost of making the improvement. The accuracy of the equations used to estimate the possible energy savings is unknown. Therefore, this study obtained the energy use before and after the improvement to assess the validity of these calculations.

Since many energy conservation opportunities are based on theories, it is important to determine if these theories are valid and if the retrofits are saving energy. If it is determined that the retrofit saves energy, the next question is if the models used to predict the energy savings do so accurately. It is important to everyone making energy conservation decisions to have accurate information regarding the energy savings so that the investment dollars can be targeted to those retrofits with the best savings to cost ratio. Even if the models do not accurately predict the energy savings, more information will be available as a result of this

project. It may be possible to know if the equations over or under predict the energy savings. It may be possible to say that some retrofits are not cost effective.

Opportunities to reduce heating and cooling loads, as well as boiler and compressor opportunities are found in nearly every facility and are the primary focus of this study. In addition to being found in nearly every facility, these items also offer a large energy savings potential.

Several companies and agencies perform energy audits. For example, Energy Analysis and Diagnostic Centers (EADC)[1] perform energy audits in manufacturing facilities. These centers are located at 28 universities around the country and are funded by the United States Department of Energy. Energy audits are performed on manufacturing facilities that have fewer than 500 employees, under $1.75 million in annual utility bills, under $75 million in annual sales, and no in-house energy expertise (Kirsch, 1993). The EADC personnel recommend ways for the facility to save money on utilities. These recommendations are called energy conservation opportunities (ECOs). It is then up to the facility personnel to decide which ECOs to implement. The EADC offices recommend several types of energy conservation opportunities, including those relating to boilers, air compressors, heat recovery, lighting, motors, etc. Nationally, over the five years from 1987-1992, EADC offices recommended heat recovery opportunities that accounted for 9.2% of the total dollars that could be saved. Compressor modifications accounted for 6.1% of the recommended savings and recommended boiler opportunities accounted for 5.0%. These are percentages based on

---

[1] As of Fiscal Year 1996, the EADCs were renamed as Industrial Assessment Centers (IAC).

the total dollars that could be saved if all of the recommended energy conservation opportunities from 1987-1992 by all of the Energy Analysis Diagnostic Centers were implemented (Kirsch, 1993). These data imply a large potential for boiler, compressor, and heat recovery energy conservation opportunities in manufacturing facilities.

In Iowa, industrial audits are performed by companies, by governmental programs, and by Iowa State University's EADC office. The data obtained from the EADC office at Iowa State University covering audits performed at 83 manufacturing facilities show recommended savings of approximately 498,500 MMBtu/year or 4.7 million $/year. Of these totals, 6.38% of the energy and 9.75% of the money that could be saved came from compressor improvements. Heat recovery opportunities accounted for 61.2% of the possible energy savings and 20% of the cost savings. Boiler opportunities accounted for 14.6% of the energy savings and 4.73% of the dollar savings. There were 123 recommendations to improve compressors, 47 for heat recovery, and 41 for boilers (Iowa State University Energy Analysis and Diagnostic Center, 1991-1994). These data imply that, in Iowa, there is a large potential for energy conservation in projects relating to boilers, compressors and heat recovery.

In order to determine energy usage, data must be collected. There are many problems associated with in-situ data collection. It is difficult to find a facility that is willing to allow data collection. Many manufacturers want to keep their processes a secret. In addition, if they allow the data collection, they require that it does not interfere with normal operations. This means that variables like loads cannot be set by the researcher.

The selection of data acquisition equipment is also important. Portability was a concern in purchasing the equipment, since it is cost prohibitive to purchase equipment to be permanently placed at the facilities.

Even if these hurdles are overcome, the actual data collection process is complicated. Facilities are not designed for data collection. Often the areas where the data must be collected have a great deal of equipment in a small space. For example, ideally when flow measurements are made in a duct, it is best if there are no bends in the duct near where the data is being collected. Often, in an actual facility it is not possible to have as large of a straight section in the duct as would be optimal. Eventually, six industrial sites were found where these problems could be minimized.

The next section of this report discusses both the industrial and campus facilities where data were collected and the information obtained at each location. Following the section on data collection sites are discussions on the basics of compressors, boilers, and reducing heating and cooling loads. Literature is reviewed for each of the areas examined. Data that were collected are provided. These data are compared to the results of the equations used to predict the energy savings of opportunities undertaken to conserve the energy used by boilers and compressors. Any time energy is reclaimed, it must be recovered from a machine, process, etc., that uses energy. For heating load reduction, the recovered energy is shown as a percentage of the energy that is used by the machine, process, etc. These data and calculations are provided in the reducing heating and cooling loads chapter. For the system studied that was installed to try to reduce the cooling load at the facility, the system was analyzed and its actual effect on the cooling load was discovered.

CHAPTER 2. DATA COLLECTION SITES

This chapter describes the locations and energy conservation opportunities studied at each location. There were six industrial facilities and one campus laboratory where data were collected for this project. In addition, data were also collected on a portable, three horsepower, reciprocating air compressor. Of the six industrial sites where data were collected, five are manufacturing plants, and one is a laboratory.

The first manufacturing facility produces meat toppings for pizza. The opportunity studied at this factory is of the heating load reduction type. Energy is currently recovered at this facility from the two ovens used to cook meat toppings. This recovered energy is used to reduce space heating loads in the winter.

The second manufacturing facility produces filters for automobiles. This factory has two 100-horsepower water-cooled screw compressors and one 50 horsepower air-cooled screw compressor. Two different compressor opportunities were studied at this facility. The first opportunity studied was the effect of changing the inlet air temperature on the power consumed by all three air compressors. The second opportunity studied was evaluating the heat recovered from the 50 horsepower air cooled screw compressor. The heat recovered from the air cooled screw compressor is used to offset space heating loads in the winter at this factory. In the summer, this warm air is ducted outside.

The third manufacturing facility produces hosiery. This factory has one cooling load reduction opportunity and two compressor opportunities that were studied. At this facility, heat that is the result of part of the manufacturing process is removed from the conditioned

space. This removed heat is ducted outside in the summer to reduce the space cooling load. In the winter, this heat is allowed to enter the conditioned space. This facility has a 100 horsepower air-cooled screw air compressor. The effect of changing the inlet air temperature on the power consumed by this air compressor was studied. The heat recovered from this air compressor was also studied.

The fourth manufacturing facility produces meat products, such as ham and summer sausage. This factory is equipped with a firetube boiler. The effect of increased combustion efficiency on the natural gas consumed by this boiler was studied.

The fifth industrial facility produces paper products. The effect of inlet air temperature on the power consumed by a 125 horsepower screw compressor was studied. The effect of lowering the exit pressure on the power consumed by the 125 horsepower air compressor was also studied. In addition, this facility has a modulated, 400 psi superheated watertube boiler. This boiler was studied in detail, including the relationship between boiler energy usage and steam generation rate, the relationship between boiler, combustion efficiencies, the effect of increasing combustion efficiency on fuel usage, and the relationship between boiler efficiency and fuel usage.

The industrial laboratory performs research on animals. This facility has a boiler opportunity that was studied. The effect of changing the air-fuel ratio on a fully modulated watertube boiler with a capacity of 40,000 lb/hour of steam was studied. When the air-fuel ratio changes, the combustion efficiency changes. In addition to studying the effect of varying the air-fuel ratio, the relationships between steam generation rate and fuel usage, between

boiler and combustion efficiencies and between boiler efficiency and fuel usage were also studied on this boiler.

The campus laboratory has a previously instrumented 150 horsepower reciprocating air compressor. The effect of lowering the compressor exit pressure on power consumption over a large pressure range was studied using this compressor.

The portable, three horsepower, reciprocating air compressor was used to study the effect of inlet air temperature on the time that the compressor operates. The energy used by an air compressor is proportional to the run time. This air compressor was used because it could be controlled during the data collection process.

Now that the data collection sites have been described, the focus shifts to air compressors. The next chapter discusses literature available relating to air compressors. Models which would be of use on an energy audit are provided. Following the compressor literature review chapter is the air compressor chapter. The air compressor chapter provides more details on the opportunities being studied, and includes data collected pertaining to the energy used by air compressors. These data are compared to the results of the equations used to predict the energy savings. The effect of inlet air temperature is studied in detail, including a review of the theory. In addition, the theoretical amount of energy that can be recovered from an air cooled screw compressor is also evaluated.

CHAPTER 3. AIR COMPRESSOR LITERATURE REVIEW

This chapter begins with a general introduction to positive displacement air compressors. This introduction is followed by a review of the information available in the literature pertaining to positive displacement air compressors. The focus of the models reviewed in this chapter is positive displacement compressor models that would be useful on an energy audit. The models discussed are in equation or graphical form. In addition to the models reviewed, several models are available on other types of air compressors, and other models are available to assist in designing air compressors. These other types of models will not be reviewed.

Both screw and reciprocating compressors are positive displacement compressors. All positive displacement compressors follow a cyclic operation. The first step is to isolate the gas within the enclosed volume. Next, the gas is compressed by reducing the volume of the enclosure. Finally the gas is released into the discharge piping (Pichot, 1986). All positive displacement compressors deliver a nearly constant volume of gas when operated at a fixed speed and a fixed exit pressure. The exit pressure of a positive displacement compressor is controlled by the loads on the system (Talbott, 1993).

Figure 3-1 shows a schematic of a screw compressor (Pichot, 1986). A screw compressor consists of two rotors enclosed in a pressure containing casing. The rotors differ in shape and are identified as male and female. The projection on the male rotor meshes with the indentation on the female rotor. As the rotors rotate, gas is drawn through the inlet into the interlobe space. As rotation continues, the rotors mesh to trap the gas and isolate it from

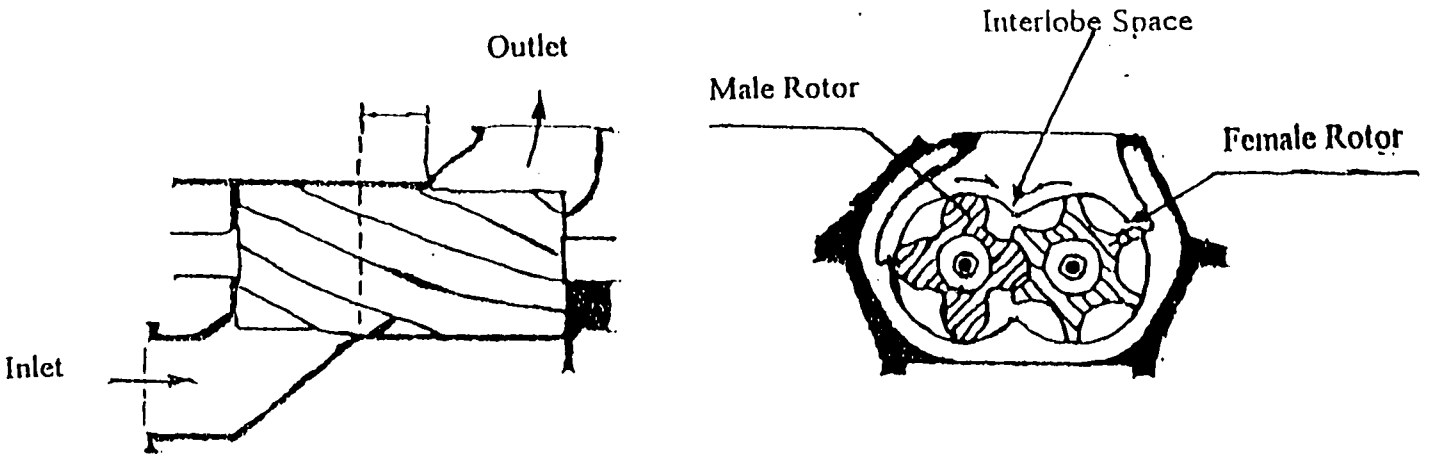

Figure 3-1. Schematic of Screw Compressor (Pichot, 1986, p.62)

the suction. The meshing point moves axially from the suction to the discharge end. The volume of the gas is constantly reduced along this path with a resulting pressure increase. The gas moves axially through the machine; a new charge is continually drawn in and compressed air is continually discharged. For screw compressors, there is no residual gas left in the interlobe space (Price, 1991).

Figure 3-2a shows a schematic of a reciprocating compressor. Figure 3-2b shows an ideal pressure-volume diagram for a reciprocating compressor. Figure 3-2b represents a single cycle. At point 1 on Figure 3-2b, the intake valve is open. The volume is increased by moving the piston. At point 2 on Figure 3-2b, the intake valve closes. This corresponds to the solid piston in Figure 3-2a. The pressure increases to point 3 on Figure 3-2b. Then the discharge valve is opened and the compressed gas is discharged from the compressor, which occurs between points 3 and 4 on Figure 3-2b. At point 4 on Figure 3-2b, the discharge valve closes. This corresponds to the dotted piston in Figure 3-2a. The residual compressed air expands, and the cycle begins again. For a reciprocating compressor, the amount of residual compressed air is dependent on the exit pressure. This is because for a reciprocating compressor there is a clearance volume that traps some of the compressed air. At higher pressures, more compressed air is trapped.

Compressors can be cooled by water or air. An air cooled compressor is cooled by atmospheric air circulated around the cylinders or casings (Rollins, 1973). This heat is rejected to the surrounding atmosphere. A water cooled compressor is cooled by water circulated through a jacket which surrounds the cylinders or casings (Rollins, 1973). This heat is then rejected to the atmosphere through a cooling tower. The air temperature in the

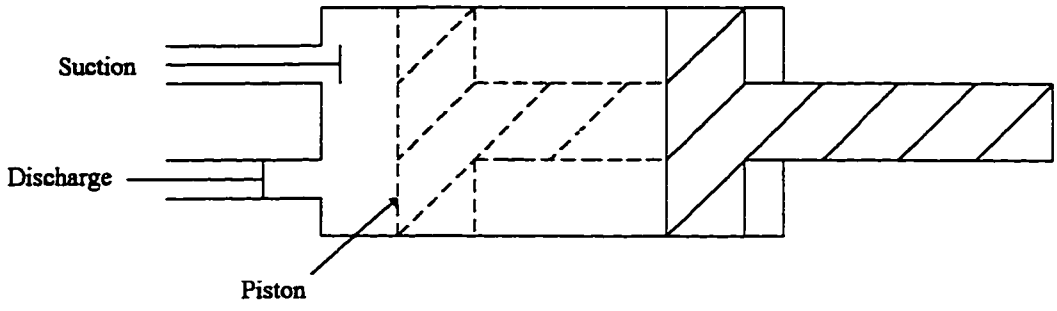

(a)

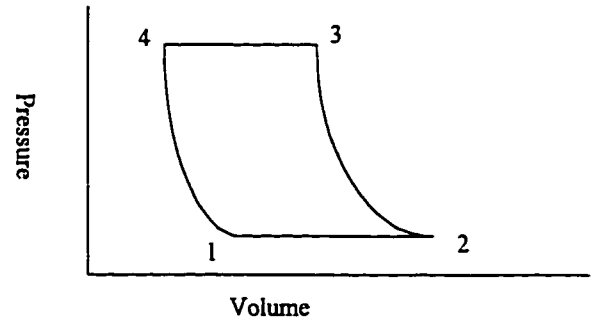

(b)

Figure 3-2. (a) Schematic of Reciprocating Compressor
(b) Typical Pressure-Volume Diagram for a Positive Displacement Compressor

area surrounding an air cooled compressor might be quite high, whereas with a water cooled air compressor the water carries away the heat and the surrounding air temperature is not significantly increased.

For positive displacement compressors, it is common to idealize the process as a polytropic compression. This means that compression occurs according to

$$p\upsilon^n = \text{constant} \tag{3-1}$$

where p is the pressure, υ is the specific volume, and n is the polytropic exponent. If n is equal to the specific heat ratio, k, the process is isentropic. Isentropic means a reversible process with no heat transfer. If n is equal to one, the process is isothermal. Isothermal means constant temperature. It is likely that the actual value of n would be somewhere between one and k.

One reference provides the following equation to calculate the horsepower requirement for single stage isentropic compression (Bloch, 1996, p.24)

$$P_T = \frac{p_1 V_{r1}}{229}\left(\frac{k}{k-1}\right)\left(r^{\left(\frac{k-1}{k}\right)} - 1\right)\left(\frac{Z_1 + Z_2}{2Z_1}\right) \tag{3-2}$$

where p_1 is the inlet pressure in psia, Z_1 is the compressibility factor at the inlet conditions, Z_2 is the compressibility factor at the exit conditions, k is the specific heat ratio, and r is the ratio of the exit pressure to the inlet pressure. The constant, 229, is a conversion factor. V_{r1} is found from (Bloch, 1996, p.24)

$$V_{r1} = V_{p1} Z_1 \tag{3-3}$$

where V_{p1} is the inlet volume in ft^3 calculated on an ideal gas basis at p_1 and T_1. The adiabatic single stage horsepower formula "represents the area of a theoretical pV diagram for the

volume per minute being handled" (Bloch, 1996, p.24). This means that V_{rl} is actually the volume per minute.

The equation for estimating the isothermal compressor power is (Bloch, 1996, p.24)

$$P_T = \left(\frac{p_1 V_{rl} \ln(r)}{229}\right)\left(\frac{Z_1 + Z_2}{2Z_1}\right) \tag{3-4}$$

where the terms in Equation 3-4 have the same meanings as in Equation 3-2 (Bloch, 1996). Both the isentropic (Equation 3-2) and the isothermal (Equation 3-4) power formulas account for deviations from the ideal gas assumption in the compressibility factor, which is a function of both temperature and pressure for a given gas. Isothermal compression takes less power than isentropic compression (Pichot, 1986). While isentropic compression is never exactly obtained, on the average, it is a good model for most positive displacement compressors (Gibbs, 1971).

The theoretical power (Equation 3-2 or 3-4) is only a portion of the power required for compression. The actual power is the theoretical power, plus the power required to overcome the dynamic flow losses and the mechanical losses. The power required to overcome the dynamic flow losses typically amounts to 10% to 15% of the total power. The power required to overcome the dynamic flow losses can be calculated from (Bloch, 1996, p.159)

$$W_d = C_f\left(\frac{L}{D}\right)\left(\frac{k}{1.4}\right)\left(\frac{p_1}{1.013}\right)\left(\frac{Q_o}{60} N_{id}\right) \tag{3-5}$$

where C_f is an empirical factor based on the wrap angle, which is described by a point on the thread of a screw as the point travels from the bottom to the top of the rotor. In this

equation, p_1 is in bars, L is the length of the rotor, D is the diameter of the rotor, and N_{id} is another empirical factor, which is based on the Mach number (Bloch, 1996, pp.160-161).

The power required to overcome the mechanical losses is estimated to be 8% to 12% of the actual power. These mechanical losses are due to viscous or frictional losses in the bearings, timing, and step-up gears (Bloch, 1996).

In addition to the power equations provided above (Equations 3-2 and 3-4), the literature offers methods for estimating the power savings achieved by reducing the compressor exit pressure. One example of this is the "rule of thumb" that states that at operating pressures around 100 psig, every extra one psi of pressure adds approximately a .5% increase in power consumption (Oviatt, 1981).

Figure 3-3 shows the approximate horsepower requirements at various discharge pressures for typical air compressors (*Site Energy Handbook*, 1976). As expected, this figure shows that as the discharge pressure increases, so does the shaft horsepower. This book references the 3rd edition of the Compressed Air and Gas Institute's book *Compressed Air and Gas Data* as being the source for this graph. Figure 3-3 does not appear in this book, therefore, it is not possible to say exactly how this figure was obtained.

Figure 3-4 shows the approximate horsepower reduction due to reduced compressor exit pressures. This figure is to be used to estimate the power savings achieved when the compressor discharge pressure is lowered on single stage reciprocating and rotary screw air compressors *(Site Energy Handbook*, 1976). Figure 3-4 implies nearly linear relationship between power consumption and exit pressure. This book references the *Air Compressor Handbook* by Caterpillar Tractor Company, 1968 as the reference for Figure 3-4. This book

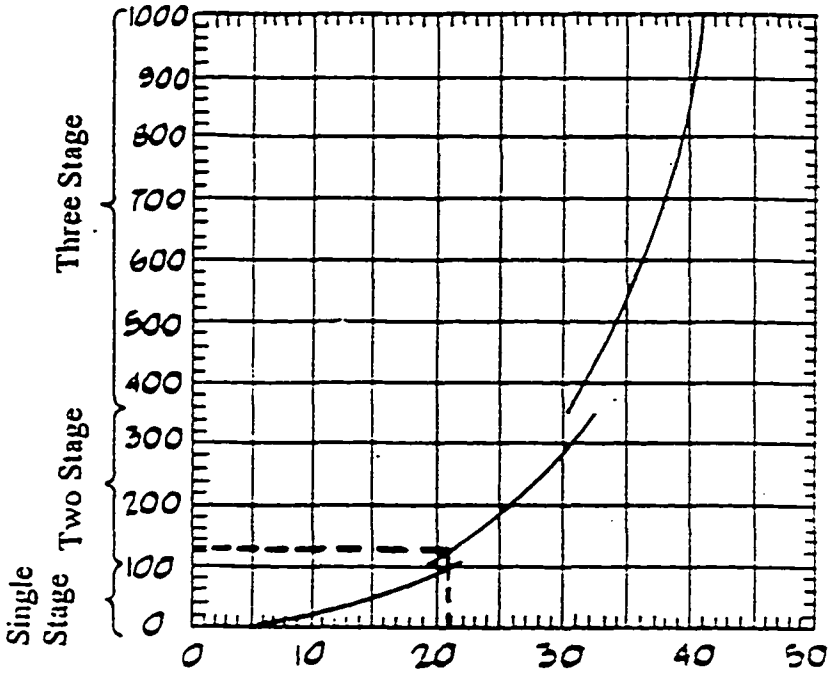

Figure 3-3. Shaft Horsepower Requirements per 100 cfm of Air at Various Discharge Pressures (*Site Energy Handbook*, 1976, p.5-87)

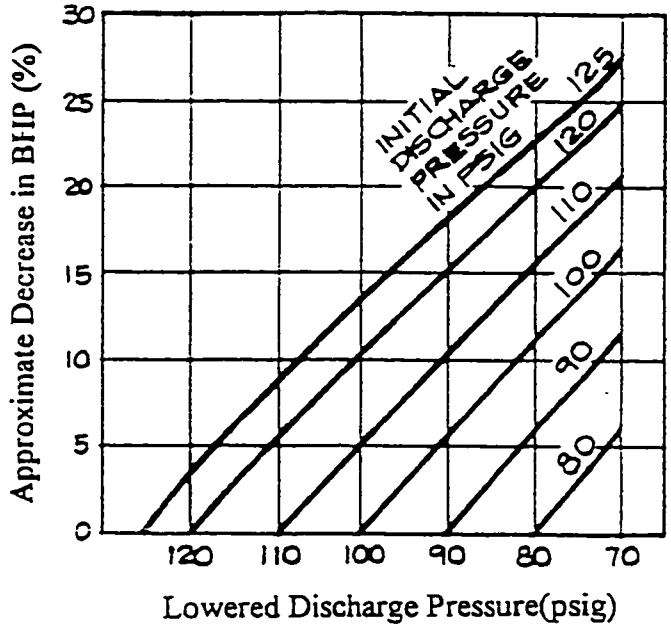

Figure 3-4. Effect of Lowered Discharge Pressure on Power Usage for Single Stage Reciprocating and Rotary Screw Air Compressors (*Site Energy Handbook*, 1976, p.5-88)

is not available, therefore, it is not possible to determine if this figure is based on experimental observations, or on theory.

Figure 3-5 shows the approximate reduction in compressor horsepower due to reduced compressor discharge pressures (*Site Energy Handbook*, 1976). This figure is valid for estimating the energy savings achieved by reducing the compressor exit pressure on two stage reciprocating and centrifugal compressors (*Site Energy Handbook*, 1976). This figure is not linear like Figure 3-4, especially at high initial discharge pressures. Figure 3-5 is from the same reference as Figure 3-4, the Caterpillar Tractor Company's *Air Compressor Handbook* As mentioned above, because this book is unavailable, it is impossible to determine how Figure 3-5 was obtained.

Figure 3-6 is an example of the effects of part load performance. This figure shows the effect that operating below 100% capacity has on power consumption at a constant discharge pressure (Price, 1991). Figure 3-6 shows how capacity control effects power consumption. The original reference calls this an example of a "good compressor". The actual power consumption at high percent capacities is very near the ideal power consumption. At low percent capacities, the actual power consumed is more than the ideal power. As the percent capacity decreases, the difference between actual and ideal power consumption increases.

Table 3-1 shows the effect of inlet air temperature on the horsepower consumed by the air compressor (Oviatt, 1981). This table shows the savings relative to a 70 °F inlet temperature. Table 3-1 shows a decrease in power consumption at temperatures less than 70 °F, and an increase in power consumption above this temperature. This table shows that if

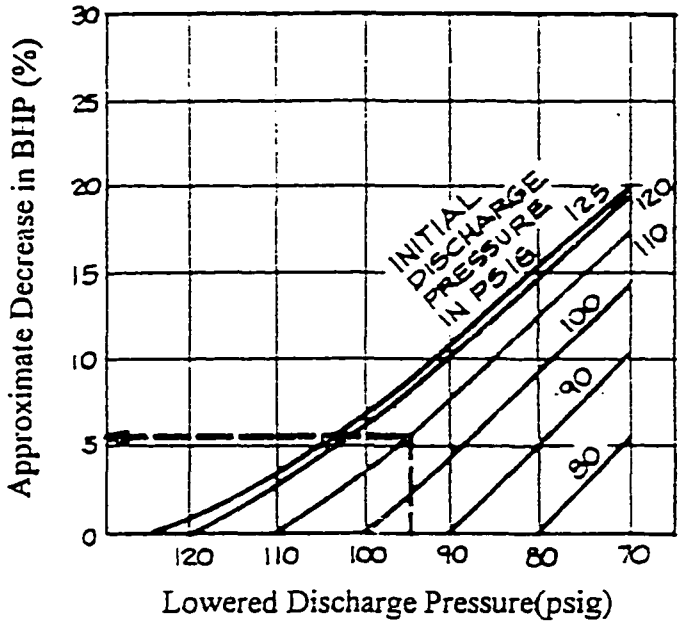

Figure 3-5. Effect of Lowered Discharge Pressures on Power Usage for Two Stage Reciprocating and Centrifugal Compressors (*Site Energy Handbook*, 1976, p.5-89)

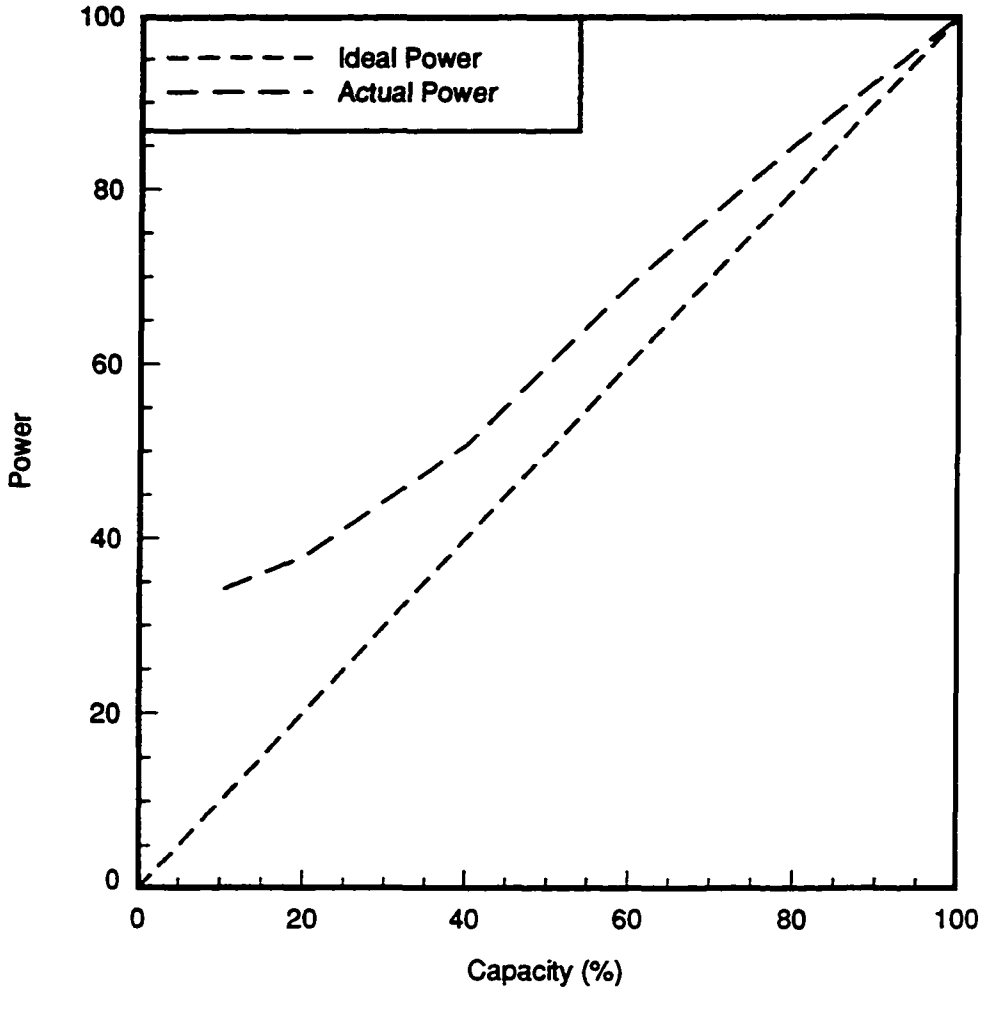

Figure 3-6. Effect of Part Load Performance on Compressor Power Consumption (Price, 1991, p.52)

lower temperature inlet air is used, an energy savings resulting from a decreased power consumption will occur. This book references *Compressed Air Data* 5th edition by Ingersoll-Rand as one of the sources for this table. This table does not appear in Ingersoll-Rand's book. Therefore, it was not possible to determine how Table 3-1 was generated.

Table 3-1. Effect of Inlet Air Temperature on Horsepower Consumed by Air Compressor (Oviatt, 1981, p.49)

Temperature of Intake Air (°F)	Intake Volume Required to Deliver 1000ft^3 of Free Air at 70 °F	% Horsepower Savings or Increase Relative to 70 °F Intake
30	925	7.5 Saving
40	943	5.7 Saving
50	962	3.8 Saving
60	981	1.9 Saving
70	1000	0.0
80	1020	1.9 Increase
90	1040	3.8 Increase
100	1060	5.7 Increase
110	1080	7.6 Increase
120	1100	9.5 Increase

Another method for determining the effect of inlet air temperature utilizes a "rule of thumb." This "rule of thumb" for reciprocating and screw compressors states that for each 5 °F decrease in inlet air temperature approximately one percent more compressed air is provided (Talbott, 1993).

One reference estimates that 80% of the electrical energy used to compress the air is converted into heat (Oviatt, 1981). Another reference estimates that 85% of the energy input to a compressor exits the compressor as waste heat (Pichot, 1986). The EADC offices estimate that 42% of the energy input to a compressor can be recovered (Iowa State University Energy Analysis and Diagnostic Center, 1994).

From the literature review, there is a basis to hypothesize that reducing the exit pressure and/or reducing the inlet air temperature can reduce the energy needed to operate positive displacement compressors. From the literature review, it appears that this energy reduction will be due to a decrease in the power required. Further, there appears to be a significant amount of waste heat that can be recovered for other uses, especially from air cooled compressors. Also, from the literature review, it is apparent that there are few models relating to positive displacement compressors available in the literature that would be useful on an energy audit. The models that are available deal with power. None of the models relate to how an air compressor in a factory is actually used. These models do not account for storage, run time, controls, multiple compressors on a common line, etc. In addition, no operating data are available in the literature, and the accuracy and validity of the models is in question, especially because it is unknown whether these models are based on theories or experimental observations. Because it is the goal of an energy audit to save money, and in

general limited resources are available to implement the energy conservation opportunities, it is important that information regarding the accuracy and validity of the models is made available.

Having reviewed the models relating to positive displacement air compressors that would be useful on an industrial energy audit, the discussion now focuses on the specifics of the air compressor energy conservation opportunities studied under this project. These energy conservation opportunities relate to the effects of inlet air temperature and compressor exit pressure on energy usage, as well as the amount of heat that can be recovered from an air compressor. Data collected are presented in the next chapter. In addition, the theories surrounding the effect of inlet air temperature are reviewed. The theoretical amount of heat recovery from a positive displacement air compressor is also discussed.

CHAPTER 4. AIR COMPRESSORS

As mentioned in the compressor literature review, there are steady-state power models available for positive displacement compressors, but due to a lack of operating data in the literature, the accuracy and validity of these models are largely unknown. This chapter discusses the energy conservation opportunities relating to positive displacement air compressors that were studied. Data collected relating to these opportunities are presented. The three compressor opportunities studied relate to the effect of inlet air temperature on power consumption and run time, the effect of exit pressure on power consumption, and the amount of heat that is recovered.

One of the goals of this study is to determine the relationship between how the equipment is operated and its energy use. For example, theory dictates that as the exit pressure from an air compressor increases, so does the energy required to operate the air compressor. A "rule of thumb" states that at operating pressures around 100 psig, every extra one psi of pressure causes approximately a .5% increase in power consumption (Oviatt, 1981), but at least one study infers that this theory is not always true (Woollatt, 1993). Several models have been proposed to quantify these relationships. Some of these models are currently being utilized by EADC personnel (Iowa State University Energy Analysis and Diagnostic Center, 1994), while others are available in the literature (*Site Energy Handbook*, 1976). Some of these models are in the form of equations, while others are graphical. A portion of this study was to determine which models provide the best estimates of the energy savings achieved by modifying compressor operation.

The effect of compressor exit pressure on power consumption was studied on a 150 horsepower reciprocating compressor in a university laboratory. This effect was also studied on a 125 horsepower screw compressor at a paper product manufacturing facility. Based on Figures 3-3 through 3-5, and Equations 3-2 and 3-4, it was expected that the collected data would show decreased power consumption with decreasing exit pressures. Unfortunately, only two facilities could be located where a large pressure range could be studied. The exit pressure from the air compressors at most facilities varies only by a few pounds per square inch.

The density of air increases with decreasing temperature. It is a widely held belief that as the inlet air temperature decreases, so does the compressor power consumption. The effect of inlet air temperature on compressor power consumption was studied on both air and water cooled screw compressors. Based on Table 3-1, the original hypothesis was that the power consumption would decrease with decreasing inlet air temperatures. When this hypothesis was proven false through theoretical and experimental verification, it was modified. The new hypothesis was that the run time would decrease with decreasing inlet air temperature. A decreased run time will result in an energy savings. The effect of inlet air temperature on the air compressor run time was studied on a portable, three horsepower reciprocating compressor. This effect was also analyzed theoretically.

The reduction in space heat loads due to utilizing the heat generated by air compressors was also evaluated. As mentioned in the literature review, one estimate is that 85% of the energy input to a compressor exits the compressor as waste heat (Pichot, 1986). Another source estimates that 80% of the electrical energy used to compress the air is

converted into heat (Oviatt, 1981). The EADC offices estimate that 42% of the power used by an air compressor can be recovered (Iowa State University Energy Analysis and Diagnostic Center, 1994). The amount of energy that can be recovered from an air compressor was studied using one 50 horsepower and one 100 horsepower air cooled screw air compressor. In addition, the theoretical fraction of input power that can be recovered was also evaluated.

The Effect of Reduced Exit Pressure on Power Consumption

Theory predicts that as the exit pressure from an compressor decreases, so does the power consumption. This can be seen by examining Equations 3-2 and 3-4 or Figures 3-3 through 3-5. Therefore, it was expected that the data collected would also show this effect.

The effect of reducing the exit pressure from an air compressor was first studied using a two-stage, water cooled, 150 horsepower reciprocating air compressor which was previously instrumented. This air compressor was used to study the effect on power consumption of lowering the compressor exit pressure under steady state loading conditions. Steady state loading means that the pressure was changed and the compressor was allowed to run until the power became constant. This air compressor was located in a campus laboratory used for teaching. Table 4-1 shows the inlet pressure, exit pressure, and power consumption measured. Table 4-1 shows that as the exit pressure of the air compressor decreases, the power consumed by this air compressor also decreases. This decrease in power consumption with decreasing compressor exit pressure was predicted by theory.

Table 4-1. 150 hp Reciprocating Compressor Power Consumption Data at Various Exit Pressures

Inlet Pressure (psia)	Exit Pressure (psia)	Pressure Ratio	Power (kW)
14.1	127.2	9.05	116.4
14.1	121.2	8.63	116.8
14.1	113.9	8.11	110.5
14.1	108.5	7.72	111.9
14.0	102.3	7.28	109.9
14.1	95.4	6.79	103.2
14.0	88.2	6.28	102.7
14.0	79.5	5.66	99.3
14.0	72.6	5.17	93.0
14.0	65.7	4.68	91.62
14.0	61.6	4.39	90.9

The effect of reducing exit pressure on power consumption was also studied on a 125 horsepower screw compressor located at a paper manufacturing facility. Appendix A contains data obtained at this facility on the 125 horsepower screw compressor. As predicted by theory, the data in Appendix A show that except for a few readings, the general trend of power increasing with increasing exit pressure is followed.

Using three different methods, an attempt was made to predict the power at the reduced exit pressure. The first method is based on assuming isentropic compression. Recall that the power required for isentropic compression is

$$P_T = \frac{p_1 V_{r1}}{229}\left(\frac{k}{k-1}\right)\left(r^{\left(\frac{k-1}{k}\right)} - 1\right)\left(\frac{Z_1 + Z_2}{2Z_1}\right) \tag{3-2}$$

If it is assumed that the inlet volumetric flow rate, V_{r1}, and the inlet pressure, p_1, are constant, and the effects of compressibility are negligible, the estimated power required at the lower exit pressure for a multi-stage compressor is

$$P_{T_{new}} = P_{T_{old}}\left(\frac{\left(\frac{p_{exit}}{p_{inlet}}\right)_{new}^{\frac{k-1}{nk}} - 1}{\left(\frac{p_{exit}}{p_{inlet}}\right)_{old}^{\frac{k-1}{nk}} - 1}\right) \tag{4-1}$$

where new is at the lower pressure, old is at the highest pressure, p is pressure, P_{Told} is the power measured at the highest exit pressure, and n is the number of compressor stages. For the evaluated reciprocating compressor, n is two. For the screw compressor studied, n is one.

Figure 3-4 provides another method to estimate the power at lowered exit pressures. This figure implies a linear relationship between power and pressure. The equation used to estimate this relationship is

$$P_{T_{new}} = P_{T_{old}}\left(\frac{\left(\frac{p_{exit}}{p_{inlet}}\right)_{new}}{\left(\frac{p_{exit}}{p_{inlet}}\right)_{old}}\right) \tag{4-2}$$

The third method is based on the "rule of thumb" mentioned in the literature review, which says that at pressures around 100 psi, every extra one psi of pressure adds approximately a .5% increase in power consumption (Oviatt, 1981). This method was applied over the entire data range. In equation form

$$P_{T_{new}} = P_{T_{old}}\left[1-\left(\frac{.5}{100}\right)(p_{old}-p_{new})\right] \tag{4-3}$$

Table 4-2 contains the predicted and experimental compressor power for the 150 horsepower reciprocating compressor. These data are graphically shown in Figure 4-1. Notice that all three methods underpredict the new power and overpredict the savings for this compressor.

Appendix B contains the predicted and experimental powers for the 125 horsepower screw compressor at various exit pressures. These data are graphically shown in Figure 4-2. Figure 4-2 shows that both the isentropic prediction and the "rule of thumb" prediction do a good job predicting the new power. Because there is no theoretical basis for the "rule of thumb" estimates, and the graphical method does a poor job of estimating the reduced power consumption for both compressors, further analysis was limited to the isentropic compressor model.

In order to determine the accuracy of the isentropic prediction model, propagation of error techniques were applied to Equation 4-1. The predicted power is actually $P_T \pm \Delta P_T$ due to measurement uncertainties. The uncertainty for values calculated using Equation 4-1 can be found from

Table 4-2. 150 hp Reciprocating Compressor Experimental and Predicted Power Consumption Data at Various Exit Pressures

Inlet Pressure (psia)	Exit Pressure (psia)	Measured Power (kW)	Isentropic Prediction (kW)	Graphical Prediction (kW)	"Rule of Thumb" Prediction (kW)
14.1	61.6	90.9	74.0	56.4	78.2
14.1	65.7	91.6	77.6	60.2	80.6
14.1	72.6	93.0	83.2	66.4	84.6
14.1	79.5	99.3	88.4	72.8	88.7
14.0	88.2	102.7	94.5	80.7	93.7
14.1	95.4	103.2	99.0	87.3	97.9
14.0	102.3	109.9	103.2	93.6	101.9
14.0	108.5	111.9	106.7	99.3	105.5
14.0	113.9	110.5	109.7	104.2	108.7
14.0	121.2	116.8	113.4	110.9	112.9
14.0	127.2	116.4	116.4	116.4	116.4

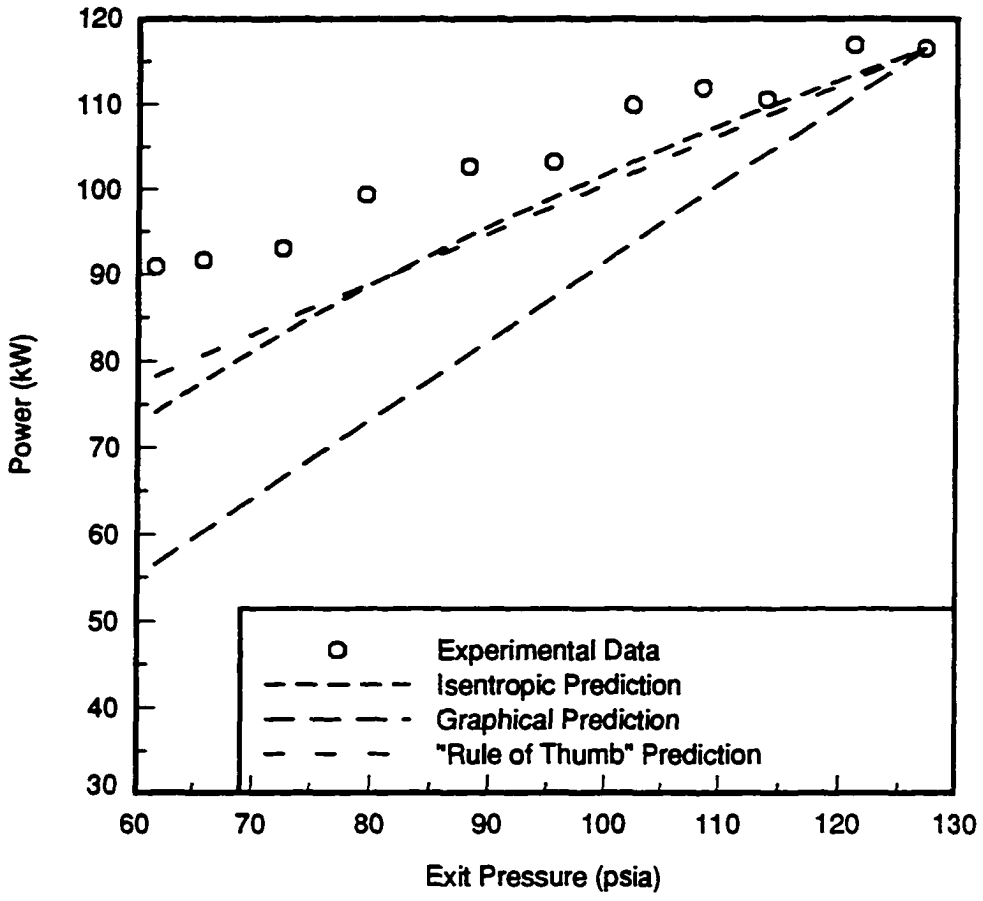

Figure 4-1. Effect of Exit Pressure on Predicted and Experimental Power Consumed by 150 hp Reciprocating Compressor

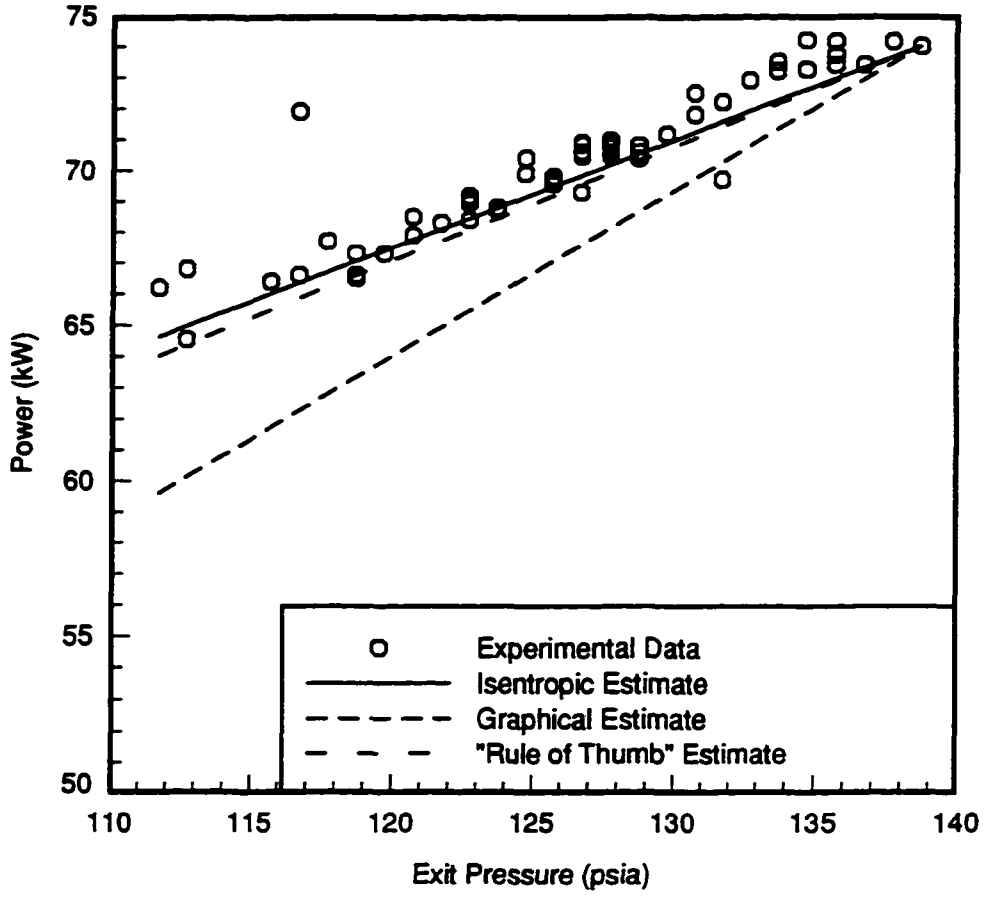

Figure 4-2. Predicted and Experimental Power Consumed by 125 hp Screw Compressor at Various Exit Pressures

$$\Delta P_{T_{new}} = \left\{ \left(\frac{\left(\frac{1}{p_{in}}\right)^{\frac{k-1}{nk}} (p_{out})_{new}^{\frac{k-1-nk}{nk}} \left(\frac{k-1}{nk}\right)\left(P_{T_{old}}\right)}{\left[\left(\frac{P_{out}}{P_{in}}\right)_{old}^{\frac{k-1}{nk}} - 1\right]} \right)^2 \left(\Delta p_{out_{new}}\right)^2 + \right.$$

$$\left(\frac{\left(\frac{p_{out}}{p_{in}}\right)_{new}^{\frac{k-1}{nk}} - 1}{\left(\frac{p_{out}}{p_{in}}\right)_{old}^{\frac{k-1}{nk}} - 1} \right)^2 \left(\Delta P_{T_{old}}\right)^2 +$$

$$\left. \left(\frac{\left(\frac{p_{out}}{p_{in}}\right)_{new}^{\frac{k-1}{nk}} - 1}{\left[\left(\frac{p_{out}}{p_{in}}\right)_{old}^{\frac{k-1}{nk}} - 1\right]^2} \left(\frac{k-1}{nk}\right)(p_{out})_{old}^{\frac{k-1-nk}{nk}} \left(\frac{1}{p_{in}}\right)^{\frac{k-1}{nk}} \left(P_{T_{old}}\right) \right)^2 \left(\Delta p_{out\,old}\right)^2 \right\}^{1/2} \quad (4\text{-}4)$$

where it is assumed that the inlet pressure is constant and known exactly. It is estimated that the power is known to ±.5 kW, and the exit pressure is measured to ±1 psi.

Table 4-3 contains the measured, isentropically predicted, and error band powers for the 150 horsepower reciprocating air compressor. Figure 4-3 is a graphical representation of these data. Note that the actual predicted isentropic power should be somewhere between the dotted lines on this figure. Because the experimental data do not lie between the dotted lines, the isentropic model does not predict the power reduction for this reciprocating compressor.

Table 4-3. Uncertainties for Isentropic Prediction for 150hp Reciprocating Air Compressor

Inlet Pressure (psia)	Exit Pressure (psia)	Measured Power (kW)	Isentropic Prediction (kW)	- Error Band (kW)	+ Error Band (kW)
14.1	61.6	90.9	74.0	73.0	75.1
14.1	65.7	91.6	77.6	76.7	78.6
14.1	72.6	93.0	83.2	82.3	84.2
14.1	79.5	99.3	88.4	87.5	89.4
14.0	88.2	102.7	94.5	93.6	95.3
14.1	95.4	103.2	99.0	98.2	99.9
14.0	102.3	109.9	103.2	102.4	104.1
14.0	108.5	111.9	106.7	105.9	107.6
14.0	113.9	110.5	109.7	108.8	110.5
14.0	121.2	116.8	113.4	112.6	114.3
14.0	127.2	116.4	116.4	115.6	117.3

As mentioned previously, this model overpredicts the savings. On an energy audit, it is customary to be conservative with the energy savings estimates. Therefore, this model should not be used for this compressor.

Figure 4-4 shows the uncertainties for the isentropic prediction for the 125 horsepower screw compressor. The data for this figure are in Appendix C. As shown in Figure 4-4, almost all of the data lie within the error bands. This figure shows that the

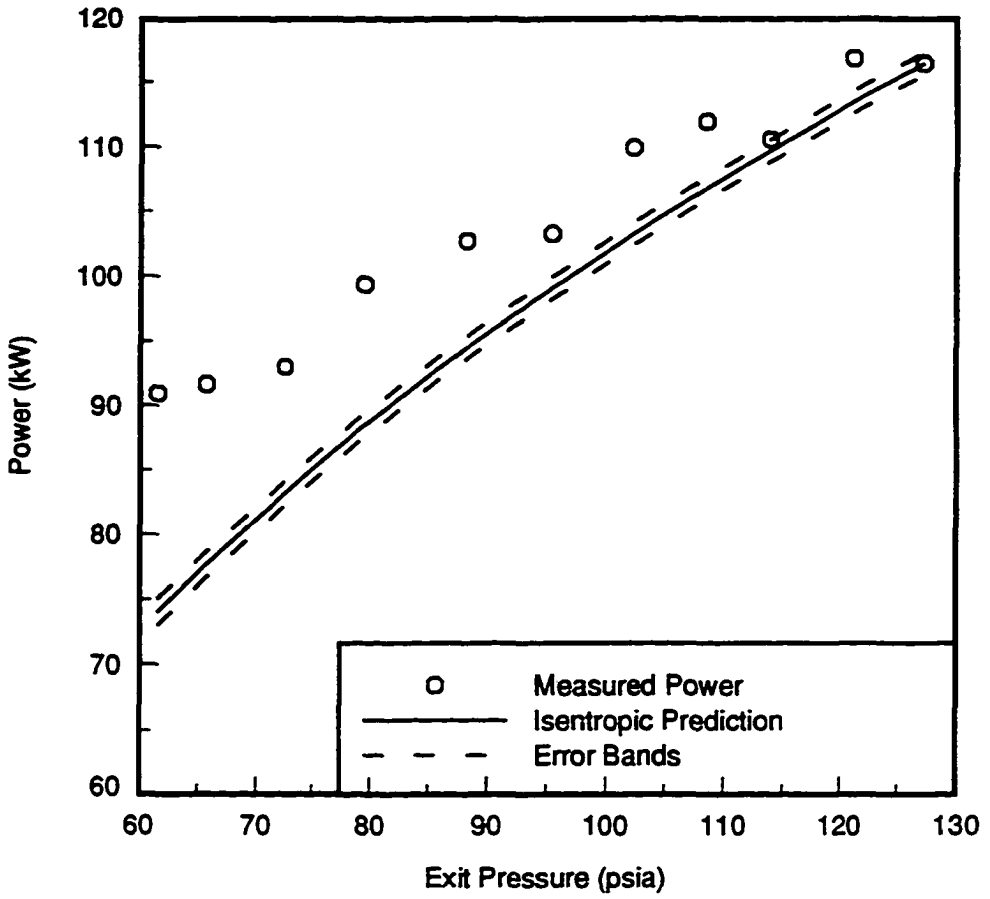

Figure 4-3. Uncertainties for Isentropic Prediction for 150hp Reciprocating Air Compressor

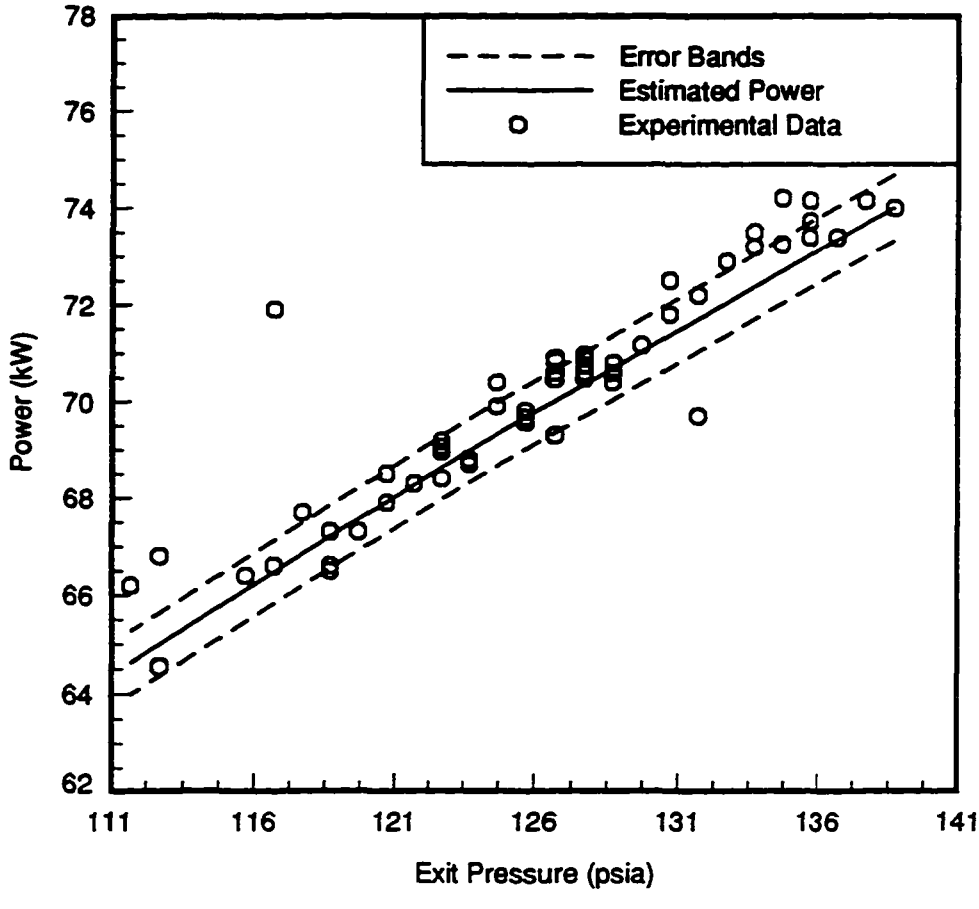

Figure 4-4. Uncertainties for Isentropic Prediction for 125hp Screw Air Compressor

predicted power is a good estimate of the measured power. Therefore, the isentropic approximation is a good predictor of the power consumed by this air compressor.

As mentioned above, Equation 4-1 assumes that the inlet volumetric flow rate and pressure do not change with the exit pressure. As mentioned in the compressor literature review, for reciprocating air compressors, the inlet volumetric flow rate is not constant because of the clearance volume. As the exit pressure increases, the inlet volumetric flow rate is decreased because of air trapped in the clearance volume. It was decided to modify Equation 4-1 to account for this effect. For the reciprocating air compressor, the following equation was used to predict the power consumed at reduced exit pressures

$$P_{T\,Reciprocating} = P_{T_{old}} \left(\frac{\left(\frac{p_{exit}}{p_{inlet}} \right)_{new}^{\frac{k-1}{nk}} - 1}{\left(\frac{p_{exit}}{p_{inlet}} \right)_{old}^{\frac{k-1}{nk}} - 1} \right) \left(\frac{1 - C\left(\left(\frac{p_{exit}}{p_{inlet}} \right)_{new}^{1/k} - 1 \right)}{1 - C\left(\left(\frac{p_{exit}}{p_{inlet}} \right)_{old}^{1/k} - 1 \right)} \right) \qquad (4\text{-}5)$$

where $P_{TReciprocating}$ is the power required for a reciprocating compressor at the new pressure, and C is the clearance fraction.

Figure 4-5 compares the experimental data to the isentropic prediction and the modified isentropic predictions. The data for Figure 4-5 are in Table 4-4. Note that as clearance fraction increases, the predicted power begins to exceed the experimental power. This occurs at clearance fractions above .1 (10%). This air compressor is a two stage, double acting air compressor. Because of this, there are four clearance fractions associated with this compressor: 1) .20, 2) .11, 3) .06, and 4) .06. The average of these clearance fractions is .11 (11%). If .11 were used in Equation 4-5, the calculated power would provide a conservative

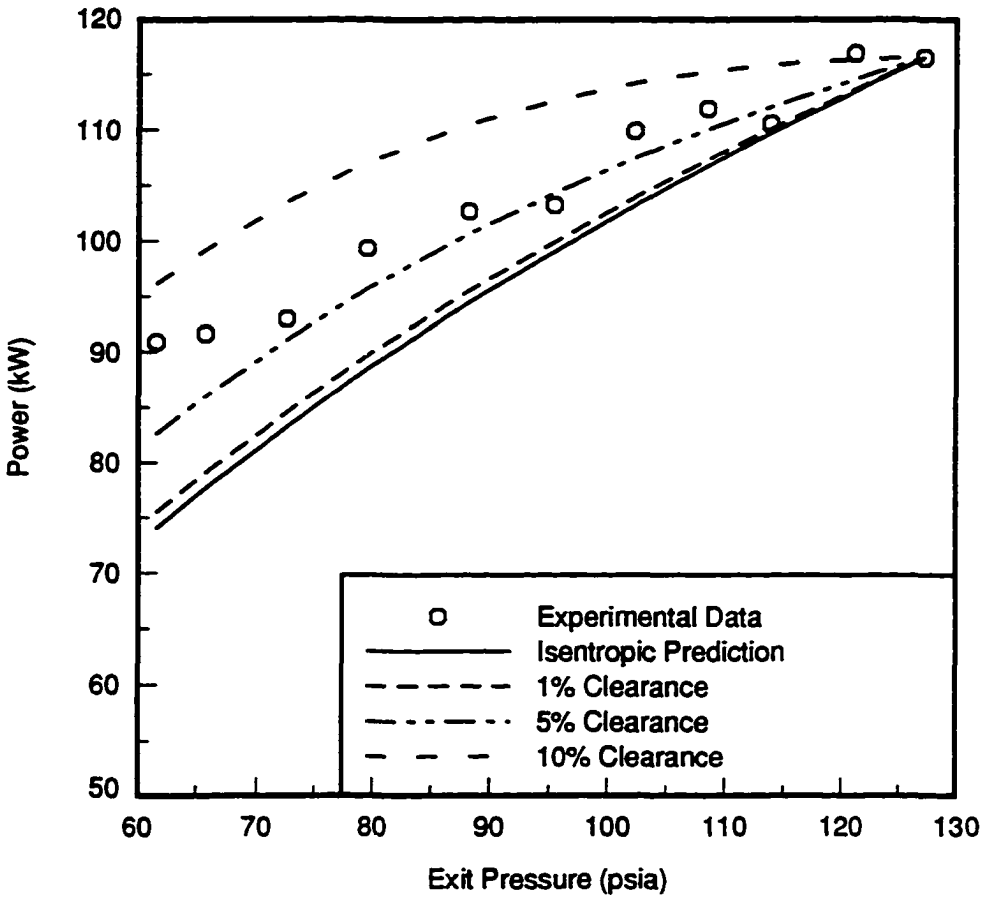

Figure 4-5. Effect of Clearance on Predicted Power for 150hp Reciprocating Compressor

Table 4-4. Effect of Clearance on Predicted Power for 150hp Reciprocating Compressor

Inlet Pressure (psia)	Exit Pressure (psia)	Measured Power (kW)	Isentropic Prediction (kW)	1% Clearance Prediction (kW)	5% Clearance Prediction (kW)	10% Clearance Prediction (kW)
14.1	61.6	90.9	74.0	75.5	82.6	96.1
14.1	65.7	91.6	77.6	79.1	86.0	99.2
14.1	72.6	93.0	83.2	84.5	91.1	103.5
14.1	79.5	99.3	88.4	89.7	95.7	107.1
14.0	88.2	102.7	94.5	95.5	100.7	110.5
14.1	95.4	103.2	99.0	99.9	104.3	112.6
14.0	102.3	109.9	103.2	103.9	107.5	114.2
14.0	108.5	111.9	106.7	107.3	110.0	115.2
14.0	113.9	110.5	109.7	110.1	112.0	115.8
14.0	121.2	116.8	113.4	113.6	114.5	116.3
14.0	127.2	116.4	116.4	116.4	116.4	116.4

estimate of the power used by this compressor. On an energy audit, conservative estimates of the power consumption are needed. Therefore, for this reciprocating air compressor, Equation 4-5 should be used to estimate the power at a reduced exit pressure.

In conclusion, the data collected for this project on a 125 horsepower screw compressor show that the isentropic compressor model accurately predicts the reduced power

due to a reduced compressor exit pressure. The data collected for this project on a 150 horsepower reciprocating compressor show that the isentropic compressor model overpredicts the power savings due to a reduced exit pressure for this compressor. If the isentropic compressor model is modified for the effects of clearance, the modified equation will provide a conservative estimate of the power at a reduced exit pressure for the reciprocating compressor studied.

The Effect of Inlet Temperature on Power Consumption

As shown in Table 3-1, the literature predicts that as compressor inlet air temperature decreases, power consumption will decrease (Oviatt, 1981, p.49). One facet of the present study involved evaluating this presumed effect by theoretical analysis and experimental verification. It was determined that no theoretical reason exists to expect a change in power consumption with changing inlet air temperature. The data also showed no effect on power consumption with decreasing inlet air temperature. It was, however, determined that a theoretical reason exists to expect decreasing run times with decreasing inlet air temperatures. This would result in an energy savings. Data were collected to evaluate this theory. This section describes the experiments and theories that led to the conclusion that energy can be saved by decreasing the inlet air temperature, but that this savings is due to decreased run time, not decreased power consumption.

An attempt was made to evaluate the effect of inlet air temperature on power consumption using two 100 horsepower water cooled screw compressors, one 50 horsepower air cooled screw compressor, and one 100 horsepower air cooled screw compressor. A series of steady-state tests were conducted where inlet air temperature, instantaneous power consumption, and exit pressure were measured. Table 4-5 contains the data collected on the 100 horsepower water cooled screw compressor, designated A. Table 4-6 is the data collected on the 100 horsepower water cooled screw compressor, designated B. Table 4-7 is the data collected on the 50 horsepower air cooled screw compressor. Table 4-8 contains the data collected on the 100 horsepower air cooled screw compressor, designated C.

Table 4-5. 100 hp Water Cooled Screw Compressor (A) Data

Average Power Usage (kW)	Exit Pressure (psig)	Inlet Temperature (°R)
66.4	115	527
67.1	115	522
67.0	115	520
71.7	121	510
59.0	121	502

Table 4-6. 100 hp Water Cooled Screw Compressor (B) Data

Average Power Usage (kW)	Exit Pressure (psig)	Inlet Temperature (°R)
77.6	116	505
72.7	116	498
83.5	115	485
84.8	115	481
84.8	115	478

Table 4-7. 50 hp Air Cooled Screw Compressor Data

Average Power Usage (kW)	Exit Pressure (psig)	Inlet Temperature (°R)
35.7	100	550
34.2	100	541
31.9	108	540
33.7	108	535
34.9	100	534
29.7	108	528

Table 4-8. 100 hp Air Cooled Screw Compressor (C) Data

Average Power Usage (kW)	Exit Pressure (psig)	Inlet Temperature (°R)
40.6	120	565
52.0	121	550
48.1	121	545

As mentioned above, the literature predicts that as the inlet air temperature decreased, the power consumed by each air compressor would decrease (Oviatt, 1981, p.49). As shown in Tables 4-5 through 4-8, this was not always the case.

The EADC office uses the following equation to estimate the compressor work fraction reduction (wr) achieved when lower temperature air is used for compressor inlet air

$$wr = \frac{T_I - T_o}{T_I} \tag{4-5}$$

In Equation 4-5, T_I is the highest intake air temperature in °R and T_o is the lower intake air temperature in °R (Iowa State University Energy Analysis and Diagnostic Center, 1994). The compressor work fraction reduction (wr) is adjusted to account for the varying exit pressures by the multiplying the calculated wr by a correction factor which assumes isentropic compression. The result of this calculation is the fractional reduction in compressor work, WR, and accounts for exit pressure and inlet temperature variations

$$WR = \left(\frac{T_I - T_o}{T_I}\right)\left(\frac{\left(\frac{P_{exit}}{P_{inlet}}\right)_{new}^{\frac{k-1}{nk}} - 1}{\left(\frac{P_{exit}}{P_{inlet}}\right)_{old}^{\frac{k-1}{nk}} - 1}\right) \tag{4-7}$$

The experimental fractional reduction in compressor work is calculated using

$$WR = 1 - \frac{Power_{low}}{Power_{high}} \tag{4-8}$$

where $Power_{Low}$ is the power at the lower temperature and $Power_{High}$ is the power at the highest temperature.

Figure 4-6 shows the predicted and experimental fractional reduction in the compressor work. The solid line in Figure 4-6 shows that Equation 4-7 does not accurately predict the fractional reduction in compressor work, at least on an instantaneous basis. If Equation 4-7 did predict the fractional reduction in compressor work, all the points in Figure 4-6 would lie on the solid line. It is possible that the problem with using Equation 4-7 to predict the energy savings calculated using Equation 4-8 is that the values cannot be measured with enough certainty. Thus, propagation of error was considered.

The values calculated using Equations 4-7 and 4-8 are $WR \pm \Delta WR$, due to measurement uncertainty. Appendix D contains the equations necessary to calculate ΔWR for the values calculated using Equations 4-7 and 4-8. Table 4-9 contains the experimental and calculated values from Equation 4-7 and 4-8 as well as the calculated ΔWRs. Figure 4-7 is a graphical representation of the data in Table 4-9 showing the magnitudes of the errors of the predicted and calculated fractional reduction in compressor work. Note that Figure 4-7

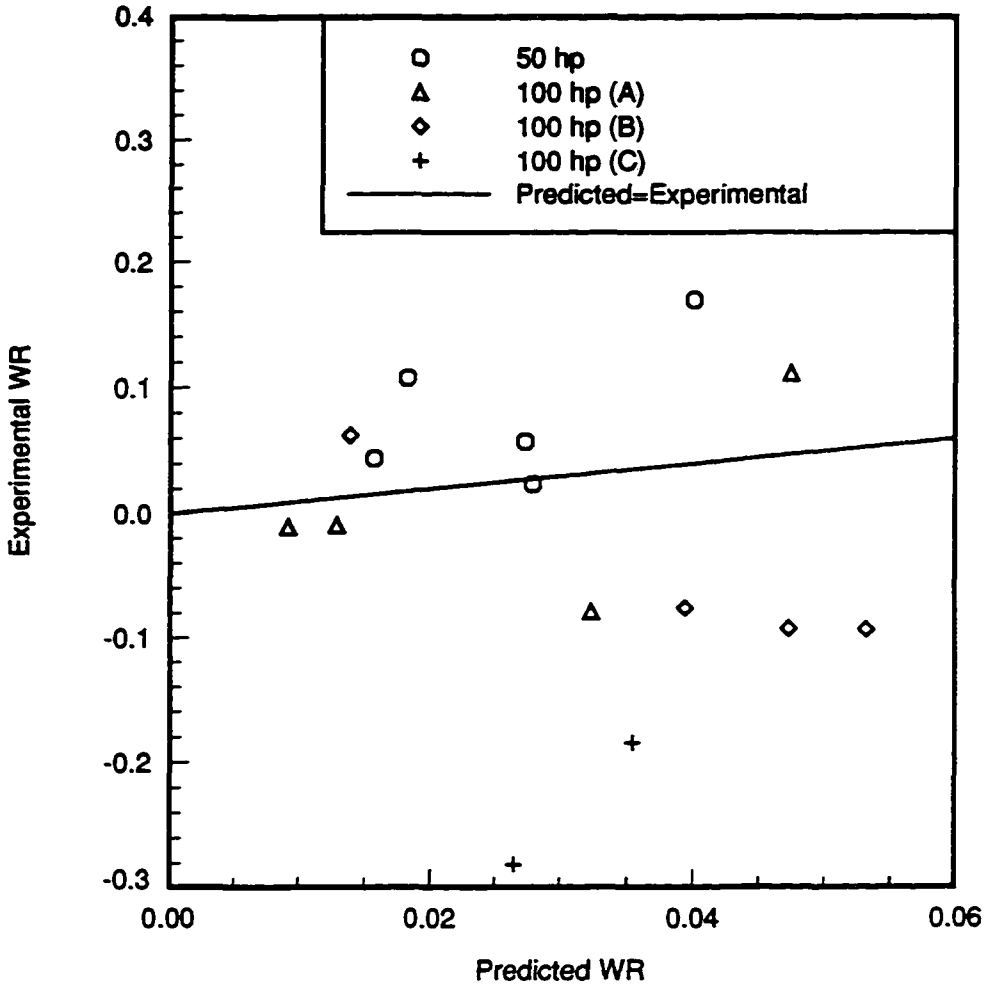

Figure 4-6. Comparison of Predicted and Experimental Fractional Reduction in Compressor Work

Table 4-9. Values and Uncertainties for Equations 4-7 and 4-8

WR_{4-7}	ΔWR_{4-7}	WR_{4-8}	ΔWR_{4-8}
.027	0.861	-.281	.020
.035	1.148	-.185	.020
.016	1.300	.042	.019
.018	1.488	.108	.019
.027	2.231	.057	.019
.028	2.312	.022	.020
.040	3.272	.170	.018
.009	0.723	-.011	.011
.013	1.012	-.009	.011
.032	2.504	-.079	.011
.048	3.683	.111	.011
.014	1.053	.063	.009
.039	2.999	-.076	.010
.047	3.599	-.093	.010
.053	4.049	-.094	.010

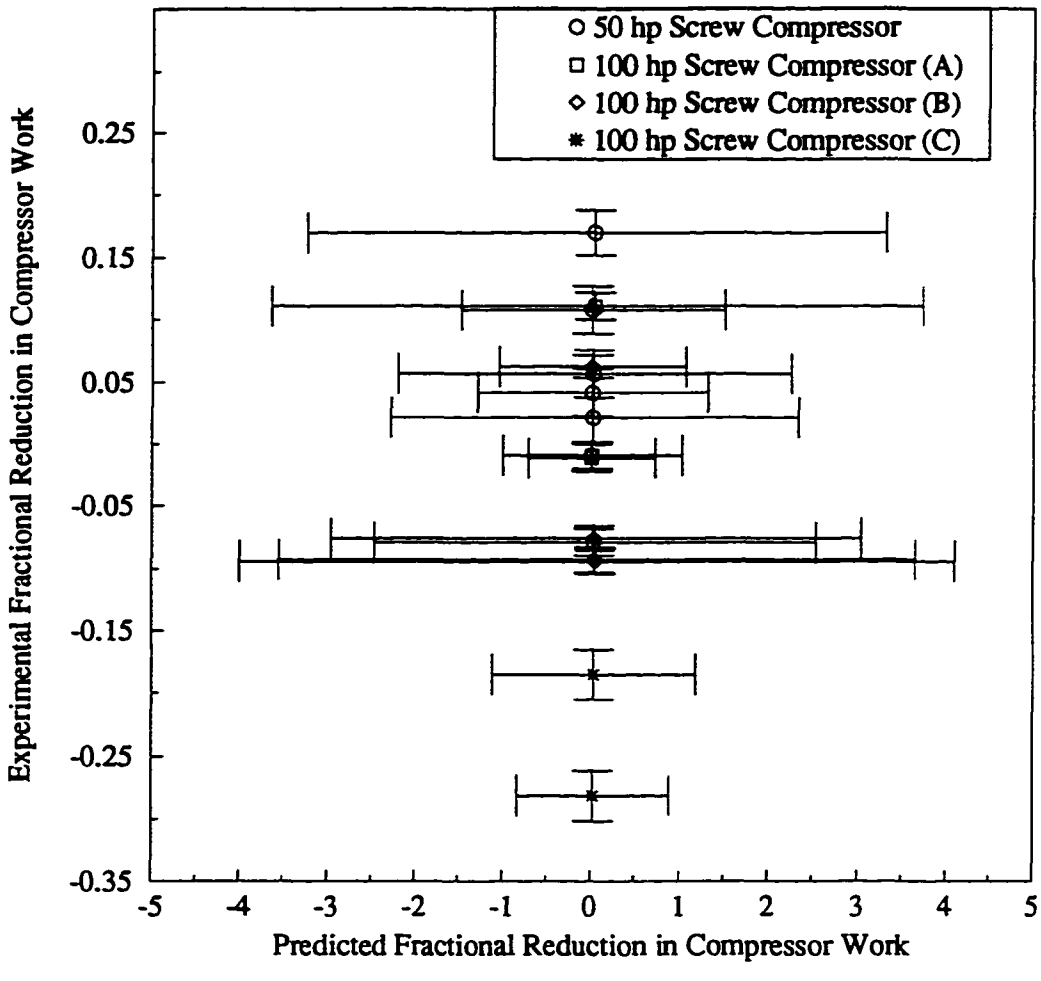

Figure 4-7. Effect of Measurement Errors on Predicted and Experimental Fractional Reduction in Compressor Work

contains the same data as Figure 4-6. The scale in Figure 4-7 has been changed so the complete error bars can be shown. This causes the data to appear to form a vertical line. The calculations to determine ΔWR assume that the inlet pressure does not change when the inlet temperature changes, and is measured to ±1 psi. These calculations also assume that the temperature is measured to ±1 °R, the power is measured to ±.5 kW, and the exit pressure is measured to ±2 psi. As shown in Table 4-9 and Figure 4-7, the uncertainties computed for the values calculated using Equation 4-7 are larger than the values themselves. Therefore, within the accuracy obtainable, no conclusions can be made as to whether Equation 4-7 predicts the savings calculated using Equation 4-8.

Once the initial data were studied, the theory was reevaluated to determine if there is a reason to expect decreasing power consumption with decreasing inlet air temperature. For a polytropic compression process, Equation 3-1 can be applied between the inlet and exit to give

$$p_1 \upsilon_1^n = p_2 \upsilon_2^n = \text{constant} \tag{4-9}$$

where p is pressure, υ is specific volume, and n is the polytropic exponent.

In order to calculate the ideal power consumed by an air compressor during polytropic compression, the following equation is used

$$\dot{W} = \dot{m} \int \upsilon dp \tag{4-10}$$

where $\dot{W}$ is the compressor power, $\dot{m} = \frac{A_1 V_1}{\upsilon_1}$ is the mass flow rate, and A_1V_1 is the inlet volumetric flow rate. Rearranging Equation 4-9 and inserting it into Equation 4-10, the expression becomes

$$\dot{W} = \dot{m}\int\left(\frac{c}{p}\right)^{\frac{1}{n}} dp \tag{4-11}$$

where c is the constant in Equation 4-9. Equation 4-11 can now be integrated between p_1 and p_2. Equation 4-9 can be incorporated into the result of the integration of Equation 4-11 to eliminate the constant, which leads to the following expression

$$\dot{W} = \dot{m}\left(\frac{n}{n-1}\right)(p_2\upsilon_2 - p_1\upsilon_1) \tag{4-12}$$

Using Equation 4-9, it is possible to substitute in for υ_2, allowing a υ_1 and a p_1 to be factored out, resulting in

$$\dot{W} = \dot{m}\left(\frac{n}{n-1}\right)\upsilon_1 p_1\left[\left(\frac{p_2}{p_1}\right)^{\frac{n-1}{n}} - 1\right] \tag{4-13}$$

By substituting for $\dot{m}$, the following equation is obtained

$$\dot{W} = \frac{A_1 V_1}{\upsilon_1}\left(\frac{n}{n-1}\right)\upsilon_1 p_1\left[\left(\frac{p_2}{p_1}\right)^{\frac{n-1}{n}} - 1\right] \tag{4-14}$$

The specific volume at the inlet conditions, υ_1, will cancel, leaving the following expression for the polytropic compressor power

$$\dot{W} = A_1 V_1 \left(\frac{n}{n-1}\right) p_1 \left[\left(\frac{p_2}{p_1}\right)^{\frac{n-1}{n}} - 1\right] \qquad (4\text{-}15)$$

Compressor inlet air temperature does not appear in Equation 4-15. Only A_1V_1, the inlet volumetric flow rate, could have a temperature dependence, and there is no theoretical reason to expect such a dependence for a positive displacement compressor. Further study was undertaken, using the data previously obtained on the 125 horsepower screw compressor, to confirm that no dependence existed. Recall that the instantaneous power data provided in Appendix A were collected at several inlet air temperatures and exit pressures.

Using the screw compressor data provided in Appendix A, and Equation 4-15, it was possible to solve for an experimental compressor inlet volumetric flow rate. In order to estimate an experimental volumetric flow rate, an inlet pressure of 14.7 psia was assumed. It was also assumed that the compression process was isentropic (n=k=1.4), and the exit pressures were converted into psia. Figure 4-8 shows the volumetric flow rate as a function of inlet air temperature. Note that it is not necessary to specify at what inlet and exit pressures these values were obtained, because these pressures appears in the power equation. From Figure 4-8, there is no systematic dependence between inlet volumetric flow rate and inlet temperature. Therefore, inlet volumetric flow rate is not a function of compressor inlet air temperature. This leads to the conclusion that compressor power is not a function of inlet air temperature.

Figure 4-9 represents a common compressed air system, consisting of an air compressor and a storage tank. In this system, the air compressor supplies the storage tank, and the storage tank supplies the compressed air to the factory. The storage tank helps to

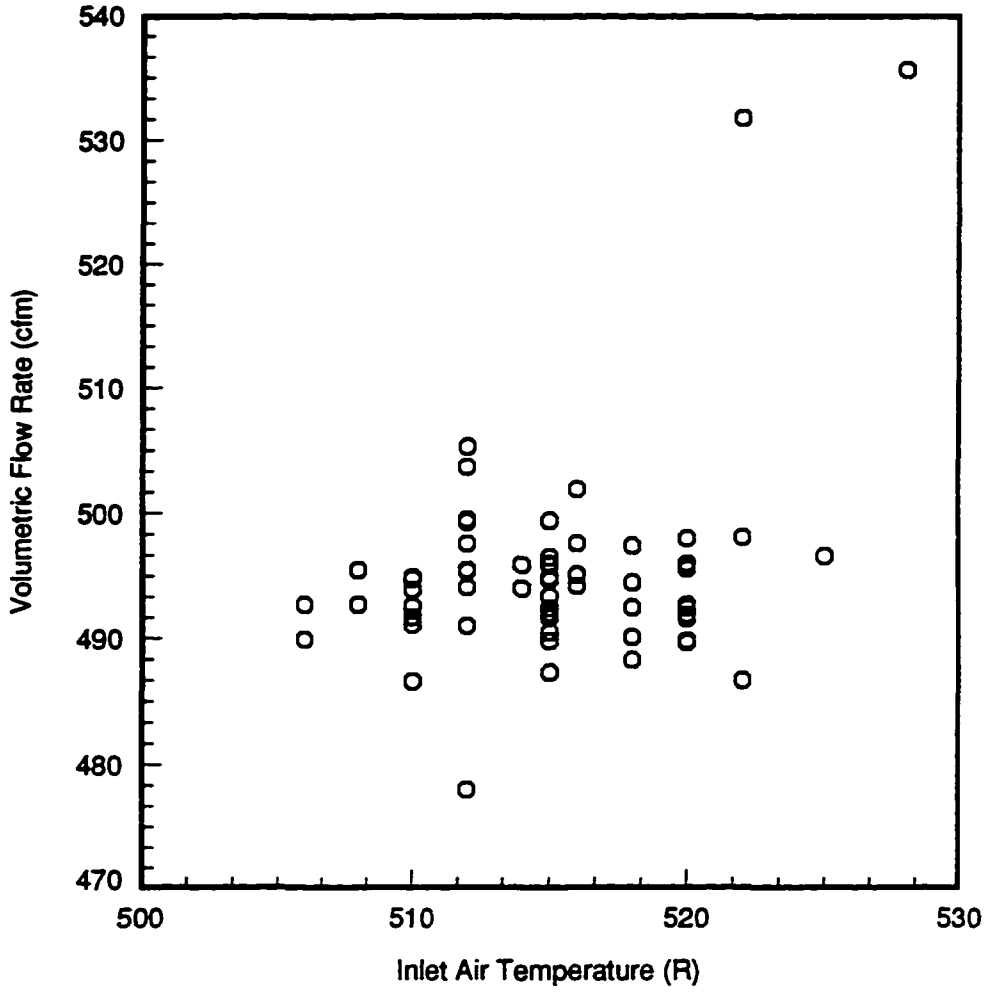

Figure 4-8. Effect of Inlet Air Temperature on Volumetric Flow Rate for 125 hp Screw Compressor

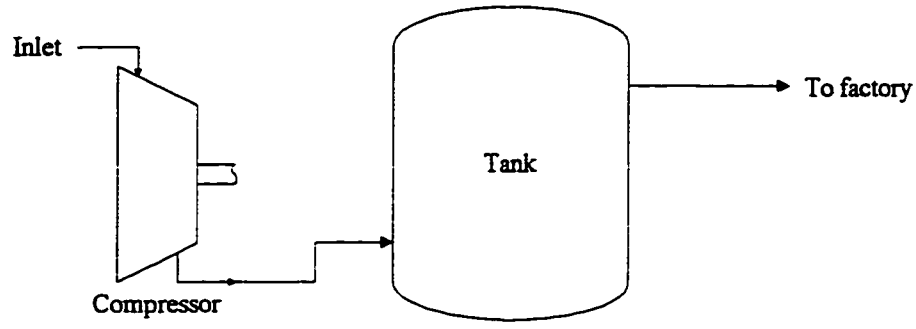

Figure 4-9. Typical Compressed Air System

maintain a relatively constant pressure. In addition, the tank helps to control compressor cycling. The compressor will cycle off when the pressure in the storage tank reaches a preset pressure. The compressor will remain off until the pressure in the storage tank drops below a preset value.

Because so many believe that lowering the inlet air temperature to an air compressor results in an energy savings, and it was determined that if the energy savings exist, they do not result from a decrease in power consumption, it was hypothesized that the savings are a result of shorter run times. A transient mass balance was performed on the compressor and tank system shown in Figure 4-9. This balance was of the form

$$\frac{dm}{dt} = \dot{m}_{in} - \dot{m}_{out} \qquad (4\text{-}16)$$

where $\frac{dm}{dt}$ is the rate of change of mass inside the tank with respect to time, $\dot{m}_{in}$ is the mass flow rate of air into the tank, and $\dot{m}_{out}$ is the mass flow rate of air out of the tank. If it is assumed that these mass flow rates do not vary with time, Equation 4-16 can be integrated to obtain

$$m = (\dot{m}_{in} - \dot{m}_{out})\Delta t + m_o \tag{4-17}$$

where m is the mass in the tank at time t, Δt is the elapsed time, and m_o is the initial mass in the tank.

The mass of air in the tank is a function of pressure and temperature. Substituting in the ideal gas law for the mass of air in the tank, the following equation is obtained

$$\frac{p_t v}{\frac{R_u}{M} T_t} = (\dot{m}_{in} - \dot{m}_{out})\Delta t + m_o \tag{4-18}$$

where p_t is the pressure in the tank, v is the tank volume, R_u is the universal gas constant, M is the molecular weight of air, and T_t is the tank temperature.

Using the definition of mass flow rate, $\dot{m} = \frac{p}{\frac{R_u}{M} T}(AV)$, and assuming that the initial mass in the tank is negligible, results in the expression

$$\Delta t = \frac{\frac{p_t v}{T_t}}{\frac{p_{atm}}{T_{inlet}}(AV)_{in} - \frac{P_{line}}{T_{line}}(AV)_{out}} \tag{4-19}$$

where $(AV)_{in}$ is the volumetric flow rate entering the compressor, $(AV)_{out}$ is the volumetric flow rate exiting the tank, T_{inlet} is the inlet air temperature, p_{atm} is the atmospheric pressure,

p_{line} is the pressure in the line leading to the factory, and T_{line} is the temperature in the line leading to the factory. This equation implies that the time that the compressor will operate is a function of the mass flow rate required by the facility, as well as the inlet air temperature.

It is possible that the factory would need so much air that the pressure in the tank never reaches the preset high pressure. If this occurs the air compressor will never cycle off. For an air compressor that never cycles off, the effect of lower compressor inlet air temperature will be an increase in the amount of air compressed, not a shorter run time or an energy savings. The amount of compressed air will increase because the density of the air is inversely proportional to the absolute temperature of the air. As long as the pressure in the tank is below the preset compressor shutoff pressure, the compressor will continue to operate. Because the energy savings associated with decreased inlet air temperature is due to a reduction in run time, if the compressor continuously operates, the run time is not decreased, and no energy is saved.

If there is no flow exiting the tank, Equation 4-19 reduces to

$$\Delta t = \frac{\frac{p_t V}{T_t}}{\frac{p_{atm}}{T_{inlet}}(AV)_{in}} \qquad (4\text{-}20)$$

Therefore, it is expected that the time required to compress the air will be a function of the inlet air temperature.

In order to evaluate this theory, a three horsepower reciprocating compressor with a 30 gallon tank was used. This air compressor was used because it could be readily controlled and instrumented during the data collection process. Also, if a relationship exists between run

time and inlet air temperature, it should have nothing to do with the size of the air compressor. The air compressor was placed outside so temperature variations could be measured.

A calibrated pressure gauge was installed in the tank. The pressure gauge could be read to the nearest psi. A valve on the tank was opened until the pressure gauge measured 0 psig. The valve was closed, the air compressor turned on, and the time required to reach 105 psig in the tank was measured. The time and the corresponding air temperature were recorded. These steps were then repeated.

Table 4-10 contains the data collected. Figure 4-10 is a graphical representation of these data. As shown in Figure 4-10, the time does not decrease with decreasing temperature. A linear curve fit to these data has a negative slope, although the correlation coefficient is so low that a linear trend is questionable. Then it was realized that at higher inlet temperatures and the same final tank pressure, the mass in the tank would actually decrease. Because it is the mass flow rate that is required by the load, the experiment was modified.

A thermocouple was installed inside the tank. The thermocouple could be read to the nearest tenth of a degree Fahrenheit. In this experiment the time required to compress 1.5 pounds of air was measured. The first step was to measure atmospheric pressure. Then the pressure required to obtain 1.5 pounds of compressed air at any given temperature was calculated according to

$$p_t = \frac{m\frac{R_u}{M}T_t}{v} \tag{4-21}$$

Table 4-10. Time to Reach a Final Tank Pressure of 105 psig

Inlet Air Temperature (°R)	Time Required to Reach 105 psig (s)
551	280
551	288
550	283
549	292
548	287
547	286
547	289
545	290
544	296
544	295
533	288
529	289
529	291
527	292

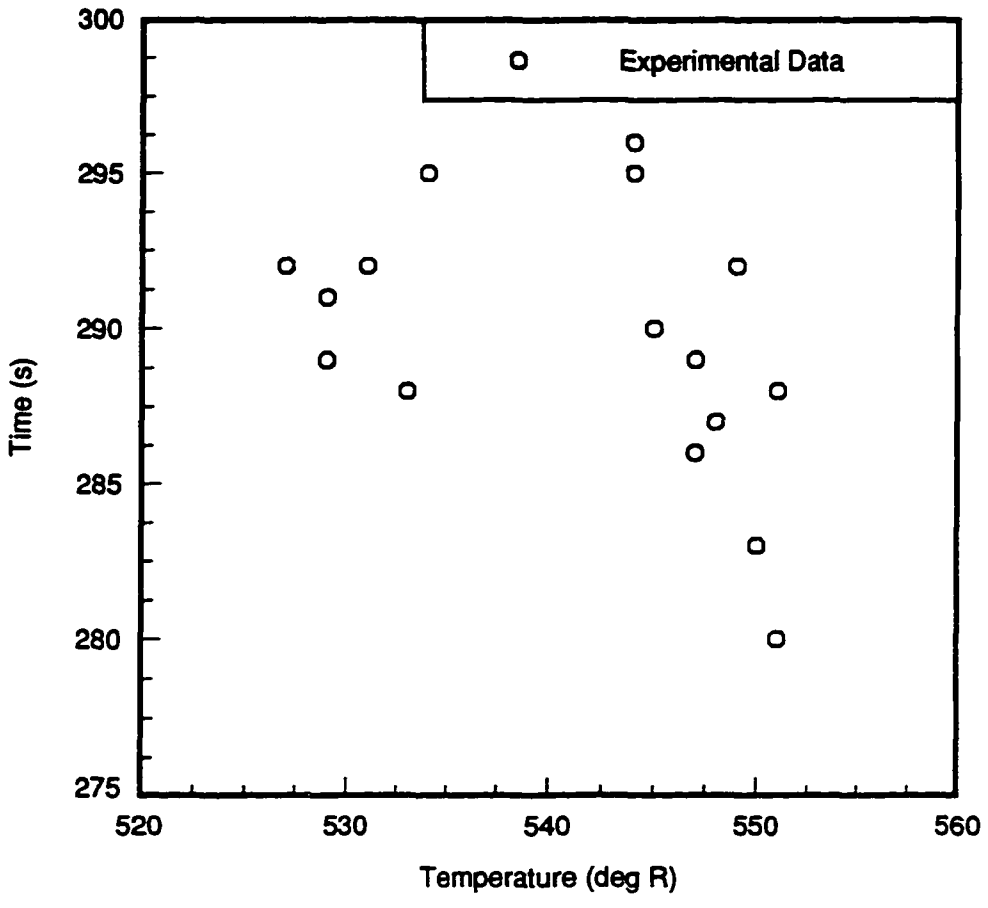

Figure 4-10. Effect of Inlet Air Temperature on
Time to Reach 105psig Tank Pressure

where m is the mass of air in the tank, p_t is the absolute tank pressure, v is the volume of the tank, R_u is the universal gas constant, M is the molecular weight of air, and T_t is the absolute temperature of the air in the tank. The valve on the tank was opened until the pressure gauge measured 0 psig. The valve was then closed, and the air compressor was started and allowed to operate until the combination of tank temperature and tank pressure resulted in a mass of approximately 1.5 pounds. The air compressor was turned off and the tank temperature, tank pressure, inlet air temperature, and run time were recorded. The valve was then opened and the process was repeated.

Appendix E contains the data collected during this experiment. Figure 4-11 is a graphical representation of these data. As expected, these data show the general trend of decreasing run time with decreasing inlet air temperature. There are also an additional savings because as the inlet temperature decreases, the pressure required to generate a given mass also decreases.

There are at least two reasons for the scatter in the experimental data. The run time for the air compressor was measured using a stopwatch. This causes some error. Another source of error is due to the pressure only being measured to the nearest psi. This translates to approximately a 5 °R range of tank temperatures that would have the same final pressure. This means that the mass in the tank is not exactly 1.5 pounds.

Equation 4-20, the relationship between inlet air temperature and run time with zero mass flow rate exiting the tank, is of the form y=mx, where y is the run time, m is the slope, and x is the inlet air temperature. This means that the relationship shown in the data should also be linear. The linear curve fit to the data in Figure 4-11 is t(s)=42.79+.2233T(°R) and

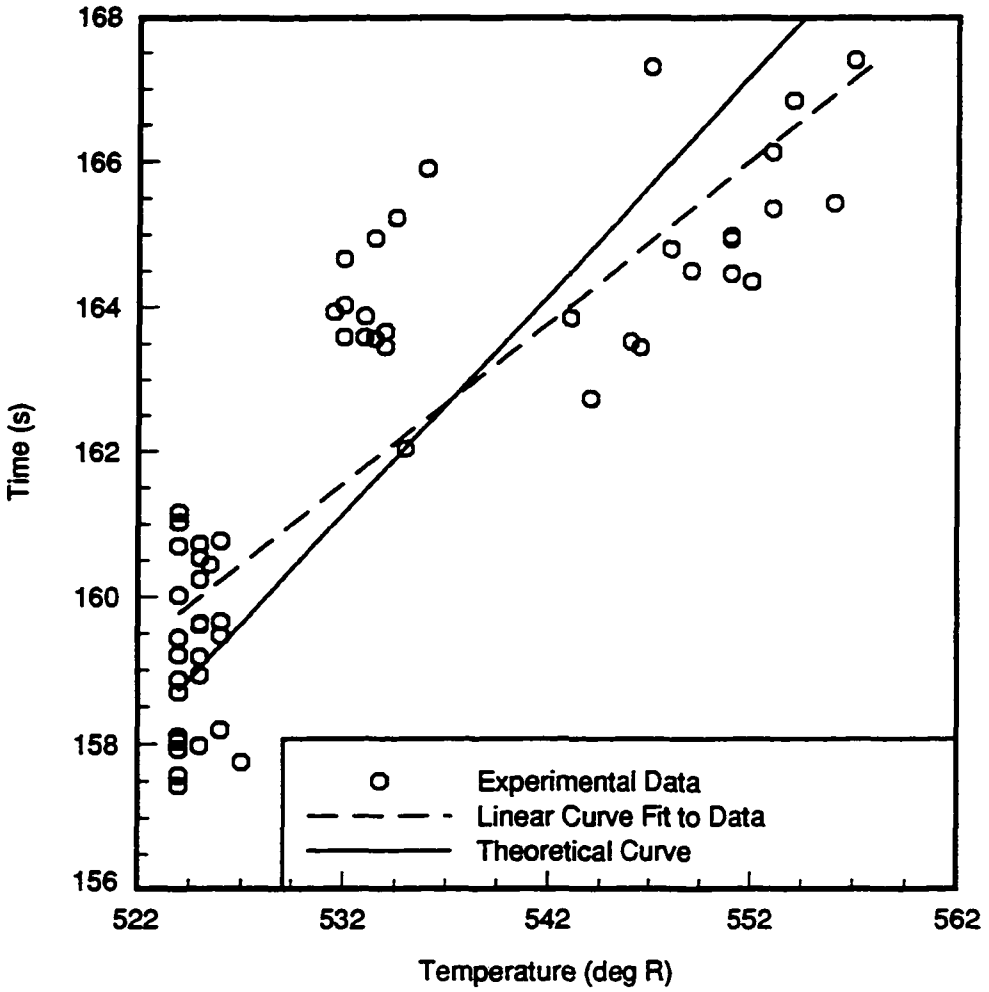

Figure 4-11. Effect of Inlet Air Temperature on Time to Compress 1.5 Pounds of Air

has a correlation coefficient of .73. The theoretical line is t(s)=.3029T(°R). As shown by Figure 4-11, the theory does a reasonable job of predicting the run time.

Now that the theory that the compressor will have a shorter run time with lower inlet air temperatures has been examined using experimental data, Equation 4-19, the run time formula, needs to be put into a form that can be used to estimate run time savings. The run time savings formula will be compared to Equation 4-6, which is used by the EADC offices to calculate the compressor work fraction reduction.

The run time savings, RTS, can be calculated using

$$RTS = \frac{\Delta t_{ht} - \Delta t_{lt}}{\Delta t_{ht}} \tag{4-22}$$

where Δt_{ht} is the value calculated from Equation 4-19 at the high temperature, and Δt_{lt} is the value calculated from Equation 4-19 at the low temperature. Recall that if the mass flow rate from the tank is zero, Equation 4-19 reduces to Equation 4-20. It is a reasonable assumption that atmospheric pressure is constant. If the compressor is a screw compressor, or if it is a reciprocating compressor and it is assumed that the clearance fraction is zero, the inlet volumetric flow rate is constant. The tank in the compressed air system has a constant volume. Therefore, with no mass flow rate exiting the tank, Equation 4-22 becomes

$$RTS = \frac{\left(\frac{p_t T_{inlet}}{T_t}\right)_{ht} - \left(\frac{p_t T_{inlet}}{T_t}\right)_{lt}}{\left(\frac{p_t T_{inlet}}{T_t}\right)_{ht}} \tag{4-23}$$

If the tank is located in the factory, and the air remains in the tank for a period of time, the temperature of the air in the tank will be approximately that of the factory, and will not be

a function of inlet air temperature. In addition, as previously mentioned, the purpose of the tank is to maintain a relatively constant system pressure. With these two assumptions, Equation 4-23 reduces to

$$RTS = \frac{T_{inlet_{ht}} - T_{inlet_{lt}}}{T_{inlet_{ht}}} \qquad (4\text{-}24)$$

Note that the right hand side of Equation 4-24 is the same as the right hand side of Equation 4-6. There are certain conditions that must be met in order to apply Equation 4-24. These conditions are: 1) no mass flow rate exiting the tank, 2) constant tank pressure, 3) constant temperature air in the tank, and 4) constant inlet volumetric flow rate.

Reducing the inlet air temperature to a positive displacement compressor can result in an energy savings, but this savings is a result of shorter run times, not a decreased power consumption as reported in the literature. This energy savings will only occur if the compressor cycles. If the compressor is constantly operating, decreasing the inlet air temperature will not decrease the energy usage, but it will increase the mass of air provided to the system.

It is interesting that with the assumptions of no mass exiting the air tank, constant tank temperatures and pressures, and a constant volumetric flow rate entering the air compressor, the formula for run time savings is equal to formula used to estimate the compressor work fraction reduction, Equation 4-6. This means that the savings estimates for air compressors with off cycles should be similar, even though the savings were previously credited to a decreased power consumption, not a shorter run time. However, because it is the run time

that is decreased, not the instantaneous power, this opportunity must be applied only to air compressors that cycle off.

Because during actual operating conditions in facilities there is a mass flow exiting the tank, Equation 4-24, the run time savings formula, should not be used. A formula must be used that accounts for the effect of the mass exiting the tank. This formula is

$$RTS = 1 - \frac{T_{inlet_R}}{T_{inlet_M}} \left(\frac{\frac{(AV)_{in} P_{atm}}{\frac{R_u}{M}} - \dot{m}_{line} T_{inlet_M}}{\frac{(AV)_{in} P_{atm}}{\frac{R_u}{M}} - \dot{m}_{line} T_{inlet_R}} \right) \tag{4-25}$$

where $\dot{m}_{line}$ is the mass flow rate exiting the tank. This formula only assumes that the load on the compressed air system is not a function of the inlet air temperature.

Figure 4-12 shows the effect of factory load on run time savings. This figure also shows the effect of using Equation 4-25 instead of Equation 4-24 to estimate the run time savings. On this figure, Equation 4-24 is represented by the line labeled zero mass flow rate. The maximum mass flow rate occurs when the compressor will not cycle off at the maximum temperature. The run time savings were calculated using Equation 4-25. The temperature ratio is the ratio of T_{in} in °R to the maximum inlet air temperature, which is assumed to be 580 °R. It is also assumed that the volumetric flow rate into the tank is a constant 800 cfm, the tank pressure varies between 105 and 115 psia, the air is inside the tank long enough to reach a constant temperature of 535 °R, the tank volume is 60 ft^3, compressor and line pressures are 110 psia, and the volumetric flow rate out of the tank is 90 cfm. Note that using Equation 4-24 to predict the run time savings will result in a conservative estimate of the energy savings

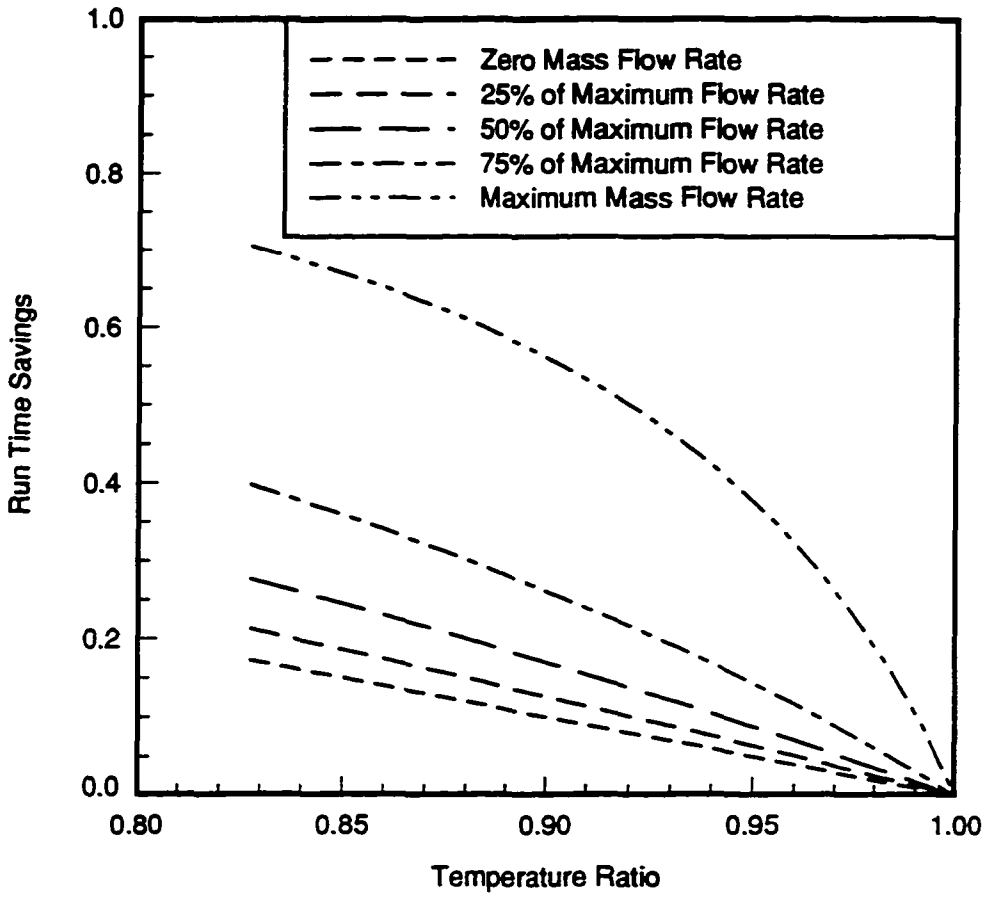

Figure 4-12. Effect of Factory Load on Run Time Savings

for this sample compressor. Also note that as the exit mass flow rate approaches zero, the run time savings approaches the compressor work fraction reduction, Equation 4-6.

Figure 4-12 could be used to estimate the savings for this sample compressor, if the fraction of time that the compressor is currently operating is known. For example, if the sample compressor is operating half of the time, the line marked 50% of maximum flow rate on Figure 4-12 could be used to estimate the run time savings. But, as previously mentioned, energy savings estimates from energy audits should be conservative. Therefore, a conservative estimate can be made using the zero mass flow rate case, Equation 4-24.

The research pertaining to the effect of inlet air temperature began with a hypothesis that power would decrease as inlet air temperature decreased. This hypothesis was based on information found in the literature. Data collected did not show a decrease in power with a decrease in inlet air temperature. The theory was reviewed, and no theoretical reason exists to expect a relationship between power and inlet air temperature. Because so many believed that it was a good idea to use colder intake air, a new hypothesis was considered. This hypothesis was that the run time would decrease with colder inlet air. This hypothesis was verified theoretically. Data collected do show that the run time is a function of inlet air temperature.

The next section discusses recovering energy from an air compressor. Although heat recovery always saves energy, it may not be cost effective if the amount of recovered energy is small. Actual experimental data is provided in the following section, as well as the theoretical maximum amount of recoverable energy.

Heat Recovery from Compressors

Although it always saves energy to recover waste heat, the decision as to whether or not to reclaim this energy is an economic one. There is a cost associated with the installation of a heat recovery system. Therefore, it is important to be able to accurately estimate the amount of heat that will be recovered. This section provides data and theory to assist in making this estimate.

In addition to studying the effect of the compressor intake air temperature on the power required by the 50 horsepower and 100 horsepower air cooled screw compressors, the waste heat recovery potential of these compressors was also studied. A byproduct of all air compression systems is heat. According to one reference, approximately 80% of the electrical energy used to compress the air is converted into heat (Oviatt, 1981). Another source estimates that 85% of the energy input to a compressor exits as waste heat (Pichot, 1986). The EADC offices estimate that 42% of the power input to an air compressor is recoverable (Iowa State University Energy Analysis and Diagnostic Center, 1994).

The heat that is recovered from the 50 horsepower air cooled screw compressor is ducted into the facility in a 14 inch by 58 inch duct and is used to offset space heating loads in the winter. The warmed air can also be ducted outside to reduce the summer cooling load. Table 4-11 contains the data necessary to calculate the heat recovered from the 50 horsepower air cooled screw compressor. Note that the difference between the inlet air temperature and the duct temperature should be positive.

The heat recovered from the 100 horsepower air cooled screw compressor enters the factory through a 24 inch by 38 inch rectangular duct. This heat is used to warm the facility in the winter, and is directed outside in the summer. Table 4-12 contains the data necessary to calculate the heat recovered from the 100 horsepower screw compressor that was studied..

Table 4-11. 50 hp Air Cooled Screw Compressor Heat Recovery Data

Average Power Usage (kW)	Exit Pressure (psig)	Inlet Temperature (°R)	Duct Air Temperature (°R)	Duct Air Velocity (feet/minute)
35.7	100	550	548	20.0
34.2	100	541	550	10.0
31.9	108	540	548	18.0
33.7	108	535	538	22.0
34.9	100	534	557	17.5
27.9	108	528	545	25.0

The energy recovered was calculated according to

$$\dot{q} = \frac{p_d}{\frac{R_u}{M} T_d} AC_p V(T_d - T_i) \qquad (4\text{-}26)$$

where p_d is the pressure in the duct, R_u is the universal gas constant, M is the molecular weight of air, A is the area of the duct through which the heated air heat flows, T_d is the

Table 4-12. 100 hp Air Cooled Screw Compressor Heat Recovery Data

Average Power Usage (kW)	Exit Pressure (psig)	Inlet Temperature (°R)	Duct Air Temperature (°R)	Duct Air Velocity (feet/minute)
40.6	120	565	580	800
52.0	121	550	570	500
48.1	121	545	580	900

absolute temperature in the duct, C_p is the specific heat of air, T_i is the absolute temperature at the compressor inlet, and V is the velocity of the air in the duct. Note that the molecular weight of air, the specific heat of air, and the universal gas constant come from standard tables (Moran, 1996). Equation 4-26 is based on a mass and energy balance.

The uncertainty in the calculated value can be obtained from

$$\Delta q = \left\{ \begin{array}{l} \left(\frac{p_d C_p V_d}{\frac{R_u}{M}} \left(1 - \frac{T_i}{T_d} \right) \right)^2 (\Delta A)^2 + \left(\frac{V_d C_p A}{\frac{R_u}{M}} \left(1 - \frac{T_i}{T_d} \right) \right)^2 (\Delta p)^2 + \\ \left(\frac{p_d C_p A}{\frac{R_u}{M}} \left(1 - \frac{T_i}{T_d} \right) \right)^2 (\Delta V)^2 + \left(\frac{V_d p_d C_p A}{\frac{R_u}{M} T_d} \right)^2 (\Delta T_i)^2 + \\ \left(\frac{V_d C_p A_d p_d T_i}{\frac{R_u}{M} T_d} \right)^2 (\Delta T_d)^2 \end{array} \right\}^{1/2} \qquad (4\text{-}27)$$

where it is estimated that the velocity is known to ±5%, the temperatures to ±5 °R, the pressure to ± 5%, and the lengths to ±.1 inches.

Table 4-13 shows the energy recovered from the 50 horsepower screw compressor. From Table 4-13, the average amount of energy recovered from the 50 horsepower air cooled screw compressor is less than 1% of the input energy. Table 4-14 shows the energy recovered from the 100 horsepower air cooled screw compressor. From Table 4-14, the average amount of energy recovered is 67% of the input energy. These tables show a large discrepancy on the amount of heat recovered. More information is needed to say what percentage of energy input to an air compressor is recoverable. Therefore, a search was made to try to locate other case studies, and a theoretical analysis was performed.

Table 4-13. Energy Recovered from 50 hp Air Cooled Screw Compressor

Input Power (kW)	Energy Recovered (kW)
35.7	-.067±.17
34.2	.149±.08
34.9	.240±.15
31.9	.112±.19
33.7	.659±.15
30.5	.712±.22

Table 4-14. Energy Recovered from 100 hp Air Cooled Screw Compressor

Input Power (kW)	Energy Recovered (kW)
40.6	21.2±7.22
52.0	18.0±4.67
48.1	55.7±8.87

A recent study purporting to be a "case study" on heat recovery from air compressors estimated that 75% of the energy input to an air compressor was available as heat (Abou-Siedo, 1992). This estimate was based on "rules of thumb" and not on data collected in a facility. Therefore, there is no reason to expect this estimate is any better than the ones presented in the literature review. No case studies could be located that had actual data collected at facilities.

In order to estimate the theoretical amount of energy that could be recovered from a positive displacement air compressor, an energy balance was performed on the 125 horsepower screw compressor. In order to obtain the temperature of the compressed air, the polytropic expression for an ideal gas was used

$$T_2 = \left(\frac{p_2}{p_1}\right)^{\frac{n-1}{n}} T_1 \qquad (4\text{-}28)$$

where p is absolute pressure and T is absolute temperature. An inlet pressure of 14.7 psia was assumed. Because the actual polytropic exponent, n, is not known, it was allowed to vary

between one, the isothermal case, and 1.4, the isentropic case. The power to compress the air, $\dot{W}$ was calculated using an equation similar to Equation 4-15

$$\dot{W} = A_1 V_1 \left(\frac{n}{n-1}\right) p_1 \left[\left(\frac{p_2}{p_1}\right)^{\frac{n-1}{n}} - 1\right] \tag{4-29}$$

where A_1V_1 is the inlet volumetric flow rate, p_1 is the inlet pressure, and p_2 is the exit pressure.

An energy balance was then performed on the air being compressed. This balance resulted in the following expression for the heat transfer rate, $\dot{Q}$, associated with the compression process

$$\dot{Q} = \dot{W} + \dot{m}(h_1 - h_2) \tag{4-30}$$

where $\dot{m}$ is the mass flow rate of air, h_1 is the enthalpy at the inlet to the compressor, and h_2 is the enthalpy of the air exiting the compressor.

A motor efficiency of 93% was then assumed (Anderson, 1995). It was now possible to calculate the theoretical fraction of input energy that is recoverable, RF, according to

$$RF = \frac{(1-\eta)\dot{W}_{in} - \dot{Q}}{\dot{W}_{in}} \tag{4-31}$$

where η is the motor efficiency and $\dot{W}_{in}$ is the power input to the motor. The expression $(1-\eta)\dot{W}_{in}$ accounts for the heat released when the motor operates.

Figure 4-13 shows the theoretical percent of input energy that is recoverable as a function of n, the polytropic exponent. Figure 4-13 shows that the percent of energy that is recoverable is a strong function of the polytropic exponent. For the isothermal case,

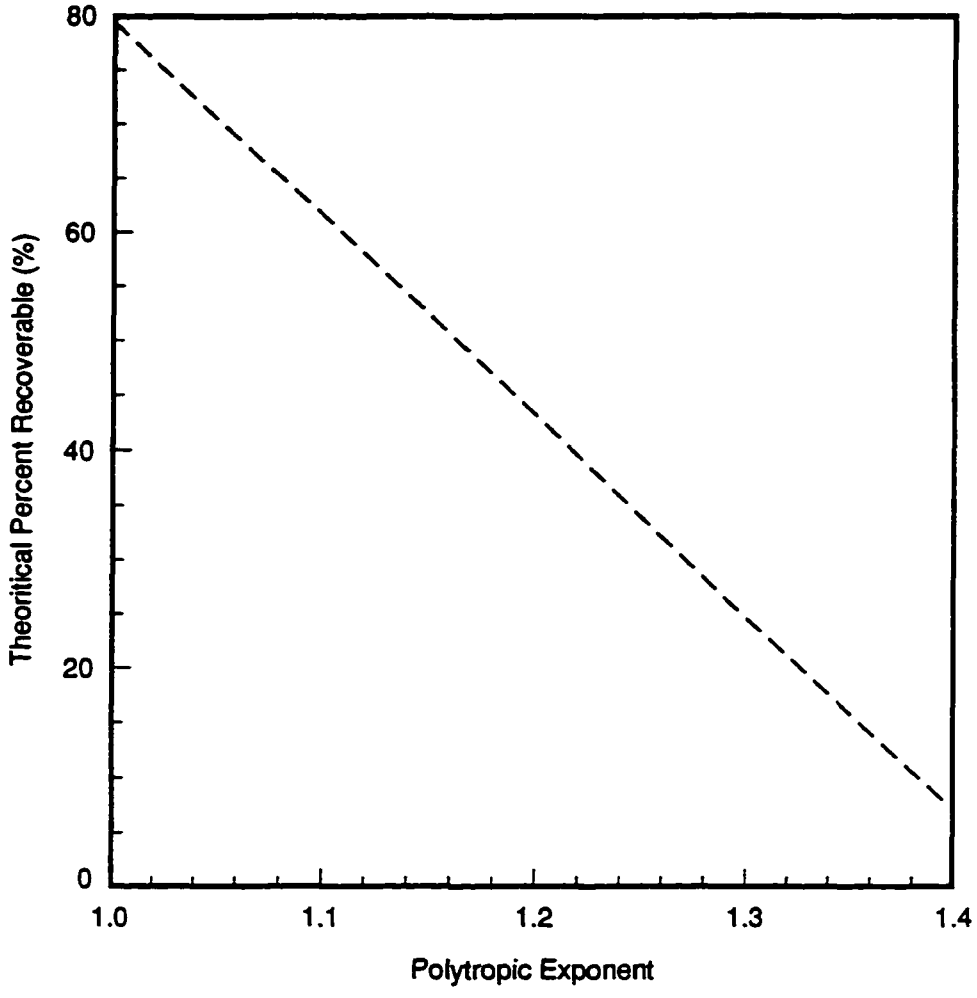

Figure 4-13. Effect of Polytropic Exponent on Theoretical Percentage of Recoverable Energy Assuming 93% Motor Efficiency

approximately 79% of the energy input to the air compressor was recoverable. For the isentropic case, it was determined that approximately 8% of the energy input to the compressor was recoverable. This means that the maximum theoretical amount of input energy to an air compressor that can be recovered is 79%.

When making the decision as to whether or not to recover the heat rejected by an air cooled screw compressor, the estimate of the percent of input energy that can be recovered is important. With higher estimated percent recovery, this opportunity appears more cost effective. This study shows that the percent of input energy that can be recovered is a function of the polytropic exponent, and always less than 79%.

Conclusions

It was possible to study three different opportunities on compressors. The effect of lowering the compressor exit pressure was studied over a large pressure range on a 150 horsepower reciprocating compressor and over a smaller pressure range on a 125 horsepower screw compressor. The effect of inlet air temperature on power consumption was studied on five different screw compressors. The effect of inlet air temperature on compressor run time was studied on a reciprocating air compressor. The heat recovery potential was studied on a 100 horsepower and a 50 horsepower air cooled screw compressor.

As predicted by theory, lowering the exit pressure from the air compressor resulted in lower power consumption. For the 125 horsepower screw compressor, it was discovered that the isentropic model did a good job of predicting the experimental power.

For a reciprocating compressor, the isentropic compressor model will underpredict the power. This will result in an overestimate of the energy savings. On an energy audit, it is desirable to provide conservative estimates of the energy savings. This means that the isentropic model should not be used to predict the power at a reduced exit pressure for this reciprocating compressor. To obtain a conservative estimate of the power at a reduced exit pressure for this reciprocating compressor, the isentropic compressor model must be modified to account for the effect of clearance volume.

It is a commonly held belief that lowering the inlet air temperature to the compressor will decrease the power consumption. Data collected for this project show that compressor power consumption is not decreased by lowering the inlet air temperature. A study of the theory behind positive displacement compressors could not find a reason to expect compressor power to increase, or decrease with changing compressor inlet air temperatures.

A theoretical reason for decreasing compressor run time with decreasing inlet air temperature was discovered. Data collected for this project show that the run time will decrease with decreasing inlet air temperatures. A decrease in run time will result in an energy savings.

It is interesting that with the assumptions of no mass exiting the air tank, constant tank temperatures and pressures, and a constant volumetric flow rate entering the air compressor, the formula for run time savings is equal to formula used to estimate the compressor work

fraction reduction, Equation 4-6. It was theoretically shown that for a sample compressor, the assumption of no mass flow provides a conservative estimate of the energy savings. It is important that caution is taken when applying this opportunity, because lowering the compressor inlet air temperature will only result in an energy savings if the compressor cycles off.

Energy is always conserved when heat is recovered. Unfortunately, the estimates of the energy savings achieved when recovering the heat from the air compressor do not accurately predict the energy savings. Even other recent studies only use "rules of thumb" to estimate the amount of energy that is recoverable (Abou-Siedo, 1992). This study provides some actual in-situ data on the amount of energy that can be recovered from an air compressor. More data will need to be collected before a definite answer is found as to what percentage of the energy input to an air compressor is recoverable. It was determined that the maximum theoretical amount of input energy that can be recovered as heat from an air compressor is 79%. This fraction can only be recovered if the compressor is operating isothermally.

The next chapter discusses the literature available relating to boilers, focusing on information that may be of use on an energy audit. The available boiler models do not account for how a boiler in a factory is actually used. These models are steady state, and do not account for seasonal effects, firing rate, boiler controls, etc. In addition, no industrial operating data are available in the literature, and the accuracy and validity of the models is in question. Therefore, this study continued with the collection and analysis of boiler data. The data and analysis are provided in the boiler chapter.

CHAPTER 5. BOILER LITERATURE REVIEW

This chapter begins with a basic introduction to boilers. This is followed by a discussion on the information available in the literature that pertains to boilers that would be useful in an energy audit. Most of the information available in the literature relating to boilers, that would be of use in an energy audit, is presented in tables and graphs. Models that relate to boiler design will not be discussed.

Boilers are used to generate hot water or steam. The heat source used for heating the water or creating the steam is usually natural gas or electricity, but it can also be fuel oil, liquefied petroleum, coal, etc. (Lipták, 1987). It is estimated that a boiler burns more than four times its original cost in fuel, yearly (Garcia-Borras, 1983).

There are two general categories of boilers; firetube and watertube. In a firetube boiler the hot combustion gases flow through the tubes, while the water flows over the tubes. In a watertube boiler the water flows through the tubes, while the hot combustion gasses flow over the tubes.

There are two efficiencies commonly used to describe how effectively the boiler is operating: combustion efficiency and boiler efficiency. Combustion efficiency is a measure of the performance of the gas burner and the heat exchange capacity of the boiler. The combustion efficiency is a function of the fuel, the excess air, the flue gas temperature, etc. The combustion efficiency of most boilers is in the 75% to 86% range (Tierney, 1994). It is defined as (Dyer, 1988)

$$\eta \equiv \frac{/h_{reactants} - h_{products}/}{HHV_{fuel}} \qquad (5\text{-}1)$$

In Equation 5-1, h is the enthalpy per pound of fuel and HHV is the higher heating value per pound of fuel. The enthalpies and higher heating values are found in standard tables. The numerator in Equation 5-1 represents the amount of energy liberated in the combustion process, while the denominator is the energy available in the fuel. The reactants in Equation 5-1 include the fuel and the moist air used for combustion. The products must be determined by performing a combustion analysis (Dyer, 1988). Improvements in combustion efficiency result primarily in reductions in the waste heat lost in the flue gases (Yaverbaum, 1979).

For a boiler with a modulated burner, the burner is always firing. Therefore, for a boiler with modulated burners, the combustion efficiency is a measure of the largest single source of boiler inefficiency, the flue losses. For all boilers, an additional energy loss occurs from the boiler jacket. In a boiler with an on/off burner, there are two additional energy loss paths: heat loss from the boiler jacket when the burner is not firing, and heat loss up the chimney when the burner is not firing (Landry, 1993). The jacket heat loss involves energy loss from the boiler's heat exchanger and water tank through convective, conductive, and radiative heat transfer to the boiler room and the ground beneath the boiler. The flue loss when the burners are not firing is a result of the heated air rising up the chimney as cold air is drawn into the combustion air inlet to replace it (Landry, 1994). Jacket losses are normally small compared to stack losses (Modera, 1988). The combustion efficiency is a useful indicator of boiler performance.

The other common measure of the efficiency of a boiler is the boiler efficiency. The boiler efficiency is a measure of how much of the energy available in the fuel is transferred to the water. This efficiency accounts for the effects of varying loads. Equation 5-2 can be used to calculate the boiler efficiency (Dyer, 1988)

$$\eta_{boiler} = \frac{\dot{m}_s(h_s - h_w)}{\dot{m}_f(HHV)} \tag{5-2}$$

where $\dot{m}_s$ is the mass flow rate of the steam, h_s is the enthalpy of the steam leaving the boiler, h_w is the enthalpy of the water entering the boiler, and $\dot{m}_f$ is the mass flow rate of fuel. It is common practice to use combustion efficiency to approximate boiler efficiency, because combustion efficiency can be calculated from measurements at the boiler stack.

Industrial boilers provide process heat, energy for space heating, and heat for other incidental loads such as domestic hot water. In a primarily process loaded boiler, the amount of steam generated by the boiler is approximately constant throughout the year. A space heating loaded boiler will not use any fuel during the months when space heating is not required. It is common to find boilers that have both space heating and process loads. This situation is illustrated by the bar graph in Figure 5-1. In Iowa, from May through October, there is typically no space heating load. During these months, the natural gas used by the boiler would be the process load. The average natural gas usage during these months is called the base load. The base load is shown as the line in Figure 5-1. Note that the natural gas used by the boiler can vary during the months with no heating due to production changes.

Still referring to Figure 5-1, there is an increase in natural gas usage over the base load from November through April. This increase in fuel usage is associated with the space heating

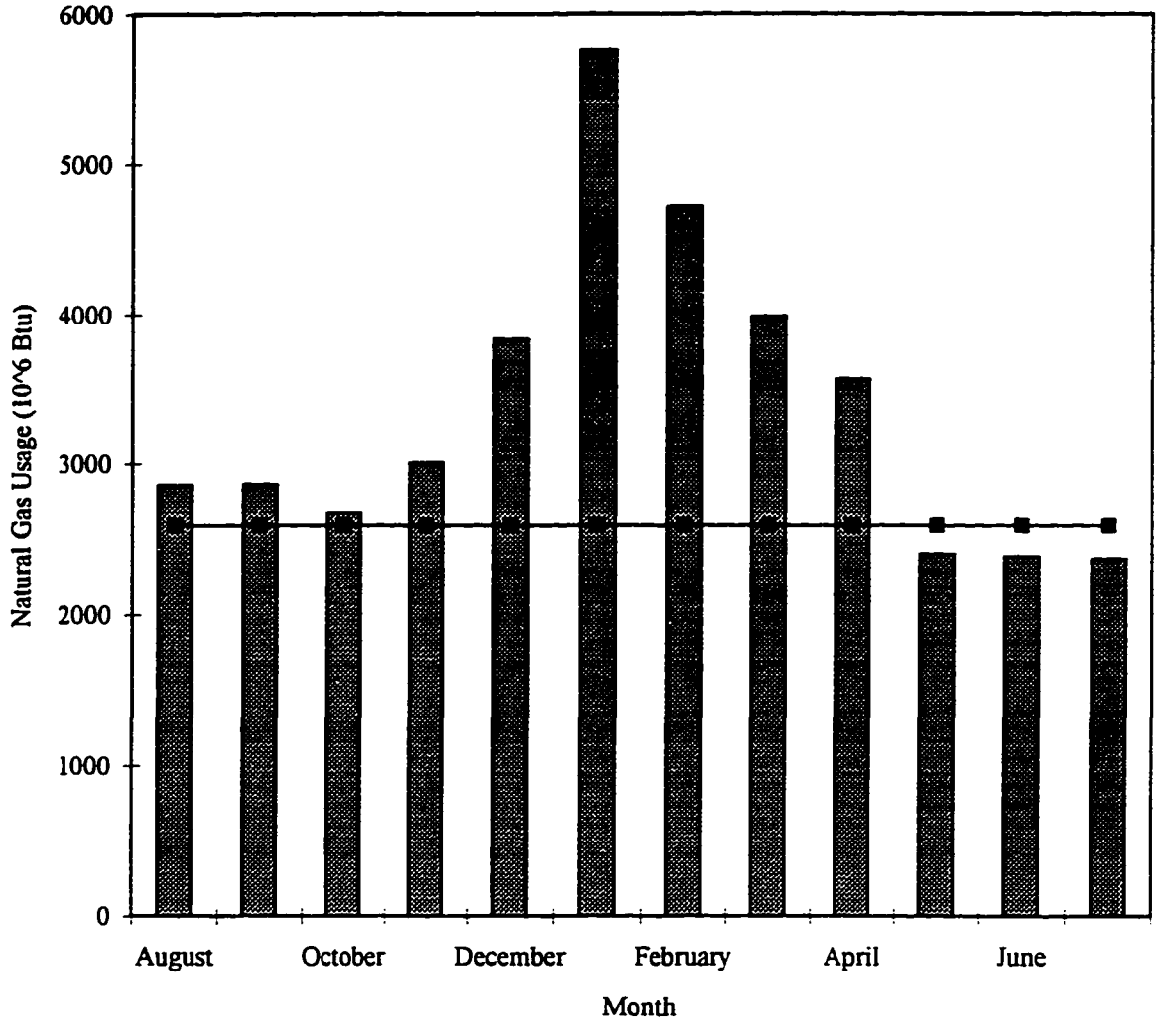

Figure 5-1. Natural Gas Usage Plot for an Industrial Boiler

load. A boiler that is used only for process loads will most likely have a fairly constant steam generation rate and boiler efficiency. A boiler that is used for space heating alone or space heating and process loads may not have a constant steam generation rate or boiler efficiency.

Figure 5-2 shows the approximate energy savings resulting from the use of preheated air (*North American Combustion Handbook*, 1952). As shown in this figure, there can be significant savings achieved by preheating the incoming air. Preheating the combustion air saves energy because less energy from the combustion process is required to raise the temperature of the air. The energy savings depend on the fuel being combusted, as well as the incoming air temperature. The information presented in this figure is approximate because it assumes that the air required per gross Btu is the same for all fuels. This was the only model showing the effect on efficiency of preheating the combustion air that could be located in the literature.

Figure 5-3 shows the effect of boiler capacity on the losses from the boiler (Dukelow, 1991). This figure looks at the individual losses: radiation, dry flue gas, and flue moisture, as well as the combined total efficiency loss. The total efficiency loss decreases at increasing percent capacity. This is because the radiation loss decreases as percent capacity increases. Radiation loss from the boiler is dependent on the amount of insulation on the surface of the boiler. Once the boiler is designed and built, the boiler operator cannot operate the boiler in any manner to reduce the radiation loss (Dukelow, 1991). The dry flue gas and flue moisture losses increase slightly as the percent capacity increases. Figure 5-3 shows that for a boiler loaded to at least 40% of capacity, the losses are approximately constant. This was the only model showing the effect of capacity on boiler losses that could be located in the literature.

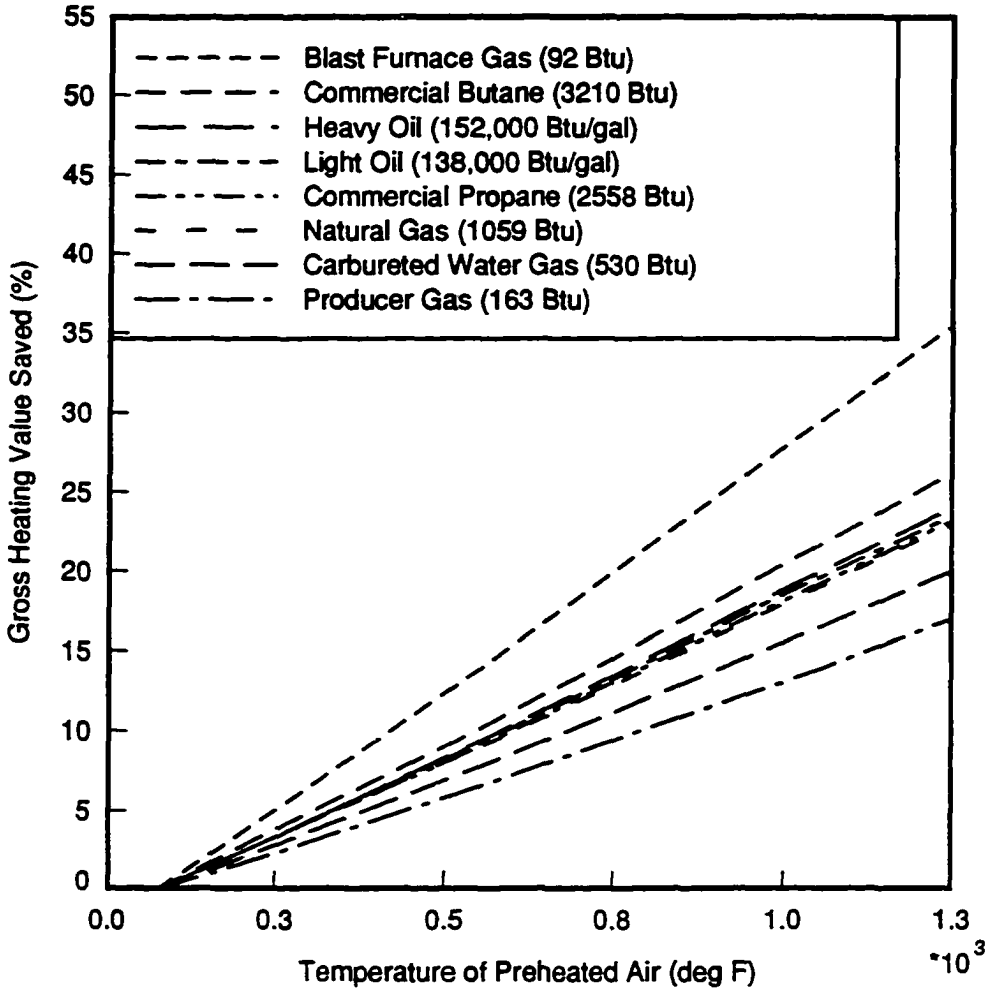

Figure 5-2. Approximate Savings Resulting from Use of Preheated Combustion Air (*North American Combustion Handbook*, 1952, p.61)

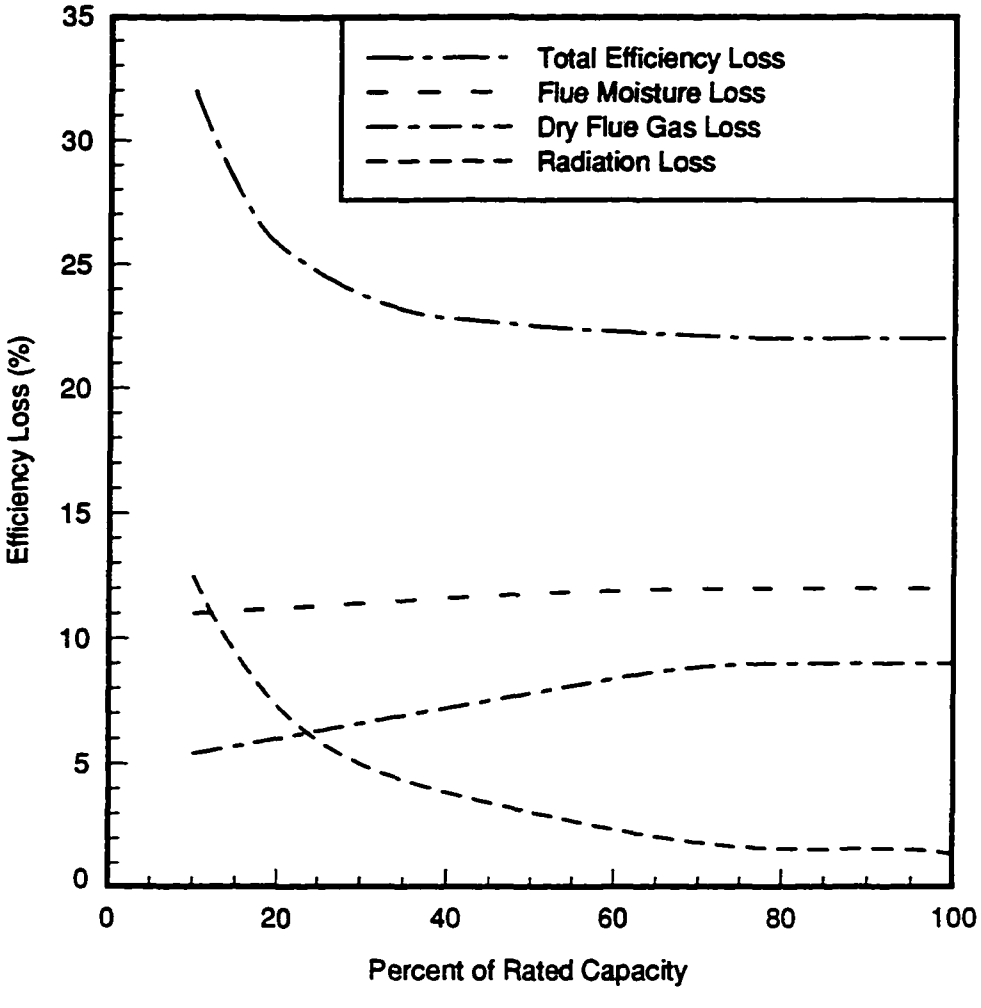

Figure 5-3. Effect of Partial Load Operation on Boiler Efficiency Losses (Dukelow, 1991, p.85)

Figure 5-4 shows the effect of the flue gas temperature on the fuel-to-steam efficiency for five different gaseous fuels (Coerper, 1995). This efficiency is a measure of the boiler heat output as a percentage of the total heat input (Utracki, 1986), and is commonly called the boiler efficiency (Equation 5-2). Figure 5-4 shows that as the flue gas temperature decreases, the efficiency increases. This is because as more of the energy is transferred to the steam, the flue gas temperature will decrease. This figure also shows that the effect of flue gas temperature is fuel specific. Figure 5-4 represents the maximum theoretical efficiency that can be obtained at a given flue gas temperature (Coerper, 1995).

Figure 5-5 shows the efficiency improvement for every 10 °F flue gas temperature reduction at various boiler excess air percentages (KVB, 1977). This figure shows that at high percent excess air, the improvement in efficiency due to lowering the flue gas temperature is greater than at lower excess air percentages. This is because more energy is needed when there is more air to be heated. According to the reference, this curve is valid for estimating efficiency improvements on typical natural gas, #2 through #6 fuel oils, and coal fuels (KVB, 1977).

Figure 5-6 shows the effect of flue gas temperature on boiler efficiency at various excess air percentages (Ottaviano, 1985). Figure 5-6 shows that as the flue gas temperature increases, the efficiency decreases at all excess air percentages. This is because more energy is lost in the stack gases at higher flue gas temperatures. This figure also shows that as excess air is increased at a constant flue gas temperature, the efficiency decreases. The efficiency decreases because with more excess air more energy must be used to heat the air to the flue gas temperature. Figure 5-6 shows that at higher flue gas temperatures it becomes more

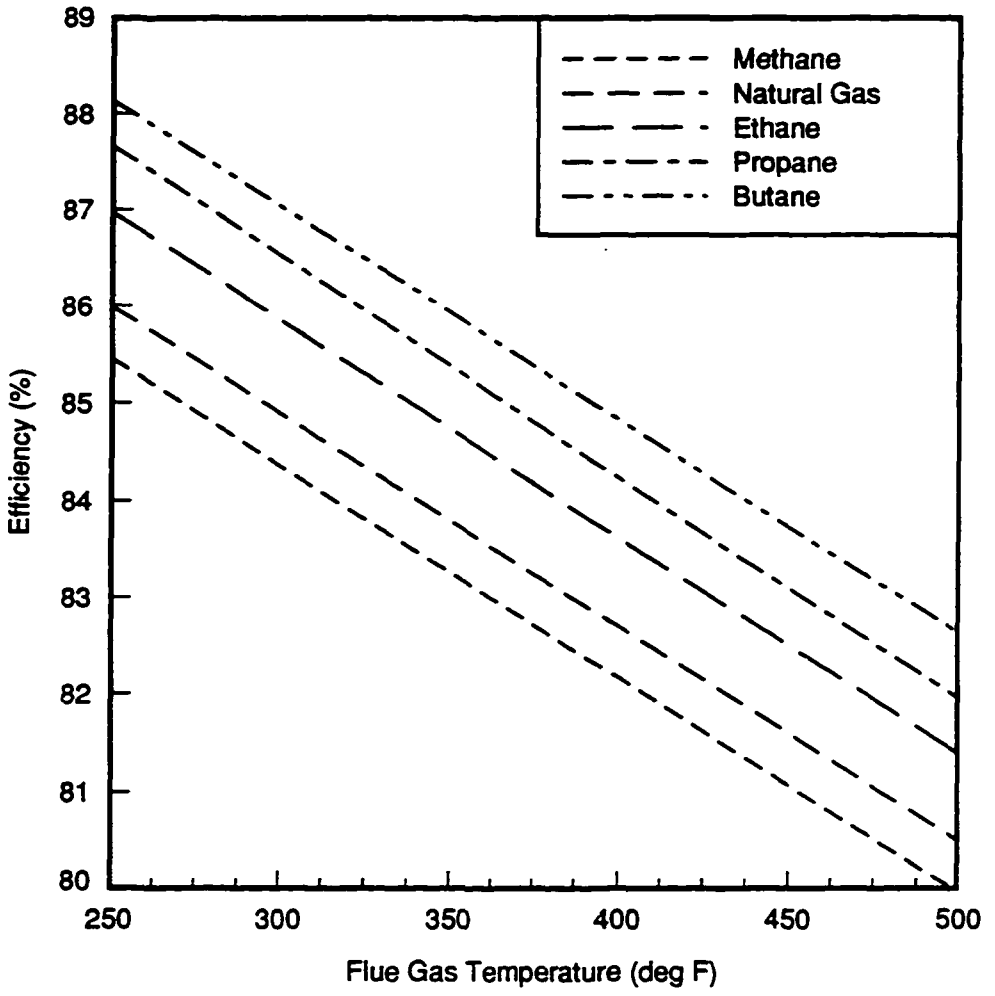

Figure 5-4. Effect of Flue Gas Temperature on Fuel-to-Steam Efficiency (Coerper, 1995, p.66)

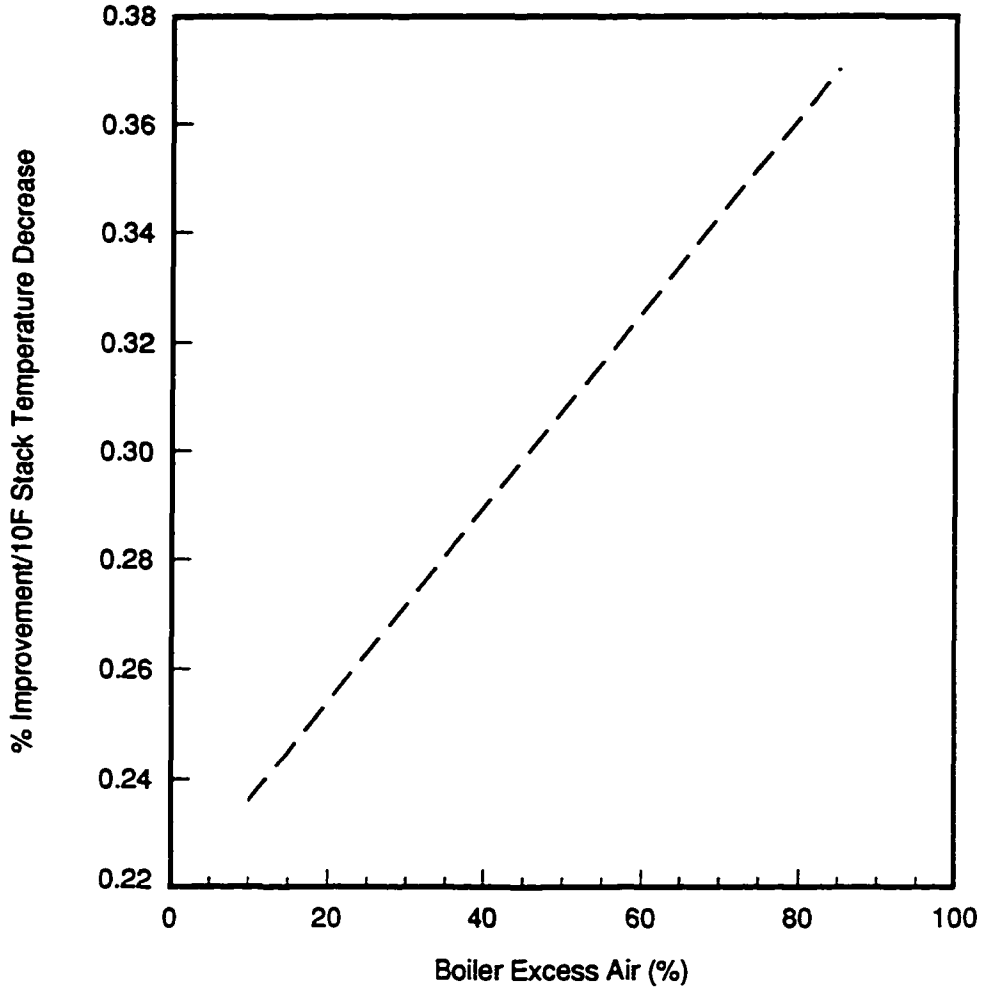

Figure 5-5. Effect of Excess Air on Boiler Efficiency for Every 10 °F Stack Temperature Reduction (KVB, 1977, p.122)

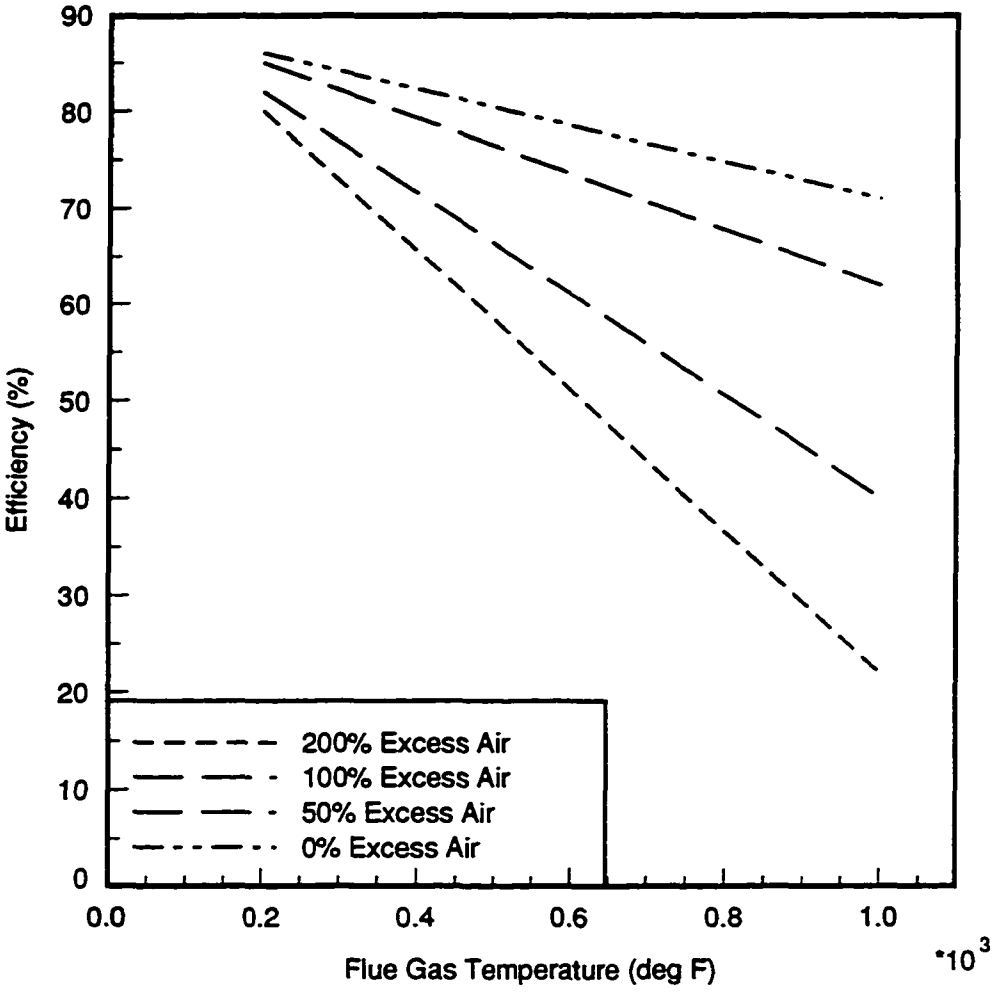

Figure 5-6. Effect of Flue Gas Temperature on Boiler Efficiency at Various Excess Air Percentages (Ottaviano, 1985, p.4.1-39)

important to control excess air (Ottaviano, 1985).

While Figures 5-4, 5-5, and 5-6 all show the effects of flue gas temperatures on boiler efficiencies, there are some differences in these curves. Figure 5-4 looks at five different gaseous fuels, but does not specify the excess air percentage. Figure 5-5 is to be used for estimating the improvements for natural gas, #2 through #6 fuel oil, and coal, at a specific excess air percentage. Figure 5-6 does not specify the fuel, but does specify the excess air in the stack. It is possible to compare the results from Figure 5-5 and Figure 5-6. These graphs do give approximately the same efficiency increases. If it is assumed that Figure 5-6 is for methane, the line labeled 0% excess air is approximately the same as the methane line on Figure 5-4. This means that these two figures also compare favorably.

Figure 5-7 shows the effect of ambient temperature on boiler efficiency (Coerper, 1995). As shown in this figure, efficiency varies approximately 3% over an ambient temperature range of 100 °F. As the ambient temperature rises, the combustion efficiency also increases. For every 20 °F ambient temperature rise, efficiency increases by approximately .5% (Coerper, 1995). This is because at warmer ambient temperatures the radiation losses decrease.

Figure 5-8 shows the effect of ambient temperature on efficiencies at various excess air percentages for methane (Ottaviano, 1985). Figure 5-8 is used for natural gas burning boilers. This figure assumes a flue gas temperature of 300 °F. Figure 5-8 shows that at a given ambient air temperature, below approximately 70 °F, as excess air increases, efficiency decreases. Above 70 °F, at 0% excess air, the efficiency rapidly decreases. The lines of excess air in Figure 5-8 are calculated at 70 °F and 14.7 psi. Therefore, at temperatures above

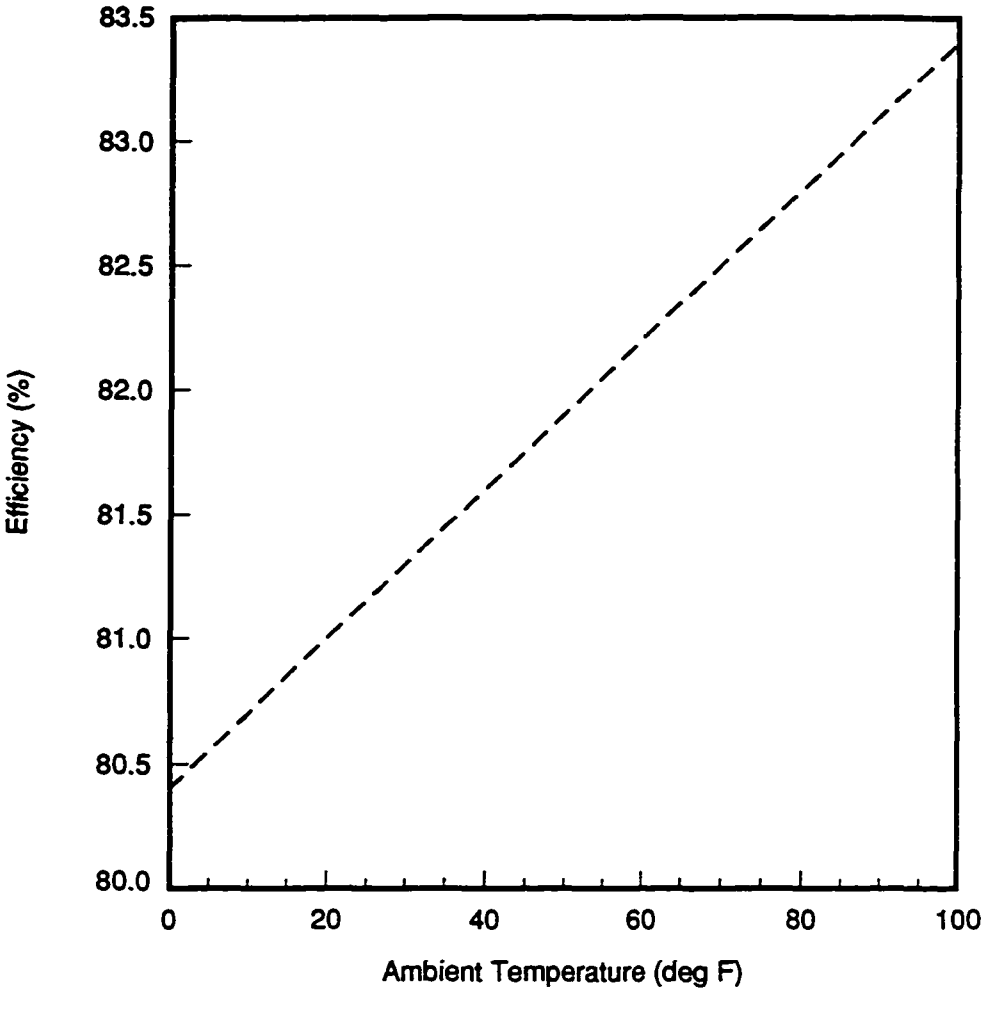

Figure 5-7. Effect of Ambient Temperature on Efficiency (Coerper, 1995, p.68)

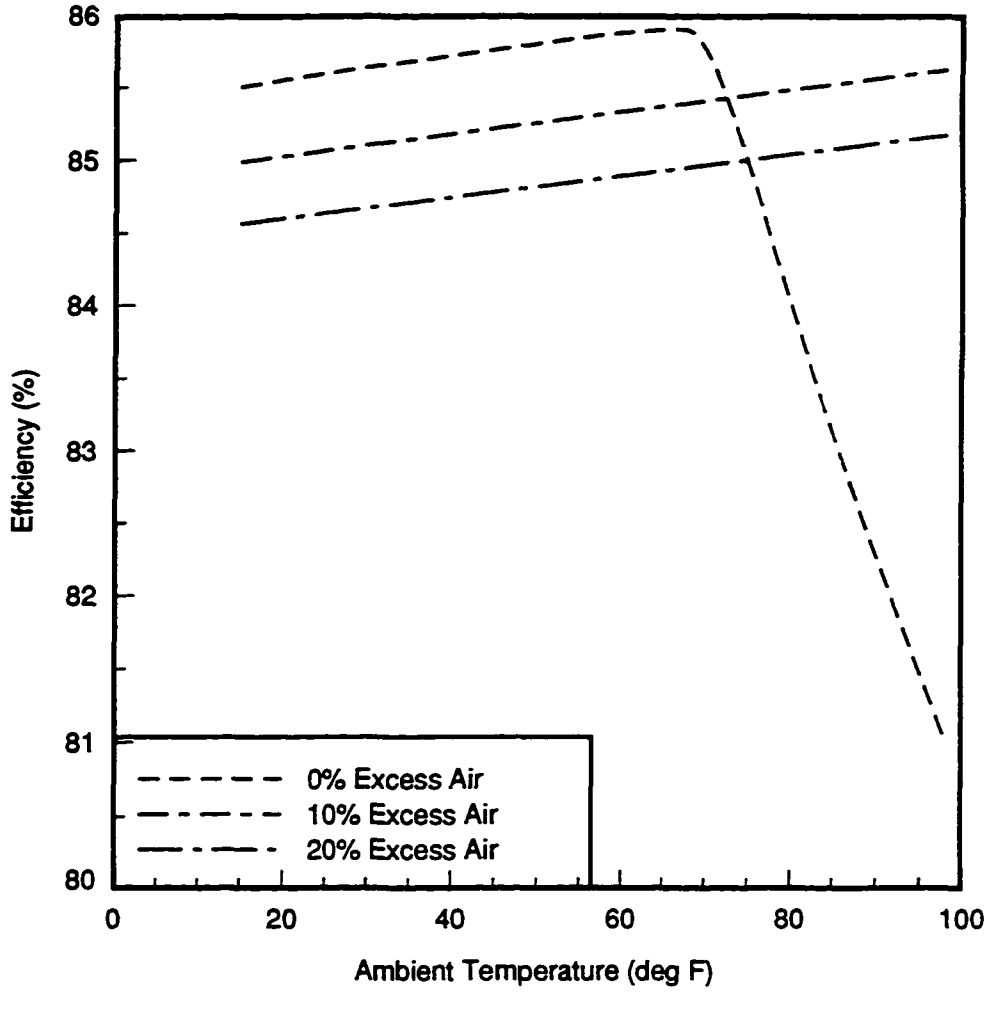

Figure 5-8. Effect of Ambient Temperature on Efficiency at Various Excess Air Percentages for Methane (Ottaviano, 1985, p.4.1-40)

70 °F, the percent excess air is actually less than indicated by the line on Figure 5-8, and the line labeled 0% excess air actually indicates deficient air. This figure provides a warning that if a boiler is tuned to 0% excess air at some ambient conditions, and these conditions change, the result can be insufficient combustion air and a decreased efficiency.

While Figures 5-7 and 5-8 both show the effects of ambient temperatures on efficiency, there are some differences in the curves. Figure 5-7 does not specify the excess air in the stack gases, while Figure 5-8 does. Figure 5-8 also considers operating with deficient combustion air. The slope of the line in Figure 5-7 is greater. This means that estimates for efficiency improvements from Figure 5-7 will be greater than from Figure 5-8. Figure 5-8 is also for a specific fuel, while the reference for Figure 5-7 does not specify the fuel.

Figure 5-9 shows the relationship between diatomic oxygen in the flue gases and the efficiency (Coerper, 1995). This figure shows that as the oxygen concentration increases, the efficiency of the boiler decreases. This is to be expected, because the excess air must be heated from ambient conditions to the flue gas temperature. If the extra air were not there, the energy used to heat the excess air could be used for creating steam.

Figure 5-10 shows the improvement in efficiency for every 1% excess air reduction at various flue gas temperatures (KVB, 1977). At high stack temperatures, there is a greater potential for improving the efficiency than at lower stack temperatures (Coerper, 1995). This is because the excess air must be heated to the same temperature as the other flue gases. At higher stack temperatures the excess air must be heated to a higher temperature, and more fuel is wasted. This curve is valid for estimating efficiency improvements for boilers using natural gas, #2 through #6 fuel oil, and coal fuels (KVB, 1977).

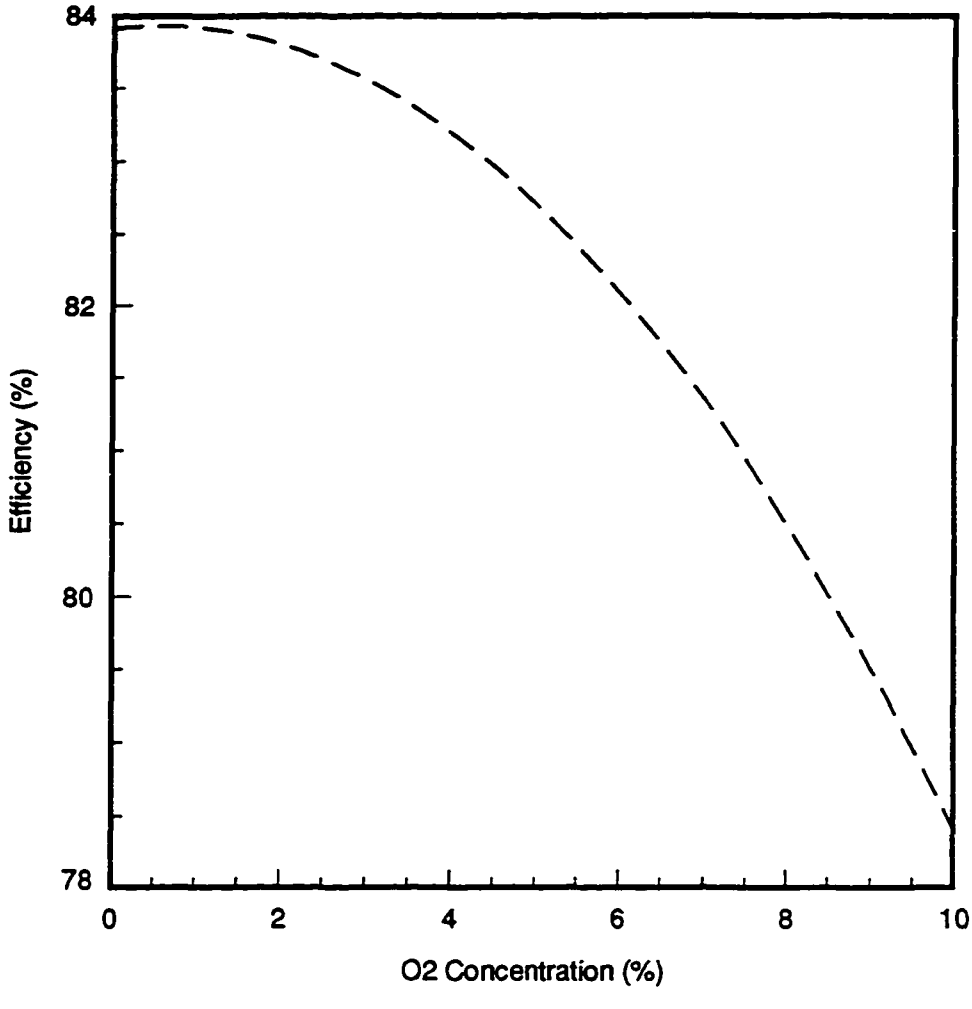

Figure 5-9. Effect of Stack Oxygen on Efficiency
(Coerper, 1995, p.67)

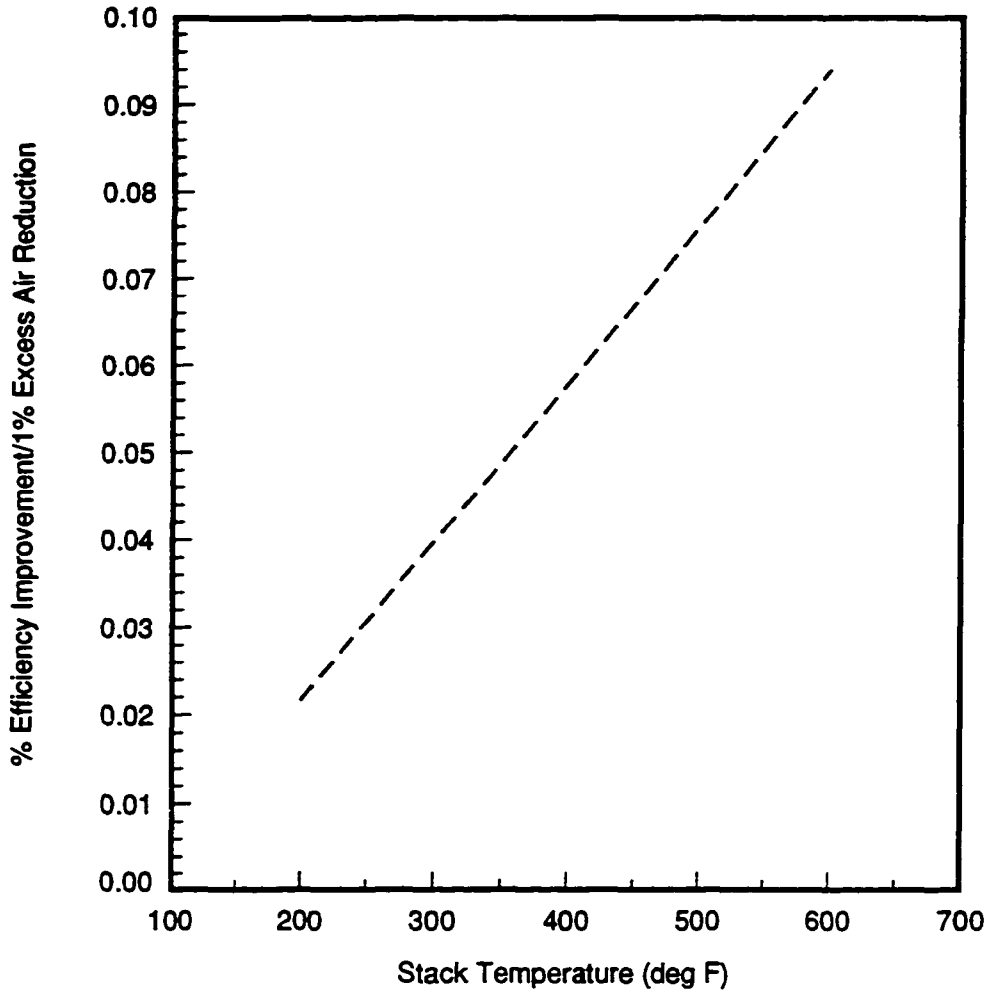

Figure 5-10. Effect of Reducing Excess Air on Efficiency Improvements at Various Stack Temperatures (KVB, 1977, p.122)

Figure 5-11 shows the effect on efficiency of percent of theoretical air for methane, at two flue gas temperatures, 300 °F and 400 °F (Ottaviano, 1985). The combustion air is assumed to be at 14.7 psia. Figure 5-11 is used for natural gas burning boilers. This figure shows that the efficiency is lower at higher flue gas temperatures, and that efficiency increases from approximately 55% to 100% theoretical air, and then decreases. Figure 5-11 shows that the drop in efficiency is more pronounced when the boiler is operated at deficient, as opposed to excess air. This is because the losses due to incomplete combustion are greater than losses due to the sensible energy in the flue gases (Ottaviano, 1985). The decrease in efficiency with higher flue gas temperatures is also to be expected, because at higher stack temperatures, more of the energy that could have been used to make steam is lost up the stack.

Even though Figure 5-9, Figure 5-10, and Figure 5-11 all relate to excess combustion air, there are some differences in these curves. Figure 5-9 looks at excess air in terms of the oxygen content of the stack gases, and only specifies the O_2 concentration. Figure 5-10 looks at the percent efficiency improvement per 1% excess air reduction at various stack temperatures. Figure 5-10 is valid for estimating efficiency improvements for boilers using natural gas, #2 through #6 fuel oil, and coal fuels. Figure 5-11 is for methane, considers the effect of flue gas temperatures, and considers the effect of operating without sufficient combustion air. Neither Figure 5-9 nor Figure 5-10 consider this possibility. These differences make it difficult to compare the three figures.

Table 5-1 shows the savings for every $100 in fuel costs by increasing the combustion efficiency. This reference defines combustion efficiency as a measure of how much of the energy that is liberated during combustion is transferred to the water. This is the definition of

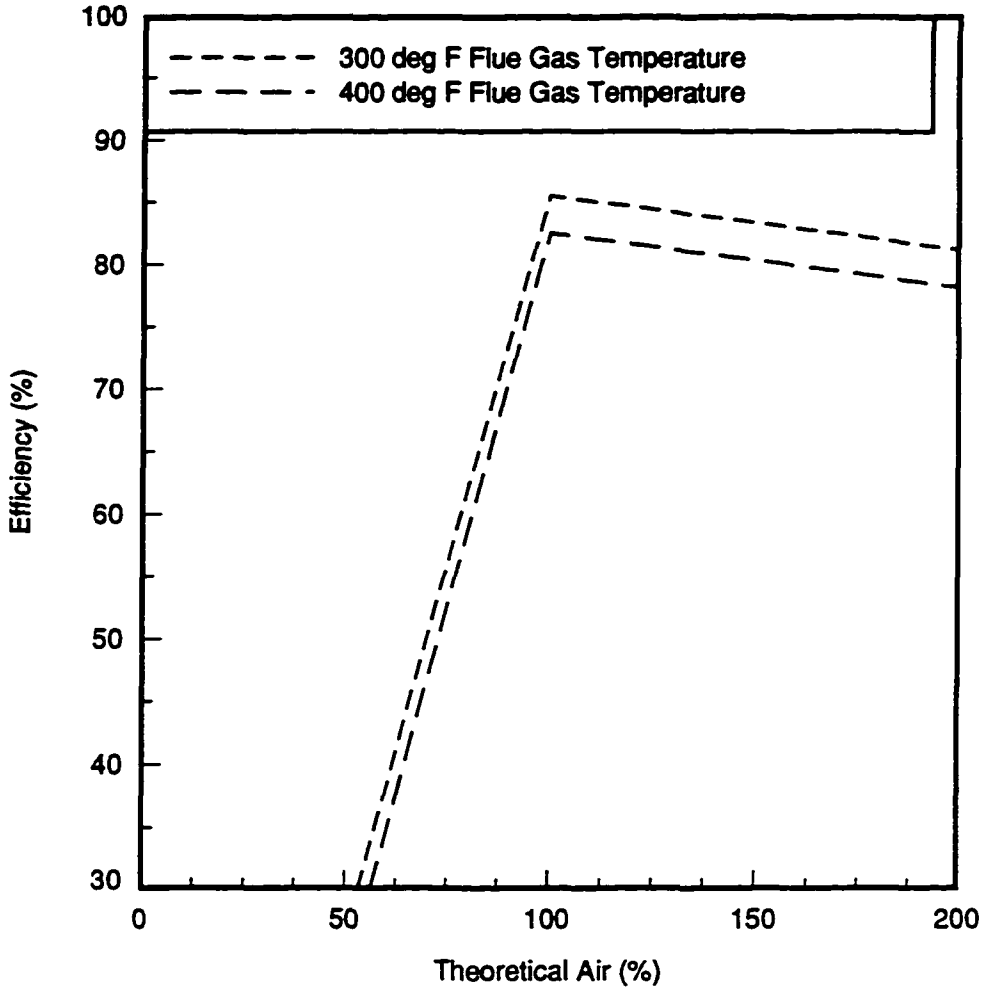

Figure 5-11. Effect of Excess Air on Efficiency at a Given Flue Gas Temperature for Methane (Ottaviano, 1985, p.4.1-39)

boiler efficiency, Equation 5-2. This table assumes constant losses (Ottaviano, 1985). If the energy costs and the current efficiency are known, Table 5-1 can be used to estimate the savings achieved by increasing the combustion efficiency. The current efficiency is located on the vertical axis. The proposed efficiency is located on the horizontal axis. Where the two intersect, the savings are found.

Table 5-1. Savings for Every $100 in Fuel Costs Due to Increased Combustion Efficiency (Ottaviano, 1985, p.4.1-1)

	To:								
From:	55%	60%	65%	70%	75%	80%	85%	90%	95%
50%	$9.10	$16.70	$23.10	$28.60	$33.30	$37.50	$41.20	$44.40	$47.40
55%		$8.30	$15.40	$21.50	$26.70	$31.20	$35.30	$38.90	$42.10
60%			$7.70	$14.30	$20.00	$25.00	$29.40	$33.30	$37.80
65%				$7.10	$13.30	$18.80	$23.50	$27.80	$31.60
70%					$6.70	$12.50	$17.60	$22.20	$26.30
75%						$6.30	$11.80	$16.70	$21.10
80%							$5.90	$11.10	$15.80
85%								$5.80	$10.50
90%									$5.30

The energy savings due to an increased boiler efficiency can be calculated according to (Ottaviano, 1985)

$$\text{Savings} = U\left(\frac{\eta_{boiler_{new}} - \eta_{boiler_{old}}}{\eta_{boiler_{new}}}\right) \tag{5-3}$$

where η_{boiler} is the boiler efficiency, old is current, new is proposed, and U is the current fuel usage.

Figure 5-12 shows the annual dollar loss due to a one percent decrease in efficiency at various steam generation rates for different fuel costs: \$2.50/10^6 Btu, \$2.00/10^6 Btu, \$1.50/10^6 Btu, and \$1.00/10^6 Btu (Ottaviano, 1985). As shown in Figure 5-12, the dollar losses increase as the steam generation rate increases. This is to be expected because more energy is needed to generate more steam. If more energy is used at a lower efficiency, more energy will be wasted.

Figure 5-12 and Table 5-1 both show the potential cost saving (or cost increase) due to changes in boiler efficiency. These two estimation techniques look at the savings based upon different information. Table 5-1 estimates the savings for every \$100 in fuel cost. The use of Figure 5-12 requires the knowledge of the steam generation rate, as well as the fuel cost. It is important to note that both table 5-1 and Figure 5-12 assume steady state operation and do not account for cycling losses and other important boiler operating parameters.

Figure 5-13 shows the effect of ambient pressure variations on efficiency at various excess air percentages for methane (Ottaviano, 1985). This figure assumes a constant flue gas temperature of 300 °F and a constant ambient relative humidity. Figure 5-12 has lines of constant excess air which are assumed to be at 14.7 psi. This figure shows that as ambient

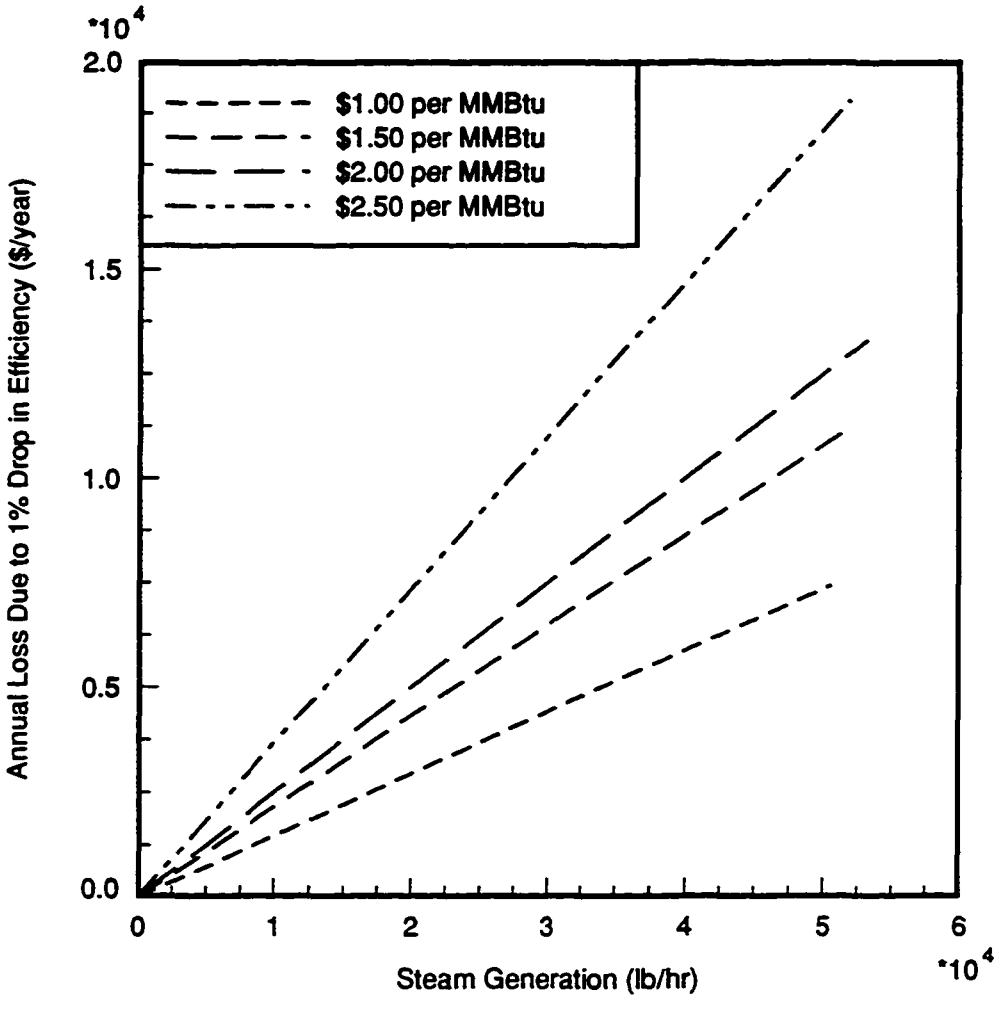

Figure 5-12. Annual Dollar Loss Due to 1% Drop in Efficiency at Various Steam Generation Rates (Ottaviano, 1985, p.4.1-38)

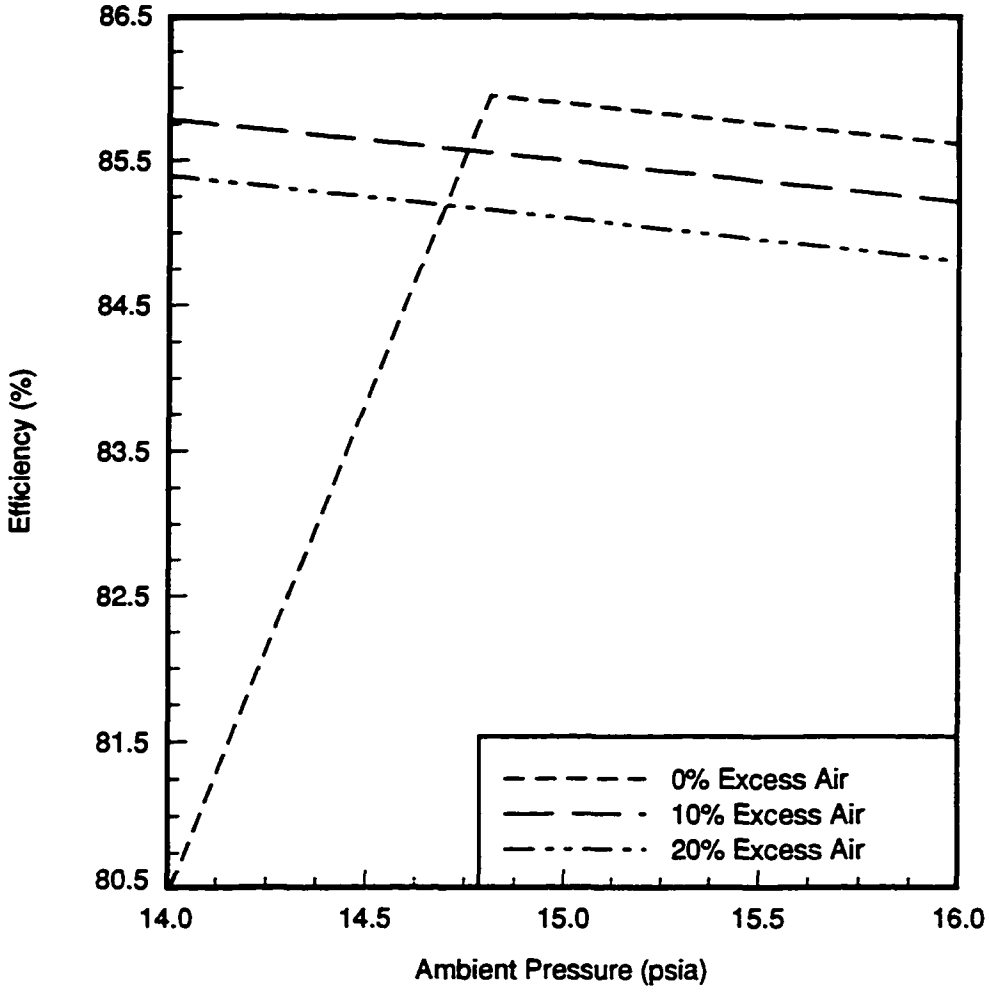

Figure 5-13. Effect of Ambient Pressure on Efficiency at Various Excess Air Percentages for Methane (Ottaviano, 1985, p.4.1-40)

pressure increases, efficiency decreases slightly. Below approximately 14.7 psi, the efficiency at 0% excess air decreases rapidly. This is because the excess air percentages were calculated at 14.7 psia, so below that pressure, 0% excess air is actually deficient air. This figure provides the same warning as Figure 5-8. The warning is that if a boiler is tuned to 0% excess air at some ambient conditions, and these conditions change, the result can be insufficient combustion air and a decreased efficiency. This was the only model showing the effect of ambient pressure on efficiency that could be located in the literature.

Figure 5-14 shows the effect of water vapor in the combustion air on efficiency at various excess air percentages for methane. The lines of excess air percentage were calculated at 0% relative humidity. This means that the lines labeled 0%, 10% and 20% excess air are really only 0%, 10% and 20% excess air at 0% relative humidity. As shown on this figure, at 10% and 20% excess air, there is no effect on efficiency, because there is still sufficient combustion air as the relative humidity increases. It is at 0% excess air that the relative humidity of the combustion air has an effect. At 0% excess air, the efficiency decreases with increasing relative humidity. This is because increased moisture causes deficient oxygen operating conditions at 0% excess air. Although relative humidity has a larger effect at 0% excess air, it is still a small effect, decreasing the efficiency less than 2% from 0% relative humidity to 100% relative humidity. This figure provides the same warning as Figures 5-8 and 5-13. The warning is that if a boiler is tuned to 0% excess air at some ambient conditions, and these conditions change, the result can be insufficient combustion air and a decreased efficiency. This was the only model showing the effect of water vapor in the combustion air on efficiency that could be located in the literature.

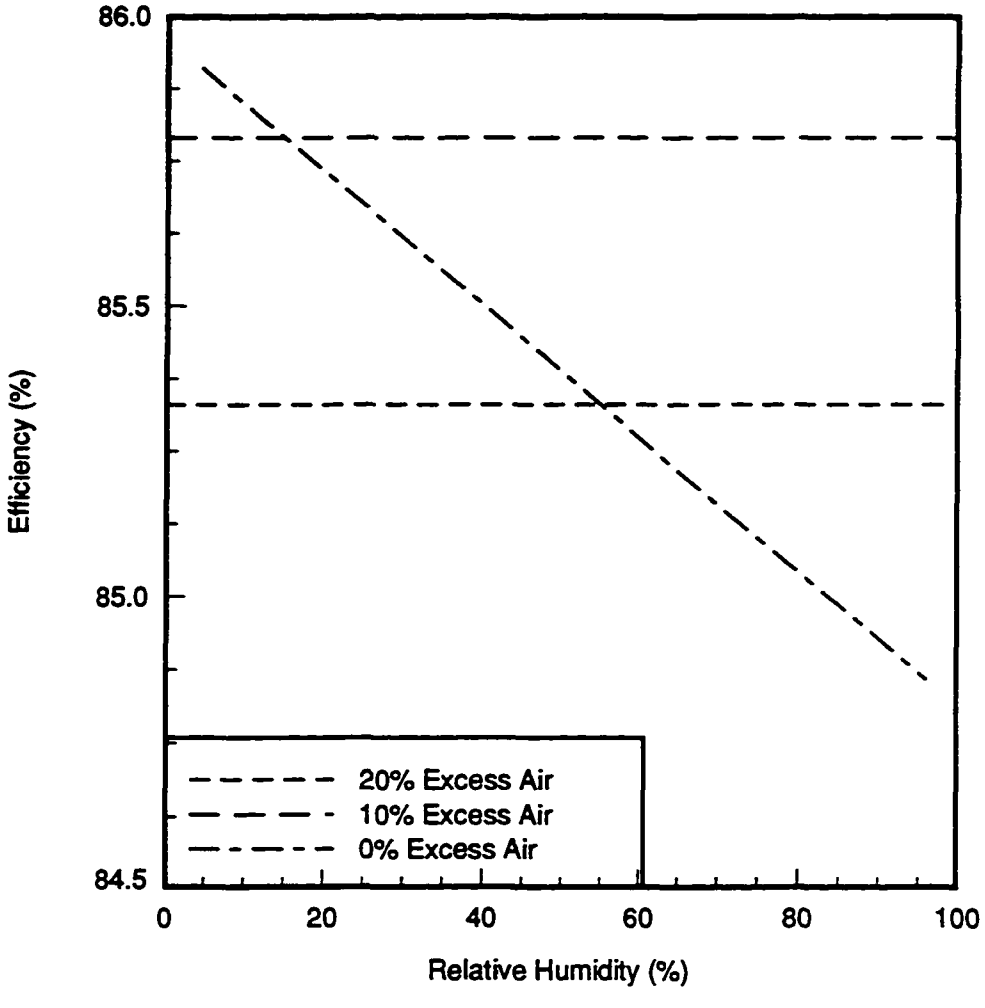

Figure 5-14. Effect of Relative Humidity on Efficiency at Various Excess Air Percentages for Methane (Ottaviano, 1985, p.4.1-41)

Figure 5-15 shows the increase in efficiency due to preheating the boiler feedwater (Ottaviano, 1985). As shown in this figure, as the temperature of the feedwater is increased, so is the boiler efficiency. This is because as the feedwater temperature is increased, the amount of energy needed to increase the temperature and boil the water decreases. As shown in Figure 5-15, efficiency can be increased by more than 10% by preheating the boiler feedwater. This was the only model showing the effect on efficiency of preheating the boiler feedwater that could be located in the literature.

It appears from the literature review, that significant efficiency improvements can be obtained by preheating the combustion air or boiler feedwater. In addition, efficiency can also be increased by controlling the excess air. The literature also shows that it is important not to operate with insufficient combustion air.

Many of the sources for the table and figures presented in this literature review did not define which efficiency was being evaluated, and none specified how the information was obtained. It cannot be stated with any certainty whether these relationships are based on theory, or on experimental observations. However, because of experimental uncertainty that would be inevitably be present in any data, it is unlikely that the cases presented here come from experimental observations.

None of the models account carefully for how a boiler in a factory is actually used. These models are steady state, and do not account for seasonal effects, firing rate, boiler controls, etc. In addition, no industrial operating data were found in the literature, and the accuracy and validity of the models is in question. Because it is the goal of an energy audit to save money, and in general limited resources are available to implement the energy

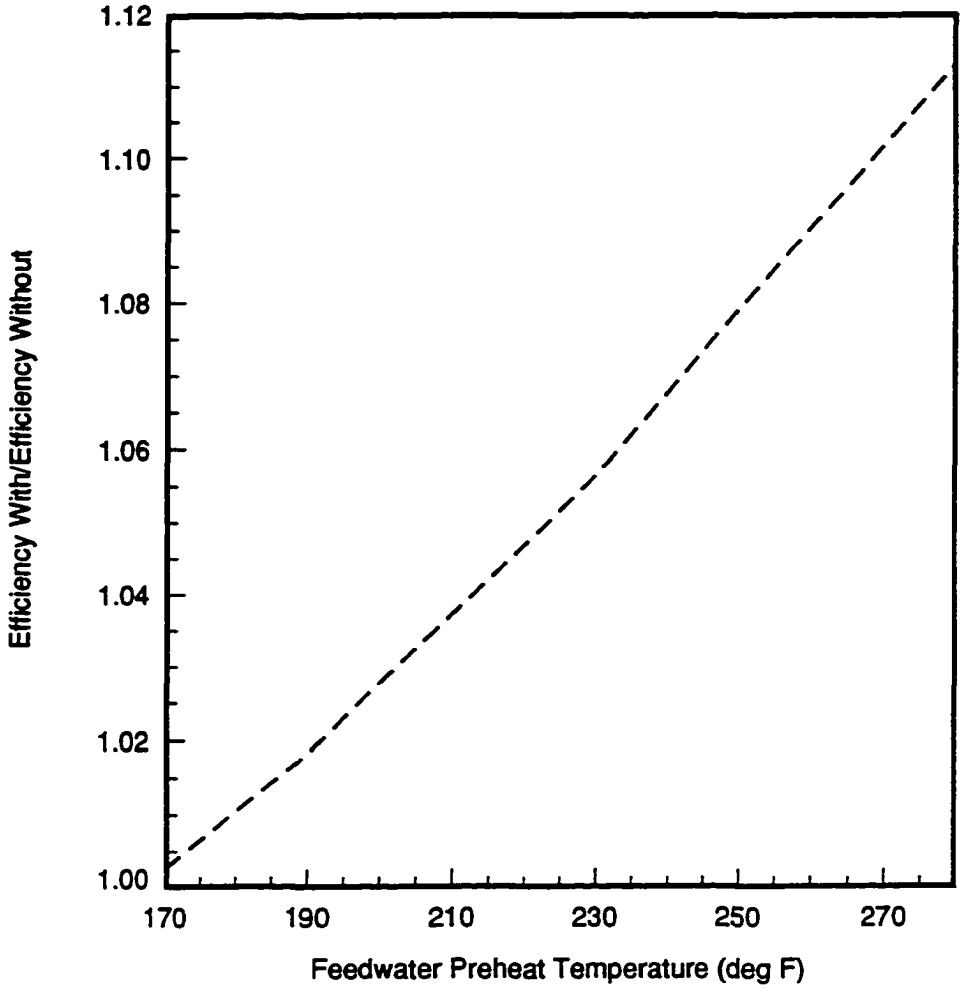

Figure 5-15. Efficiency Improvement Due to Preheating Boiler Feedwater (Ottaviano, 1985, p.4.1-43)

conservation opportunities, it is important that information regarding the accuracy and validity of the models is made available.

Now that the literature pertaining to boilers has been reviewed, the next chapter reviews the specifics relating to the energy conservation opportunities studied. The boiler data collected are also provided in the following chapter. The boiler portion of this study evaluated the equations used to predict the energy savings due to increased combustion efficiency. In addition, the relationships between boiler and combustion efficiencies, boiler efficiency and fuel usage, and steam generation rate and fuel usage were also evaluated.

CHAPTER 6. BOILERS

As mentioned in the literature review, current boiler models do not account for all of the factors that effect a boiler operating in an actual factory. It was also mentioned that no actual operating data were found in the literature. This project tested industrial boilers under actual operating conditions. As a result of this project, more information will be available about how natural gas fueled boilers actually operate in industrial settings.

This section discusses the locations and types of boilers being studied, as well as what was studied on these boilers. This is followed by a section describing the data collection process and the data collected. Then, the equations used to estimate the energy savings due to increased combustion efficiency are studied. In addition, the relationships between boiler and combustion efficiencies, boiler efficiency and fuel usage, and steam generation rate and fuel usage are also studied.

A 350 horsepower firetube boiler at a processed meat factory was studied under this project. The air-fuel ratio on this boiler was adjusted, and the combustion efficiency measured. According to the information reviewed in the literature, higher combustion efficiency should correspond to a lower fuel consumption rate. This boiler has two firing rates; high fire and low fire.

A watertube boiler with modulated firing rates and a capacity of 40,000 lb/hour of steam was studied at an industrial animal laboratory. Modulated firing rates means that the firing rate of the boiler can be changed to closely match the amount of steam that is required. For this boiler, the air supply was also modulated to achieve a specified level of stack oxygen.

This type of boiler fires constantly, but at small steam demand times, the firing rate is very low. Natural gas meters were installed on the boiler. Personnel at this facility agreed to allow the evaluation of the effects of increased combustion efficiency on natural gas usage. In addition, the relationships between combustion efficiency and boiler efficiency, boiler efficiency and natural gas usage, and steam generation rate and fuel usage were also studied using this boiler.

The third boiler studied under this project was a 400 psi superheated vapor watertube boiler at a paper manufacturing facility. This boiler has modulated firing rates and an air preheater, and had been previously instrumented by facility personnel. For this boiler, the air supply remained fixed as the fuel supply was modulated. The previously installed instruments measure: 1) stack temperature, 2) percent oxygen in the stack, 3) combustion air temperature, 4) steam temperature, 5) feedwater flow rate, 6) steam pressure, 7) feedwater temperature, and 8) natural gas used. The relationships between combustion efficiency and natural gas usage, combustion efficiency and boiler efficiency, boiler efficiency and natural gas usage, and steam generation rate and fuel usage were studied using this boiler.

All three boilers studied under this project provide steam for both process and space heating. At the processed meat facility and the paper manufacturing factory, the load is primarily process, with some space heating. At the animal laboratory, the load is primarily space heating, with some process.

The next section of this chapter discusses the operating data collected and the data collection process. This is followed by the study of the effect of combustion efficiency on energy usage. Propagation of error techniques are used to assist in the analysis of the effect of

combustion efficiency on fuel usage. This is followed by the evaluation of the relationships between boiler and combustion efficiencies, boiler efficiency and fuel usage, and steam generation rate and fuel usage.

Boiler Data

This section contains the operating data collected on the three boilers studied under this project. The equipment used to collect this data is described. These data will be analyzed in the following sections.

Data were obtained on a 350 horsepower firetube boiler. Combustion data were obtained using a Bacharach Fyrite II combustion analyzer. This analyzer was factory calibrated and compared against two other units to confirm proper operation. Table 6-1 shows the data obtained with this meter. As shown in Table 6-1, as percent oxygen decreases, percent carbon dioxide increases. This is as expected.

Table 6-1 shows additional data which were obtained for this boiler. The inlet air velocity and inlet air temperature were measured using an Omega portable air velocity kit which also measures temperature. With these measurements, it was only possible to estimate the inlet air flow, because the inlet was not ducted. Flue gas flow rates were measured using a pitot tube. This measurement was obtained at the approximate center of the duct, and then multiplied by .9, as instructed by the manufacturer, to obtain the average velocity. A strip chart recorder at the facility was used to record the steam flow rate, and natural gas usage

Table 6-1. Combustion Data on 350 hp Firetube Boiler

Combustion Efficiency (%)	O_2 (%)	CO_2 (%)	Stack Temperature (°R)	Stack Loss (%)	Excess Air (%)	Inlet Temperature (°R)	Inlet Air Flow Rate (ft^3/s)	Natural Gas Flow Rate (ft^3/s)	Flue Gas Flow Rate (ft^3/s)	Steam Generated (10^3 lb/hr)
81.3	10.7	5.7	748	18.7	93	534	19.49	2.22	2368	5.0
83.6	6.7	8.0	769	16.4	41	536	14.62	1.61	1444	5.0
84.4	5.8	8.5	753	15.6	34	536	13.78	1.75	1675	3.5
84.5	5.8	8.5	747	15.5	34	534	13.22	1.82	1386	3.0
83.3	7.7	7.4	761	16.7	51	532	19.49	1.92	1733	1.0
84.1	7.5	7.5	743	15.9	49	538	16.70	2.17	1473	1.0

was estimated by timing the natural gas meter at the factory. Unfortunately, the natural gas meter measures all gas used by the facility. In addition, the gas meter was not in the boiler room, so it was impossible to tell what was occurring when the meter was being read. Note that the units of measurement on the steam strip chart recorder were lb/hour, and that the time for 100 ft^3 of natural gas was approximately one minute. The control system for this boiler did not allow the steam generation rate to be controlled during the tests. Fortunately, other boilers were located that have dedicated gas meters.

The second boiler studied has a capacity of 40,000 lb/hour of steam, and is a watertube type boiler. The control system on this boiler is much more sophisticated than on the 350 horsepower firetube boiler. With this boiler, the air-fuel ratio was varied, which resulted in varying combustion efficiencies, at four different nominal steam generation rates: 1) 25% of boiler capacity, 2) 37.5% of boiler capacity, 3) 50% of boiler capacity, and 4) 60% of boiler capacity. The data were collected using a Bacharach combustion analyzer. This analyzer measures all of the data that the Bacharach Fyrite II measures, and also measures sulfur dioxide and nitrous oxides, as well as calculating and outputting the carbon monoxide in the flue gas. Table 6-2 shows the data collected on this boiler at 25% of capacity, Table 6-3 is the data at 37.5% of capacity, Table 6-4 is the data at 50% of capacity, and Table 6-5 is the data at 60% of capacity. The sulfur dioxide ppm (parts per million) was zero for all the data, so it is not listed.

As shown in Tables 6-2 to 6-5, the natural gas usage does vary slightly, even at a set percent capacity. One reason for this is that there is actually a slight variation in the steam generation rate even though the percent capacity is controlled.

Table 6-2. Data Collected on 40,000 lb/hour Watertube Boiler at 25% of Capacity

Stack Temperature .(°R)	O_2 (%)	Combustion Efficiency (%)	NO_x (ppm)	CO (ppm)	Excess Air (%)	Loss (%)	CO_2 (%)	Natural Gas (scfm)
786	4.6	83.1	104	0	24	16.9	9.3	373
797	4.3	83.3	114	0	23	16.7	9.3	404
792	4.0	83.4	111	0	21	16.6	9.5	337
794	2.9	84.2	114	0	14	15.8	10.2	378
794	2.6	84.5	69	0	12	15.5	10.3	351
797	3.0	84.7	114	0	14	15.3	10.1	346

Table 6-3. Data Collected on 40,000 lb/hour Watertube Boiler at 37.5% of Capacity

Stack Temperature (°R)	O_2 (%)	Combustion Efficiency (%)	NO_x (ppm)	CO (ppm)	Excess Air (%)	Loss (%)	CO_2 (%)	Natural Gas (scfm)
815	5.1	84.1	92	0	28	15.9	8.9	452
813	4.7	84.3	92	0	25	15.7	9.1	440
805	2.3	84.3	120	0	11	15.7	10.5	471
810	4.0	84.4	91	0	21	15.6	9.5	463
810	3.3	84.8	110	0	16	15.2	9.9	420

Table 6-4. Data Collected on 40,000 lb/hour Watertube Boiler at 50% of Capacity

Stack Temperature (°R)	O_2 (%)	Combustion Efficiency (%)	NO_x (ppm)	CO (ppm)	Excess Air (%)	Loss (%)	CO_2 (%)	Natural Gas (scfm)
825	4.6	83.0	95	0	25	17.0	9.2	553
822	3.5	83.4	110	1	18	16.6	9.8	491
820	2.9	83.8	113	0	13	16.3	10.2	490
819	4.2	83.9	95	0	23	16.1	9.4	531
825	5.3	84	88	0	30	16.0	8.8	521
819	2.3	84.7	115	0	11	15.3	10.5	533

Table 6-5. Data Collected on 40,000 lb/hour Watertube Boiler at 60% of Capacity

Stack Temperature (°R)	O_2 (%)	Combustion Efficiency (%)	NO_x (ppm)	CO (ppm)	Excess Air (%)	Loss (%)	CO_2 (%)	Natural Gas (scfm)
836	3.9	82.5	96	0	21	17.5	9.5	599
839	5.1	83.2	82	0	28	16.8	8.9	595
833	2.8	84.0	107	0	13	16.0	10.2	600
834	4.5	84.0	91	0	24	16.0	9.3	609
827	2.3	84.4	111	1	11	15.6	10.5	592
832	3.3	85.8	101	0	16	14.2	10.0	598

The third boiler studied under this project was located at a paper product manufacturing facility. At this facility, boiler data are collected automatically during every shift on a 400 psi superheated watertube boiler. These values are then averaged into daily boiler data. Appendix F contains the daily boiler data collected. All of the values in Appendix F are average daily values, except for the natural gas usage and feedwater flow rate, which are totals for the day.

To aid in the analysis of the 400 psi superheated boiler a routine was written that utilizes the computer program Interactive Thermodynamics to calculate the air-fuel ratio and combustion efficiency at all of the data points, given the inlet combustion air temperature, the amount of oxygen in the flue gases, and the flue gas temperature. In addition, this routine calculates the amount of energy liberated during the combustion process, the amount of energy absorbed during the water to steam transformation, and the boiler efficiency, given: the water and natural gas flow rates, the steam temperature and pressure, and the feedwater temperature. These calculations assume that natural gas is pure methane, with a higher heating value of 383,030 Btu/lb_m (Moran, 1995), complete combustion occurs, the fuel enters at 530 °R, and that no additional power is needed by pumps, fans, etc. A copy of this routine is included in Appendix G.

The next section investigates the relationship between combustion efficiency and fuel usage. The data described above are used in the analysis of this presumed effect. This section is followed by the analysis of the relationship between boiler and combustion efficiencies, boiler efficiency and fuel usage, and steam generation rate and fuel usage.

Effect of Combustion Efficiency on Energy Usage

It would be expected that as the combustion efficiency of the boiler increases, the natural gas required by the boiler to produce a given amount of steam decreases. Table 5-1 and Figure 5-12 both imply that as efficiency increases, energy use will decrease. This study investigated the energy savings achieved by properly adjusting the boiler air-fuel ratio, which results in an increased combustion efficiency, on three different boilers; one firetube and two watertube. Propagation of error techniques were applied to determine the uncertainties on the predicted and experimental energy savings.

The following equation can be used to predict the energy savings achieved by increasing the combustion efficiency

$$ES_{predicted} = U * \left(1 - \frac{\eta_c}{\eta_p} \right) \tag{6-1}$$

where $ES_{predicted}$ is the predicted energy savings, U is the current energy usage, η_c is the current combustion efficiency, and η_p is the proposed combustion efficiency. Equation 6-1 assumes that combustion efficiency is equal to boiler efficiency. Equation 6-1 is of the same form as Equation 5-3 (Ottaviano, 1985).

The energy savings achieved by increasing the combustion efficiency is the difference between the energy usages at the current and proposed efficiencies. To calculate the measured energy savings, subtract the energy used at the higher efficiency from the energy used at the lower efficiency. In equation form

$$ES_{measured} = U - Pr \tag{6-2}$$

Figure 6-1 is a plot of the predicted energy savings versus the measured energy savings achieved by increasing the combustion efficiency on the boiler, at the various capacities studied, for the 350 horsepower firetube boiler and the 40,000 lb/hr watertube boiler. The data from the 400 psi superheated watertube boiler are not included in this figure. For the 350 horsepower firetube boiler, the savings were calculated using the data at 84.5% as the proposed energy usage. The estimated energy savings at 25% of capacity are based on savings if the efficiency were improved to 84.7%. At 37.5% of capacity, the estimated energy savings are based on improving the efficiency to 84.8%. At 50% of capacity, the savings are based on improving the efficiency to 84.7%. At 60% capacity, the savings are based on improving the efficiency to 85.8%. The line in Figure 6-1 represents the situation where the predicted energy savings is equal to the measured energy savings.

As shown in Figure 6-1, Equations 6-1 and 6-2 do not give the same results. Equation 6-1 is normally used on an annual basis. In order to predict the annual energy usage of a boiler, Equation 6-1 would require a steady state efficiency. It is difficult, if not impossible to define a steady state efficiency for a heating loaded boiler or a boiler with heating and process loads.

Another reason that Equations 6-1 and 6-2 do not provide the same results is due to measurement uncertainty. The data used to plot Figure 6-1 are in Appendix H. In addition, Appendix H also contains the uncertainty for the calculated values, ΔES, for each of the methods used to calculate the energy savings. These uncertainties were calculated using the propagation of error method. This method allows uncertainties on measurements to be propagated through the calculation. For the predicted energy savings, Equation 6-1,

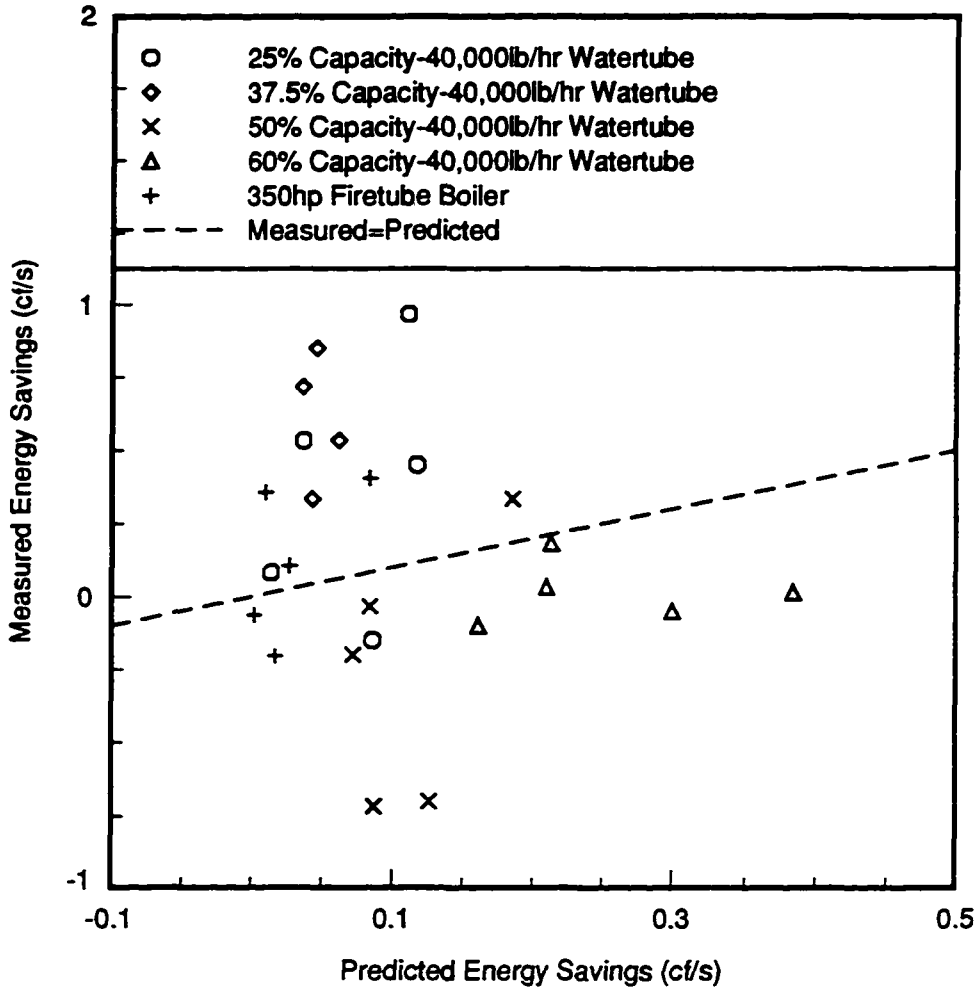

Figure 6-1. Comparison Between Predicted and Actual Energy Savings on Two Studied Boilers

propagation of error gives the following formula

$$\Delta ES_{predicted} = \sqrt{\left(1-\frac{\eta_c}{\eta_p}\right)^2(\Delta U)^2+\left(\frac{U}{\eta_p}\right)^2(\Delta\eta_c)^2+\left(\frac{U\eta_c}{\eta_p^2}\right)^2(\Delta\eta_p)^2} \qquad (6\text{-}3)$$

where $\Delta ES_{predicted}$ is the uncertainty on the predicted energy savings, ΔU is the uncertainty on the measured energy usage, which is assumed to be ± 5 ft^3/s, and $\Delta\eta$ is the uncertainty on the measured combustion efficiency, proposed or current, which is estimated to be $\pm .5\%$.

For the measured energy savings, using propagation of error techniques, the following formula estimates the uncertainty for the measured energy savings

$$\Delta ES_{measured} = \sqrt{(\Delta U)^2+(\Delta Pr)^2} \qquad (6\text{-}4)$$

where ΔPr is the uncertainty on the measurement of the natural gas usage at the proposed efficiency.

As shown in Appendix H, the uncertainties for the quantities calculated using Equation 6-2 are of the same magnitude, or larger than the results calculated using Equation 6-2. The uncertainties for the quantities calculated using Equation 6-1 are approximately of the same magnitude as the values calculated using Equation 6-1. Figure 6-2 graphically demonstrates the errors associated with these calculations. Figure 6-2 contains the same data as Figure 6-1. Note the large errors associated with Equation 6-2. Within the accuracy obtainable, it is impossible to tell if Equations 6-1 and 6-2 give the same results.

Because it was determined that within the accuracy obtainable, it cannot be known if the equation used to predict the energy savings achieved by increasing the combustion efficiency predicts the energy savings, it was decided not to use Equation 6-1 to analyze the 400 psi superheated watertube boiler data. Instead, the combustion efficiency and fuel usage

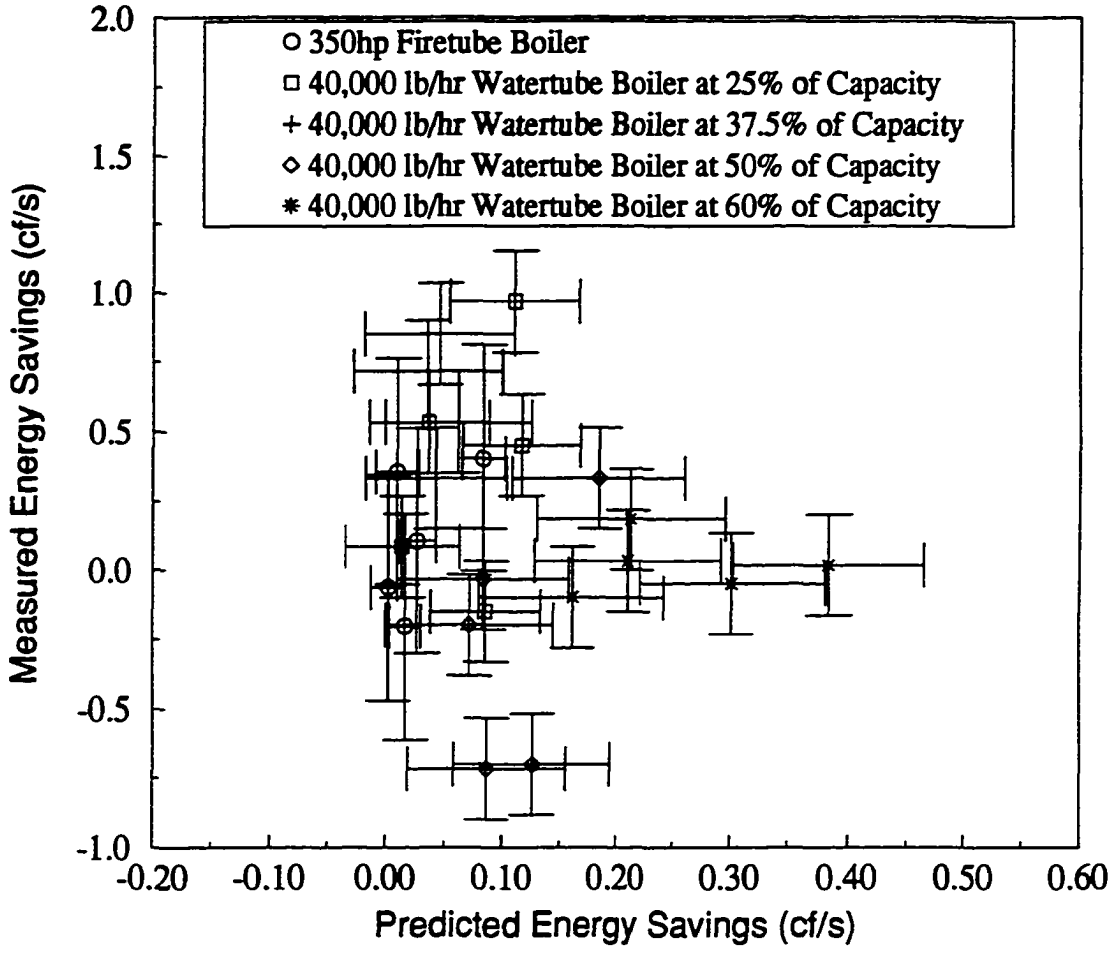

Figure 6-2. Effect of Measurement Errors on Energy Savings Achieved by Increasing Combustion Efficiency

for this boiler are shown in Figure 6-3. Note that the combustion efficiencies for this graph were calculated from the data using the Interactive Thermodynamics routine in Appendix G. As shown in this figure, the combustion efficiency varies less than 3% while the fuel used varies approximately $4x10^5$ scf/day. The data in this figure also show that more than one fuel usage is possible at a given combustion efficiency.

This analysis has shown that combustion efficiency alone cannot be a measure of fuel usage. Due to measurement inaccuracies, it is not possible to know if Equation 6-1 predicts the energy savings due to an increased combustion efficiency. This is an important finding of the present study, since many energy audits base proposed savings on a relationship such as Equation 6-1.

The assumption that boiler efficiency can be approximately by the combustion efficiency was made in Equation 6-1. This assumption will now be examined, by investigating the relationship between boiler efficiency and combustion efficiency.

Comparison Between Boiler Efficiency and Combustion Efficiency

As previously mentioned, it is common practice to approximate boiler efficiency using combustion efficiency. This is because it is easy to measure combustion efficiency. A portable combustion analyzer can be used, and within seconds the combustion efficiency is known. Obtaining the actual boiler efficiency requires more measurements. Some of the instruments required to make the measurements necessary to calculate the boiler efficiency are

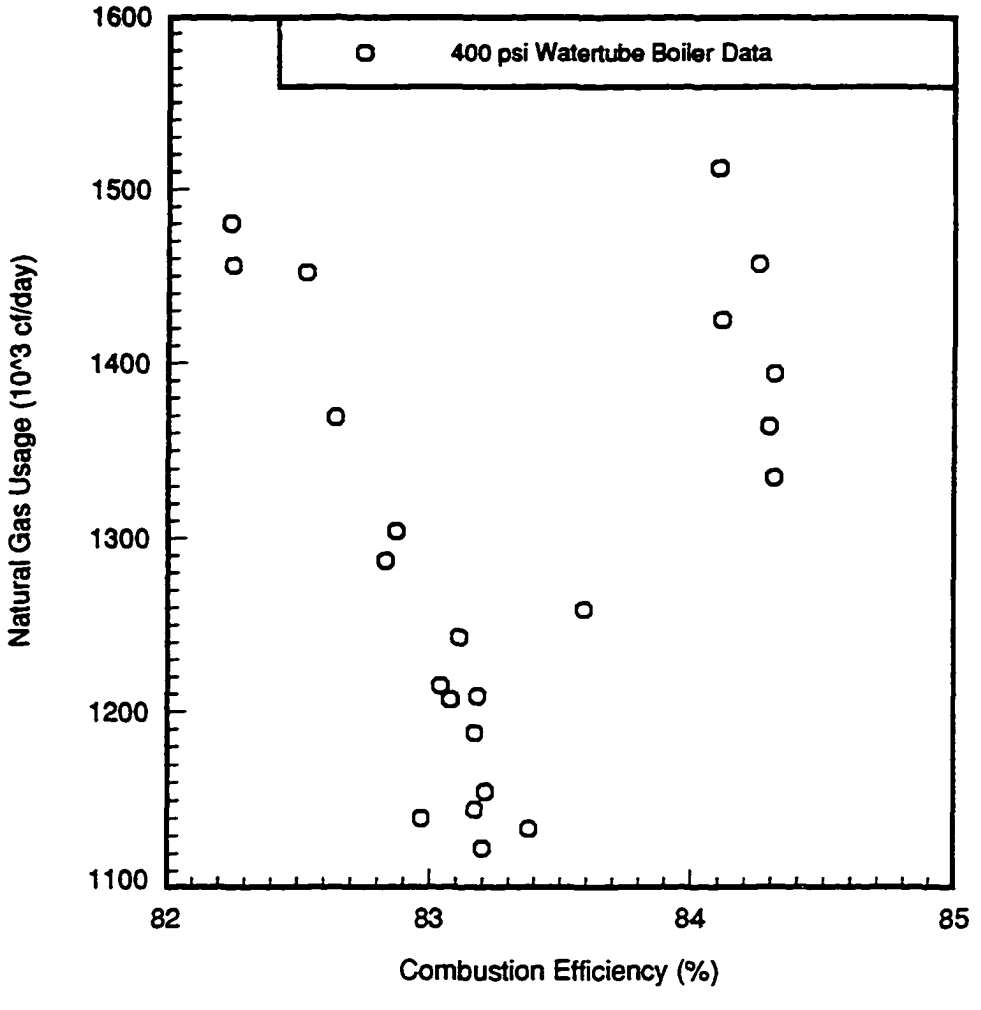

Figure 6-3. Relationship Between Combustion Efficiency and Natural Gas Used by Superheated Watertube Boiler

not commonly installed in industrial facilities.

Figure 6-4 shows the boiler and combustion efficiencies for the 40,000 lb/hr watertube boiler at the percent capacities studied. As shown in this figure, the boiler efficiency varies approximately 25% while the combustion efficiency varies approximately 3%. Figure 6-4 also shows that, for this boiler, as percent capacity increases, boiler efficiency increases. Figure 6-4 shows that more than one boiler efficiency is possible at a given combustion efficiency, and more than one combustion efficiency is possible at a given boiler efficiency.

Figure 6-5 shows the boiler and combustion efficiencies for the 400 psi superheated watertube boiler. The data for this boiler were separated into nominal flow rates. For example, a 7.75×10^5 lb/day nominal flow rate means that the measured flow rate is between 7.50×10^5 and 8.00×10^5 lb/day. Across all nominal flow rates, the boiler efficiency varies approximately 7%, while the combustion efficiency varies less than 3%. It is hypothesized that the smaller variation in boiler efficiency is due to a smaller range of flow rates. Figure 6-5 shows that more than one boiler efficiency is possible at a given combustion efficiency, and more than one combustion efficiency is possible at a given boiler efficiency.

Figures 6-4 and 6-5 show that the combustion efficiency should not be used to approximate the boiler efficiency. It is interesting to note that the 400 psi superheated watertube boiler has a higher boiler efficiency than the 40,000 lb/hr watertube boiler. The boiler efficiency also varies less on the 400 psi superheated watertube boiler. It is hypothesized that this is because the 400 psi boiler is operating near 100% of capacity, while the 40,000 lb/hr watertube boiler is only loaded to 60% of capacity. For a boiler that is primarily heating loaded, the boiler efficiency can vary greatly, especially from winter to

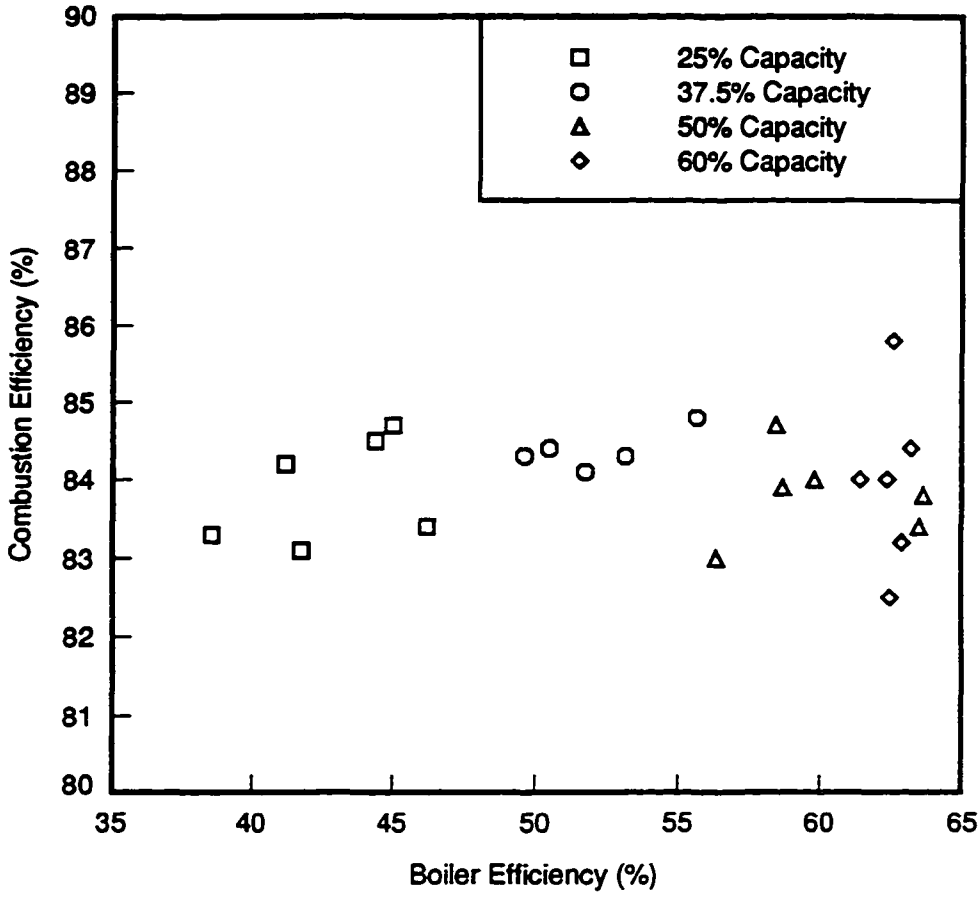

Figure 6-4. Relationship Between Combustion Efficiency and Boiler Efficiency for the 40,000 lb/hr Watertube Boiler

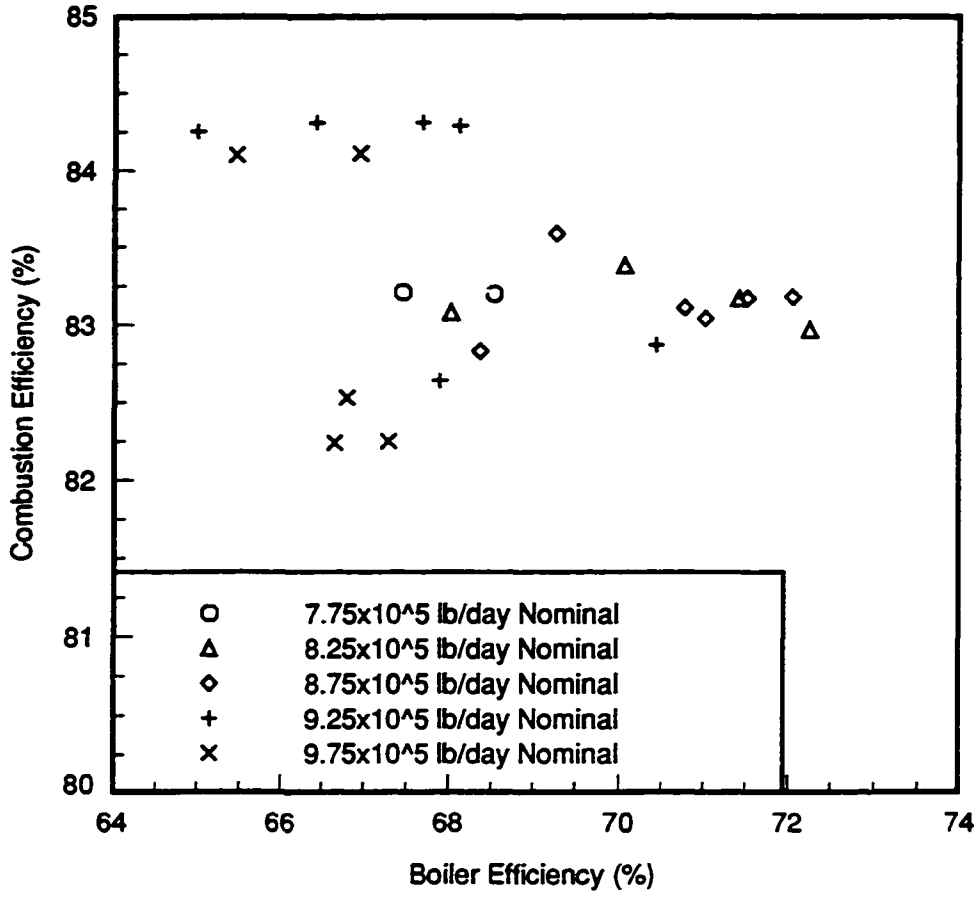

Figure 6-5. Relationship Between Combustion Efficiency and Boiler Efficiency for the 400 psi Superheated Watertube Boiler

summer. A boiler that is primarily process loaded will operate near 100% capacity continuously. As shown in Figure 5-3, it is good practice to operate near 100% capacity.

Efforts should be made to obtain the actual boiler efficiency, not to approximate it using the combustion efficiency. This is because combustion efficiency does not accurately represent the boiler efficiency. Data analyzed so far have shown that inaccuracies preclude determining if increases in combustion efficiency correlate directly with decreased fuel consumption. In addition, it was also shown that for the two watertube boilers studied, great inaccuracies can occur if boiler efficiency is approximated by combustion efficiency. Because the equation used to estimate the savings achieved by increasing the combustion efficiency assumes that the combustion and boiler efficiency are equal, and it has been shown for these two boilers that these efficiencies are not equal, the next step is to determine if increases in boiler efficiency will result in measurable decreased fuel usage.

Relationship Between Boiler Efficiency and Fuel Usage

It has been shown that for the two watertube boilers studied, there is no singular relationship between boiler and combustion efficiency. It has also been shown that due to measurement uncertainty, it is unknown if there is a fuel savings achieved by increasing the combustion efficiency. This section evaluates the hypothesis that an increased boiler efficiency means a decreased fuel usage.

Figure 6-6 shows the relationship between boiler efficiency and fuel usage for the 40,000 lb/hr watertube boiler at the percent capacities studied. As predicted by theory, for this boiler at a given percent capacity, as the boiler efficiency increases, the fuel usage decreases. These data also seem to imply that as percent capacity increases, so does boiler efficiency.

Figure 6-7 shows the relationship between boiler efficiency and natural gas usage for the 400 psi superheated watertube boiler. Also shown on this figure are lines of constant nominal flow rate. These lines were generated by a least squares curve fit to the data in the nominal flow rate range. The equations for the lines, and the coefficients of determination for these lines are in Appendix I. The coefficient of determination is a measure of the difference between the actual value and the value determined by the curve fit. The coefficient of determination varies between zero and one, zero meaning no correlation and one meaning that the actual value and the value from the curve fit are equal. Note that all of the coefficients of determination in Appendix I show strong correlations. The data in Figure 6-7 show that at a given nominal flow rate, as boiler efficiency increases, natural gas usage decreases. These data seem to imply that as nominal flow rate increases, boiler efficiency decreases. This appears to be the opposite to what Figure 6-6 showed.

It is hypothesized that it is possible that at a given capacity, the boiler can operate at many different boiler efficiencies. Unfortunately, the variation in boiler efficiency seems to be unpredictable. Nothing that was varied in the data collection process had a systematic effect on this efficiency. It may be that the boiler system is so complicated that there is nothing one can do to systematically increase the boiler efficiency. The question remains, what can be

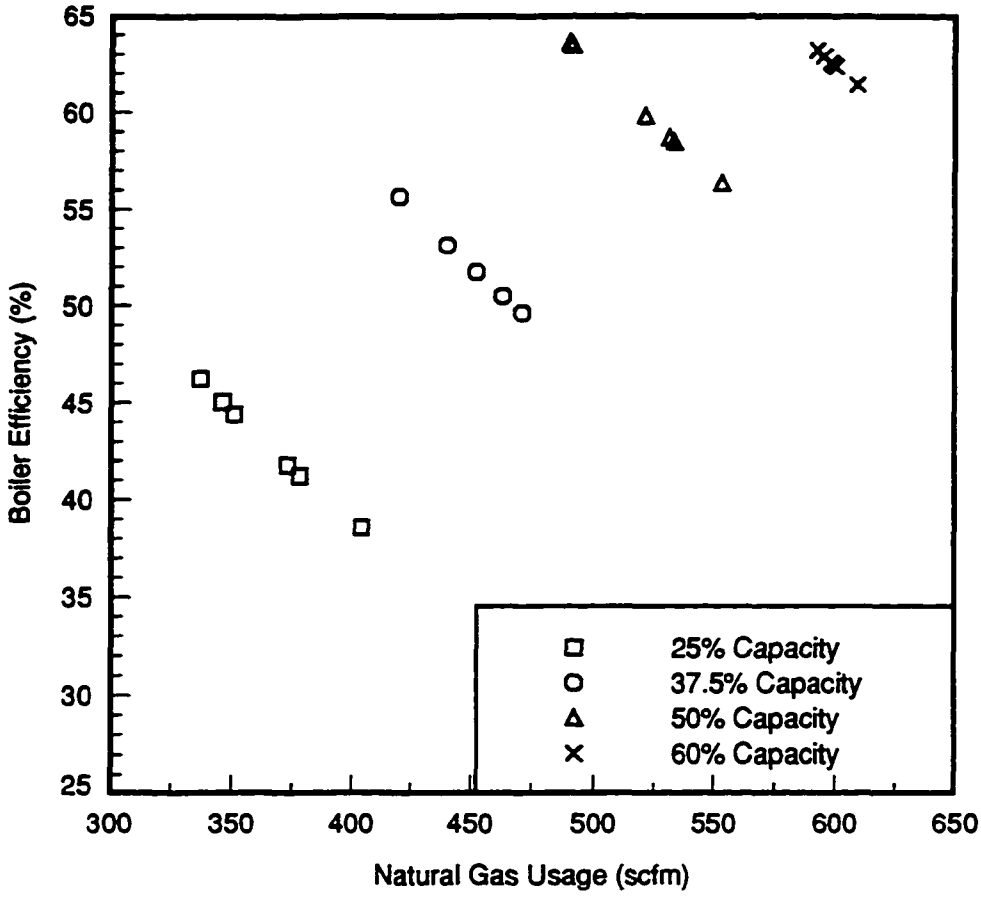

Figure 6-6. Relationship Between Boiler Efficiency and Fuel Usage for the 40,000 lb/hr Watertube Boiler

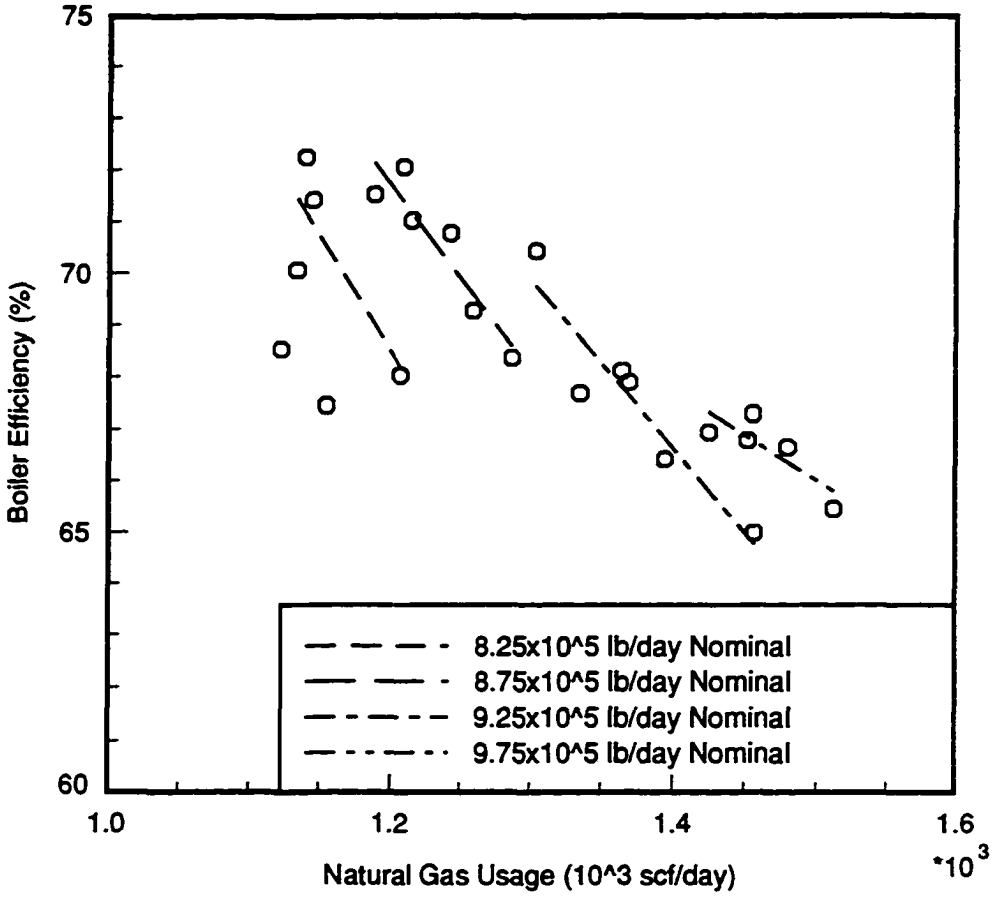

Figure 6-7. Relationship Between Boiler Efficiency and Fuel Usage for the 400 psi Superheated Watertube Boiler

done to save energy in a boiler. One possibility would be to decrease the steam generated. The next step was to confirm the hypothesis that a decreased steam generation rate would result in an energy savings.

Effect of Steam Generation Rate on Energy Usage

It has been shown that at a given percent capacity, an increase in boiler efficiency will result in an energy savings. Unfortunately, no scheme has emerged from the present study to systematically increase this efficiency. Perhaps the best way to decrease the energy used by a boiler is to decrease the steam generated. It is expected that as steam generation rate increases, fuel usage will increase, and conversely. The data previously collected were analyzed to show this relationship.

Figure 6-8 shows the natural gas usage for the 40,000 lb/hour steam capacity watertube boiler at the percent capacities studied. Data for Figure 6-8 are found in Tables 6-2 through 6-5. As expected, as the amount of steam generated increases, so does the amount of natural gas used. Of the variables that could be measured on the 40,000 lb/hour steam capacity boiler, the amount of steam that was generated had the largest effect on natural gas usage.

Figure 6-9 shows the relationship between the feedwater flow rate and the natural gas used by the 400 psi superheated watertube boiler. The feedwater flow rate is approximately equal to the steam generation rate. The data for this figure are in Appendix F. As the

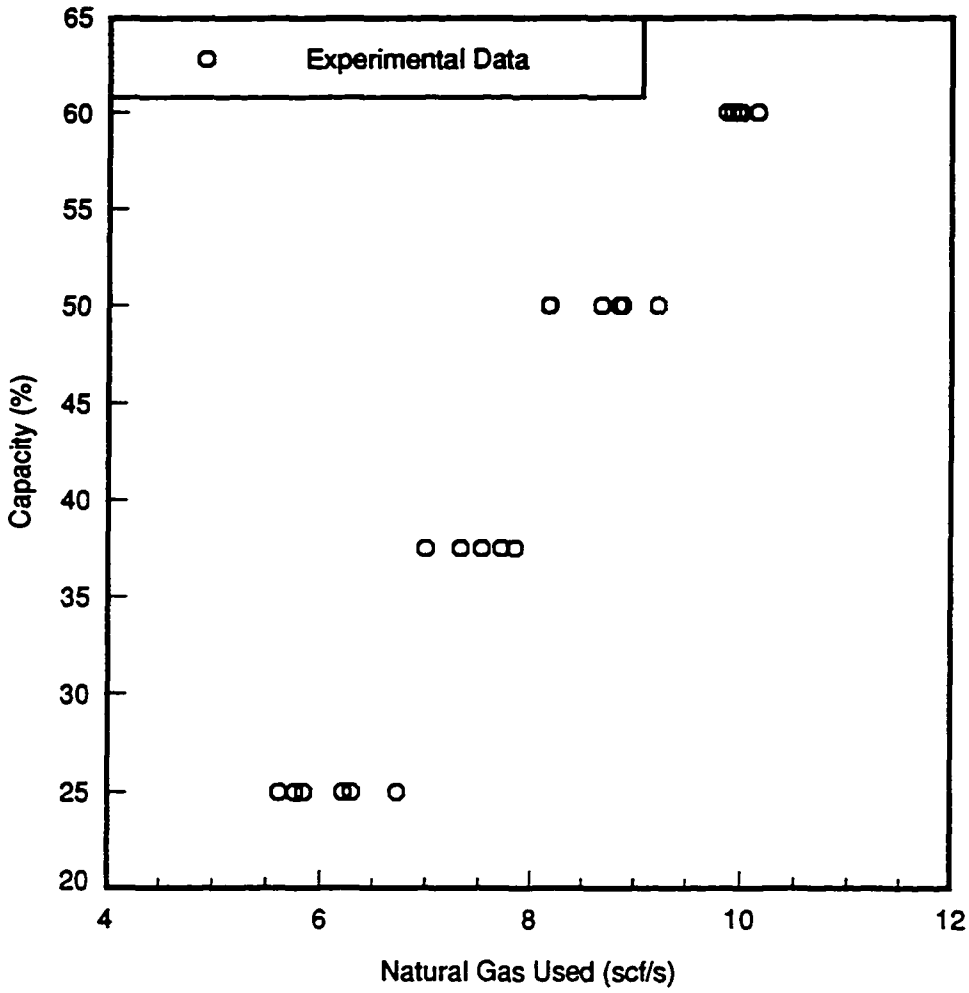

Figure 6-8. Effect of Percent Capacity on Natural Gas Used by 40,000 lb/hour Watertube Boiler

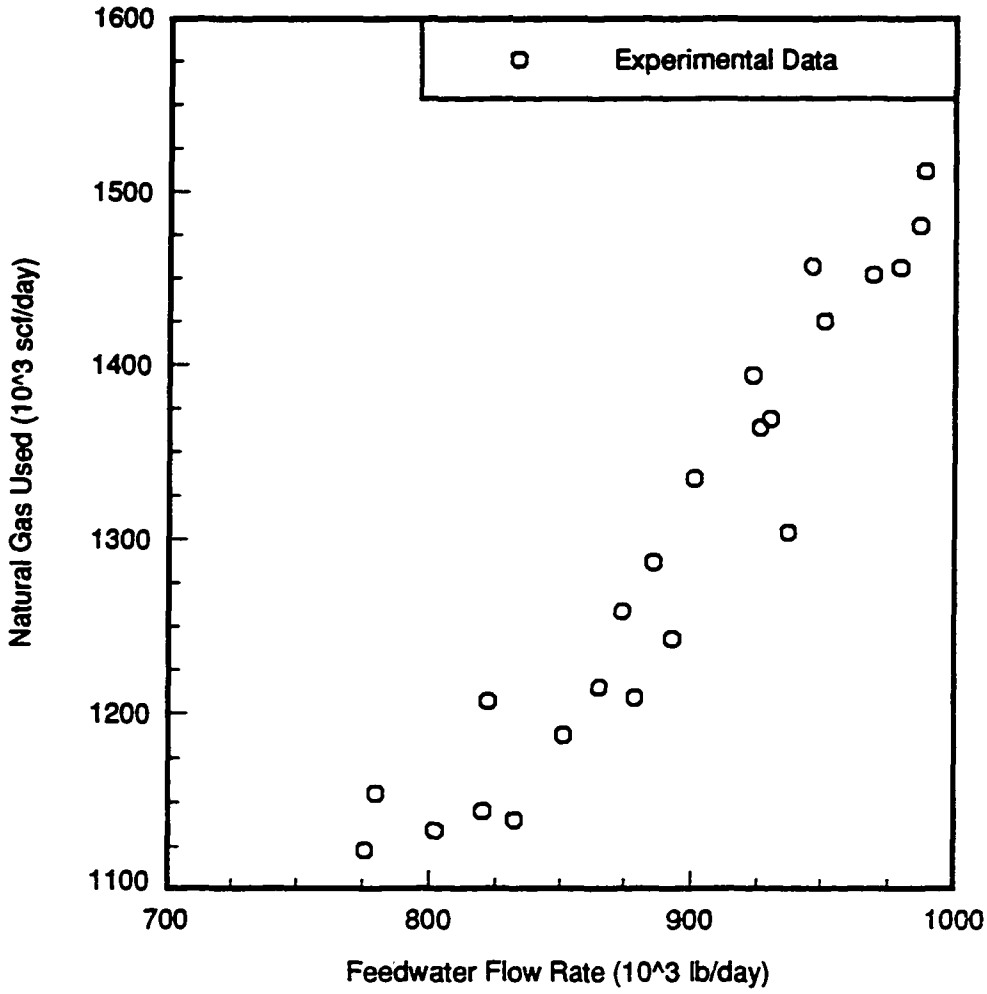

Figure 6-9. Relationship Between Feedwater Flow Rate and Natural Gas Used by Superheated Watertube Boiler

feedwater flow rate is increased, the natural gas usage also increases. This is the same pattern as shown in Figure 6-8 for the 40,000 lb/hr watertube boiler.

It appears that the only certain way to decrease the fuel used by a boiler is to reduce the steam generation rate. While other modifications may decrease the fuel usage, the present study has been unable to confirm a systematic method to assess such effects in actual boiler applications.

Conclusions

Boiler data have been collected at three facilities; a processed meat factory, an animal laboratory, and a paper manufacturing facility. The processed meat factory has a 350 horsepower firetube boiler, the animal laboratory has a watertube boiler with a capacity of 40,000 lb/hour of steam, and the paper manufacturing facility has a 400 psi superheated watertube boiler. Each of the boilers was studied over a range of combustion efficiencies. Theory states that as the combustion efficiency increases, the fuel usage will decrease. The energy savings was predicted using the measured combustion efficiency and energy usage. The experimental energy savings was determined by measuring the fuel usage at different combustion efficiencies. It was determined that for the processed meat factory boiler and for the animal laboratory boiler, these two methods do not give the same results. Therefore, these methods were not applied to the 400 psi superheated watertube boiler.

Part of the reason that these two methods do not give the same results is because of the uncertainty in the measurement process. It was determined that with ordinary data acquisition equipment, it is not possible to measure with enough precision so that the uncertainty on the calculated value is always smaller than the value itself.

In analyzing the data collected on the two watertube boilers, it was determined that it is inaccurate to use combustion efficiency to approximate boiler efficiency, because boiler efficiency varies over a much wider range than combustion efficiency. It is also possible to have the same combustion efficiency at more than one boiler efficiency, and the same boiler efficiency at more than one combustion efficiency.

The data collected on the two watertube boilers also show that at a given steam generation rate, as the boiler efficiency increases, the fuel usage decreases. Unfortunately, it is unknown what caused the boiler efficiency to increase. None of the modifications made to the boiler had any systematic effect on the boiler efficiency. The only change in operating conditions that always had a systematic effect on fuel usage was changing the steam generation rate. It appears that the only method currently known that definitely reduces the fuel usage is to reduce the need for steam at the facility.

All of the boilers located for this study were already operating within suggested ranges. A boiler that is operating with too much or too little air wastes fuel. It is important that a boiler be "tuned" (i.e. operating within suggested ranges). Once the boiler is operating within suggested ranges, like the two watertube boilers with modulating burners, the amount of steam being generated has the largest effect on the natural gas used by these boilers. This study did not investigate the effects of operating with deficient air or extreme amounts of

excess air. It is still hypothesized that either of these operating conditions would waste fuel. The data did seem to imply that it was not worth the effort required to reduce the stack oxygen from 6% to 3%, although it is unknown at this time at what point the effort becomes worthwhile.

In order to assure that a boiler is properly tuned, an O_2 sensor and a stack temperature gauge are required. It is common for boilers to have a steam temperature and/or pressure gauge to assure that the steam being produced is what the process requires. In addition, it is important that the amount of steam being produced can be measured. This is important because the amount of steam being produced has a large effect on fuel usage. Also, the measurement of steam being generated can aid in minimizing steam leaks. As long as the boiler is operating properly, effort should be placed on decreasing the need for steam at the facility.

CHAPTER 7. REDUCING HEATING AND COOLING LOADS

The final portion of this study was to evaluate two systems already installed in facilities. One is a heat recovery system. The other system has the purpose of reducing the cooling load. This section describes the these systems, as well as the facilities in which they are located. The next section discusses the available literature relating to reducing heating and cooling loads.

Waste heat is energy that is released but not utilized within the facility. It is found in fluid steams that are discharged at temperatures differing from ambient conditions. In the warmer months, waste heat streams located inside a cooled space increase the cooling load. In the cooler months, these waste heat streams can be used to reduce space heating loads. At any time of year these streams may also be used to reduce process energy usage, such as to preheat water before it enters a hot water heater. The strategy to use the waste heat depends on the temperature and the type of fluid stream but is ultimately a question of economics. The benefits of utilizing heat recovery technology are a reduction in energy use and in equipment cost and size (Sengupta, 1983).

Opportunities for reducing heating and cooling loads were evaluated by studying systems that had already been installed. The goal was to try to estimate the amount of energy that was saved. These estimates are for specific systems at particular facilities. The particular estimates are not transferable to other systems or facilities. However, the methods used to estimate the savings should be of interest to other researchers.

Personnel at a local facility agreed to allow the study of their heat recovery project. At this site, meat is cooked in one of two natural gas ovens. Heat exchangers have been installed to reclaim some of the energy in the oven exhaust gases and reduce the space heating load. The hot gases from each oven stack pass through an intermediate air to water-glycol mixture heat exchanger, transferring energy to the liquid. The heated water-glycol mixture is then used to warm fresh air which is ducted into the facility. The energy recovered from the exhaust gases reduces the energy required to heat the incoming fresh air.

Personnel at another location agreed to allow the study of their cooling load reduction project. Energy from machinery which is used in the production of socks is ducted outside in the summer to reduce the cooling load. The energy is allowed to enter the facility in the winter.

In addition to the projects described above, space heating loads can be reduced in a facility by utilizing the heat generated when compressors, boilers, or other equipment are operated. Compressor heat recovery was evaluated at two facilities, and was discussed in the chapter on compressors.

The following section discusses the literature available relating to reducing heating and cooling loads. This is followed by two case studies, one reducing heating loads, the other reducing cooling loads. It will be discovered that both of these systems do not save the energy that they should. In both cases, one reason that the systems do not save as much energy as possible is poor system design.

Literature Review

Many books are available that discuss the basics of reducing heating loads by utilizing heat recovery, although the information they provide is basically the same. These books explain the benefits of heat recovery, which include a reduction in energy cost, a reduction in equipment cost and size, and a reduction in energy use (Reiter, 1983). These books also discuss the methods used to recover this energy, such as which type of heat exchanger should be used for a particular type and temperature waste stream (Kiang, 1981). A waste stream is a gas, liquid, or vapor which has energy that can be recovered. Heat recovery equipment provides a means for transferring the waste heat from the source in a form acceptable by the user of the energy (Reiter, 1983). Besides using a heat exchanger, this recovered energy could also be used directly, or the temperature of the stream could be raised by a heat pump, etc. (Sengupta, 1983). These books also explain how to decide where and how to reclaim this energy, and where and how to utilize the energy (Reiter, 1983).

Heat recovery can generally be divided into three types. High temperature heat recovery occurs when the waste stream is at a temperature above 1660 °F. Low temperature heat recovery occurs when the waste stream is at a temperature below 910 °F. Medium temperature heat recovery is when the temperature of the waste stream is between 910 °F and 1660 °F (Goldstick, 1986).

Heat recovery is site-specific. The best method to recover the energy, as well as the best way to use the energy all depend on the distance between the source of the unused

energy and the process that will use this energy, the temperature of waste stream and the process that will use the energy, etc. (Reiter, 1983). These items can all vary from factory to factory or building to building. Therefore, there are not a lot of methods in the literature to estimate the recovered energy. However, there is one "rule of thumb" for heat recovery mentioned in literature that may be of use in an energy audit. In general, each Btu recovered will save about three Btu in fuel (Goldstick, 1986). This is because of losses inherent in any process. For example, if the recovered energy is used to heat a room, the heating load in the room will decrease. This means that the furnace will not have to operate as much. Because the amount of heat the furnace is producing is decreased, the fuel used by the furnace is also decreased. Furnaces are not 100% efficient, so by reducing the amount of fuel used, inefficient fuel use is also decreased.

There do not appear to be any discussions relating to reducing cooling loads by removing space heat in literature. However, reducing heating and cooling loads both use heat exchangers, ducting, fans, etc. Therefore, some of the information related to reducing heating loads will be applicable.

The next section describes the heating load reduction part of this study. A description of the system is included. Data are presented in this section, as well as an analysis of the amount of heat that is recovered. Design suggestions that would have increased the amount of heat recovery are also included. This is followed by the reducing cooling loads case study. Data will also be presented in this section, as well as an analysis of the system. Design suggestions that would have improved the energy savings will also be discussed.

Case Study: Reducing Heating Load Using Energy from Oven Stack

This heating load reduction case study evaluates the waste heat recovered from the oven stacks at a local facility. The ovens are used to cook meat. This section describes the heat recovery system, the data collected, and suggestions that would have increased the amount of recovered energy.

Figure 7-1 shows a schematic of this heat recovery system. The data collected include temperatures and flow rates from each 16 inch diameter oven stack, as well as temperatures and flow rates in the duct leading to the factory. Notice that by the point that the duct measurements were obtained, the air has been affected by the energy recovered from both stacks. The heat exchangers HX1 and HX2 in Figure 7-1 use the stack gases to warm a water-glycol mixture, while HX3 uses the warmed water-glycol mixture to increase the temperature of the air that is brought in from the outside. All three heat exchangers are the counter-flow type.

A this production facility, two ovens are used to cook meat and remove the fat. Each oven has two burners, with each burner having a rating of 2.15 MMBtu/hour. The exhaust gases entering HX1 had a temperature of 570.5 °R, and an average velocity of approximately 2100 feet/minute. The exhaust gases entering HX2 had a temperature of 630 °R and an average velocity of approximately 2200 feet/minute.

Several measurements were made of the temperatures and velocities in the 36 inch by 36 inch duct carrying the heated air to the facility. Due to equipment and space limitations a complete velocity distribution in the duct could not be obtained. Table 7-1 contains the

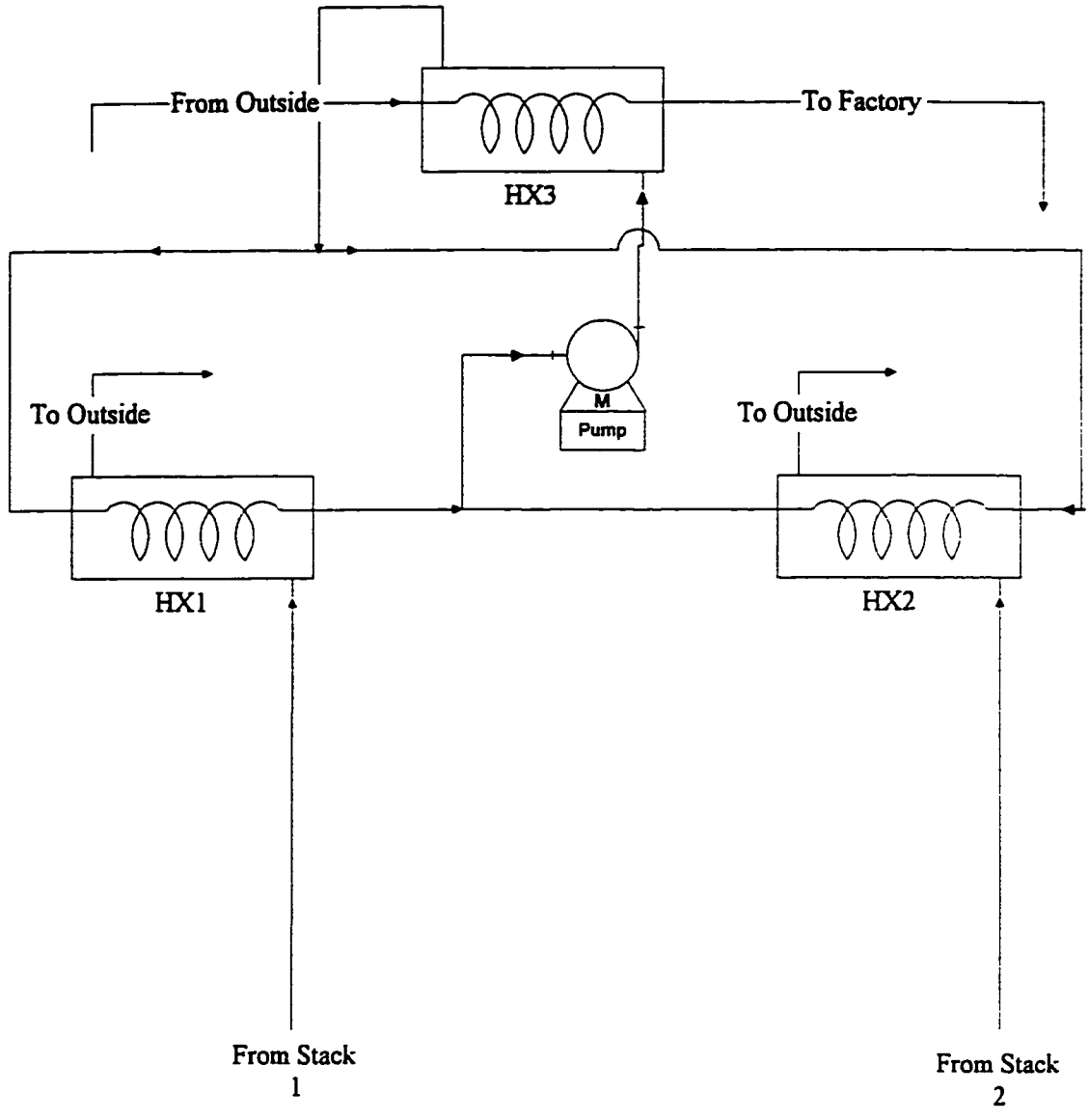

Figure 7-1. Schematic of Heat Recovery System

measured velocities and the locations where these velocities were measured. Figure 7-2 is a graphical representation of these data. The data in Figure 7-2 were curve fitted using the equation $V(x,y) = a_o + a_1x + a_2y + a_3xy + a_4x^2 + a_5y^2 + a_6xy^2 + a_7x^2y + a_8x^2y^2$. This equation was integrated over the area of the duct to obtain the average velocity in the duct. The average velocity in the duct was approximately 1164 feet/minute.

Table 7-1. Values Used to Estimate the Energy Recovered From the Oven Stacks

x(in)	y(in)	V(feet/min)	T(°R)
6	4	600	545
6	16	250	550
6	28	525	555
12	4	700	555
12	16	400	550
12	28	450	557
16	4	1100	559
16	16	1000	557
16	28	900	557
28	4	2300	570
28	16	2100	568
28	28	2150	570

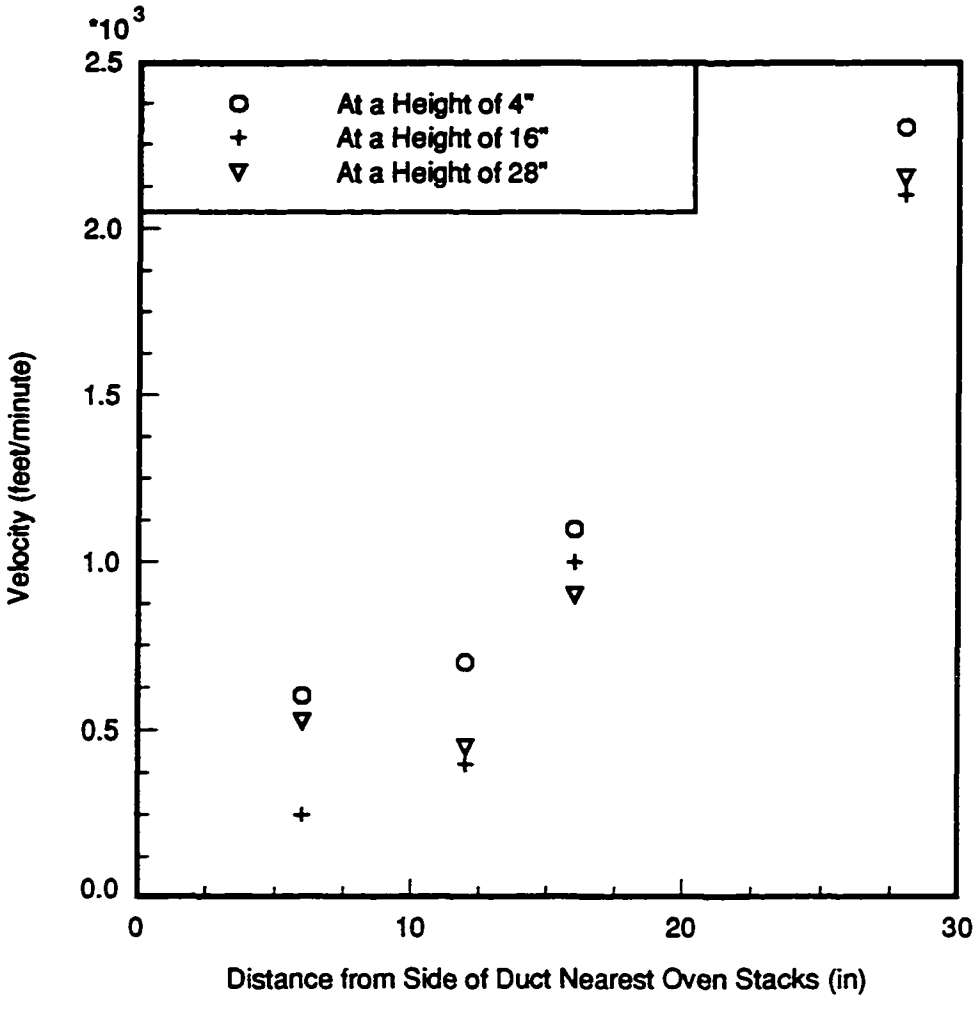

Figure 7-2. Velocity Distribution in 36 Inch by 36 Inch Duct

Table 7-1 also contains the temperatures measured in the duct leading to the facility. Figure 7-3 is a graphical representation of these temperature data. Due to equipment and space limitations a complete temperature distribution in the duct could not be obtained. The average duct temperature must be estimated. A curve fit was obtained for the data in Figure 7-3, using an equation of the form $T(x,y) = a_o + a_1x + a_2y + a_3xy$. This equation was then integrated over the area of the duct, and the average temperature inside the duct was obtained. On the day that the data were taken, the average duct temperature was approximately 553 °R, and the outside temperature was approximately 510 °R.

In order to determine the amount of energy recovered on the day that the data were collected, a mass balance and an energy balance were performed on the warm air side of the duct, resulting in the following equation

$$q = \dot{m} C_p (T_d - T_o) \tag{7-1}$$

where q is the heat transfer rate, $\dot{m} = \rho_d A_d V_d$ is the mass flow rate on the warm air side of the duct, C_p is the specific heat of air, T_o is the absolute outside air temperature, T_d is the absolute temperature of the air in the duct leading to the facility, V_d is the velocity of the air entering the facility, and A_d is the area of the duct.

The density of the air in the duct leading to the factory can be calculated using the ideal gas law (Equation 7-2)

$$\rho_d = \frac{p_d}{T_d \frac{R_u}{M}} \tag{7-2}$$

where p_d is the pressure in the duct.

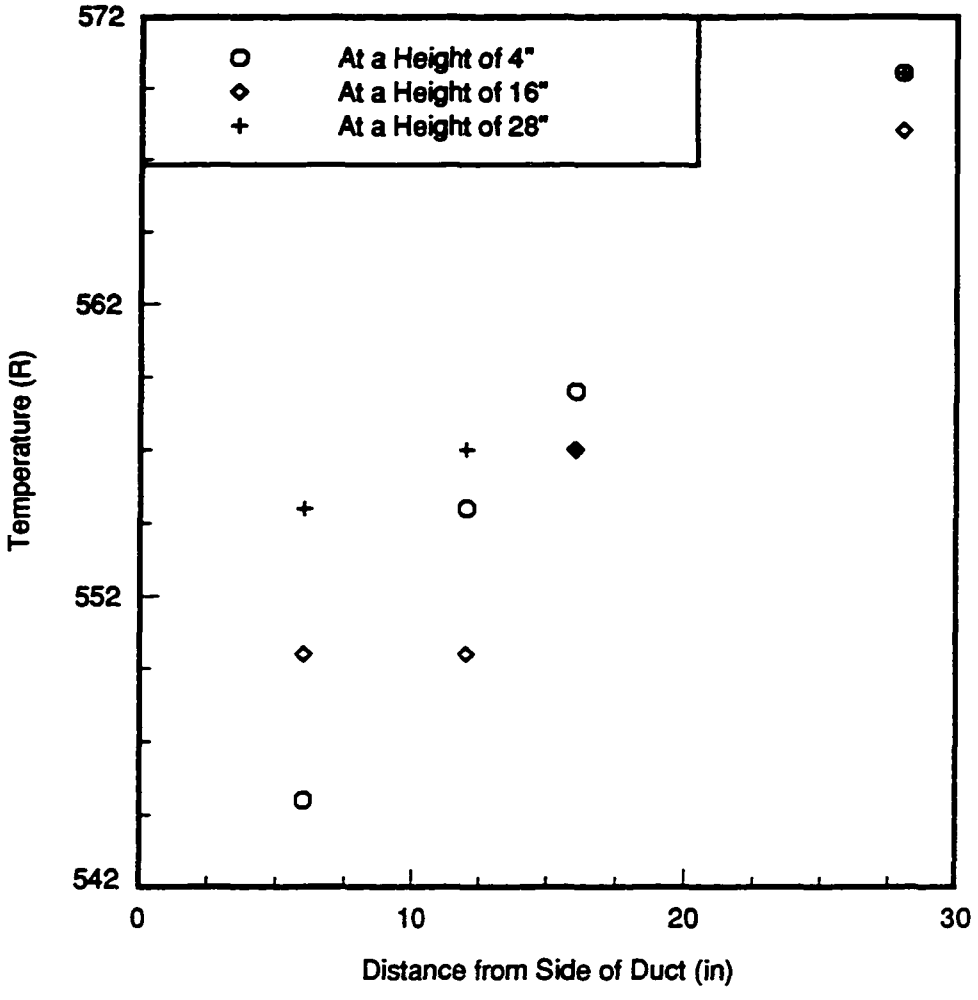

Figure 7-3. Temperature Distribution in 36 Inch by 36 Inch Duct

With these substitutions, the energy balance on the warm air side of the duct reduces to

$$q = \frac{p_d A_d}{T_d \frac{R_u}{M}} C_p V (T_d - T_o) \tag{7-3}$$

The uncertainty on the calculated heat transfer rate can be found from

$$\Delta q = \left\{ \begin{array}{l} \left(\frac{p_d C_p V_d}{\frac{R_u}{M}} \left(1 - \frac{T_o}{T_d} \right) \right)^2 (\Delta A_d)^2 + \left(\frac{V_d C_p A_d}{\frac{R_u}{M}} \left(1 - \frac{T_o}{T_d} \right) \right)^2 (\Delta p_d)^2 + \\ \left(\frac{p_d C_p A_d}{\frac{R_u}{M}} \left(1 - \frac{T_o}{T_d} \right) \right)^2 (\Delta V_d)^2 + \left(\frac{p_d A_d C_p V_d}{\frac{R_u T_d}{M}} \right)^2 (\Delta T_o)^2 + \\ \left(\frac{p_d A_d C_p V_d T_o}{\frac{R_u T_d^2}{M}} \right)^2 (\Delta T_d)^2 \end{array} \right\}^{1/2} \tag{7-4}$$

It was estimated that each linear dimension was known to ±.1 inches. This means that ΔA is .00007 ft^2. It was estimated that the velocity was known to within 5%, or ΔV was 3492 ft/hr. It was also estimated that the duct pressure was measured to ±5%, and that the temperatures were known to ± 5°R.

Table 7-2 contains the data used in Equations 7-3 and 7-4 to estimate the energy recovered from the two oven stacks. Note that the universal gas constant, as well as the specific heat and molecular weight of air were obtained from standard tables (Moran, 1996).

Table 7-2. Values Used in Equations 7-3 and 7-4 to Estimate the Energy Recovered from Oven Stacks

Equation Variable	Value (Units)
p_d	2117 (lb_f/ft^2)
A_d	9 (ft^2)
V_d	1164 (feet/minute)
C_p	.24 (Btu/lb_m-°R)
M	28.97 (lb_m/lb_{mol})
R_u	1545 (ft-lb_f/lb_{mol}-°R)
T_d	553 °R
T_o	510 °R

With the values from Table 7-2, the energy recovered from the two oven stacks is .47 ± .39 MMBtu/hour. Since the total energy used by the two ovens is 8.6 MMBtu/hour, this system recovers about 5.5% of the energy. There are a number of reasons for such a low fraction of energy recovery. One reason is a low effectiveness in the heat exchange design, particularly because there is an intermediate heat exchange loop. The most efficient way to recover this energy would be direct use. Because of the grease from the cooking process in the exhaust gases this is not possible. A heat exchanger system without the intermediate loop would have a higher effectiveness than this system. Another reason for the low fraction of energy recovery was fouling of the heat exchanger due to grease from the cooking process.

If it is assumed that the effectiveness of the heat exchangers is approximately constant, then difference between the duct temperature and the outside temperature should also be approximately constant. This means that it is possible to estimate the total energy recovered in a heating season by multiplying the value obtained on this one day by the number of hours during the heating season. In order to estimate the energy recovered in a heating season by this system, it is necessary to know how many hours the ovens are in operation during the heating season. Based upon the number of hours this facility is operating, the ovens are in use approximately 3634 hours during a heating season. Therefore, in a heating season, this system will recover approximately 1692 MMBtu of energy.

A similar case study was performed by another researcher. At this facility, two ovens were used in a paper drying process. It was suggested to facility personnel that by installing plate type air-to-air heat exchangers in the oven stacks they could save money. Each of the ovens used 14 MMBtu/hr of natural gas. It was estimated that it would be possible to reclaim 9.3 MMBtu/hr from each oven, 66% of the input energy. These estimates were provided to the researcher by a heat exchanger manufacturer, and were not measured (Abou-Siedo, 1992). Because the estimated amount of heat recovery was not measured, this prediction is suspect.

Although this system will save energy, proper design and maintenance would save more energy. This case study shows that design and maintenance have a large effect on the energy savings achieved in heat recovery projects. The next section evaluates a cooling load reduction case study. It will be shown that proper design is also important for these types of projects.

Case Study: Reducing Cooling Loads by Removing Energy from the Space

This case study involves a system that was designed to try to reduce the cooling loads at a hosiery manufacturing facility. It will be shown that improper design made this system inefficient.

At the hosiery manufacturer, autoboards are used to form the shape and size of a sock using steam or electric heating. When a new sock is made, it is tubular in shape. It is then placed over a sock form on the autoboard, and heated. The heat causes the sock to take on the desired shape of the autoboard form. The temperature is controlled by a thermostat, which is set to approximately 705 °R. Two of the autoboards at this facility are electric and six use steam to heat the socks. The electric autoboards use approximately 44 amps and 208 volts. The power factor was estimated by facility personnel to be .9. The steam autoboards are fed by a boiler which generates saturated steam at 118 psig. The steam heats the socks and then is discharged into the room. A 1 1/4 inch steam line is reduced to 3/4 inches at the machines. The main steam velocity could not be measured but is estimated to be 50 feet/second. This should give a conservative estimate of the steam flow. The temperature of the water in the condensate tank was approximately 580 °R.

To determine the energy used by the steam coil autoboards, an energy balance was performed. Because steam is discharged to the surroundings, the energy used by the autoboard is the difference between the energy content of the boiler feedwater and energy

content of saturated steam at 118 psig. This assumes that there are no losses between the boiler and the autoboard. The energy balance reduces to

$$EU = \frac{\rho AV(h_2 - h_1)}{\eta} \tag{7-5}$$

where ρ is the density of saturated steam at 118 psig, .295 lb_m/ft^3, V is the velocity of the steam, A is the area of the 1 1/4 inch diameter pipe, η is the efficiency, which is assumed to be .8, h_1 is the enthalpy of the feedwater, and h_2 is the enthalpy of saturated steam at 118 psig.

Due to measurement uncertainties, the exact amount of energy used by the steam coil autoboards is not known. In order to determine the range within which the actual energy use will be found, the following equation was used

$$\Delta EU = \left\{ \begin{array}{l} \left(\frac{\rho V(h_2 - h_1)}{\eta}\right)^2 (\Delta A)^2 + \left(\frac{\rho A(h_2 - h_1)}{\eta}\right)^2 (\Delta V)^2 + \left(\frac{AV(h_2 - h_1)}{\eta}\right)^2 (\Delta \rho)^2 + \\ \left(\frac{\rho VA(h_2 - h_1)}{\eta^2}\right)^2 (\Delta \eta)^2 + \left(\frac{\rho VA}{\eta}\right)^2 (\Delta h_2^2 + \Delta h_1^2)^2 \end{array} \right\}^{1/2} \tag{7-6}$$

It is estimated that P_2 is known to ± 5psi. This leads to a $\Delta\rho$ of .004 lb_m/ft^3 and a Δh_2 of .75 Btu/lb_m. It is estimated that T_1 is known to ± 5°R. This leads to a Δh_1 of 5 Btu/lb_m. It is estimated that the pipe diameter is known to ±.1 inches. This leads to a ΔA of .00005 ft^2. It is estimated that the velocity is measured to within 10%, and the efficiency is known to ± .1%.

The enthalpy of the steam at 118 psig is 1193 Btu/lb_m, and the enthalpy of saturated liquid water at 580 °R is 88.0 Btu/lb_m. Using Equations 7-5 and 7-6, the steam coil autoboards add a total of 625 ± 28 MBtu/hr to the space cooling load.

The following equation is used to determine the energy used by each electric autoboard

$$EU = \sqrt{3}(V_o)(I)(PF)(C4) \tag{7-7}$$

where V_o is the voltage, I is the current, PF is the power factor, and C4 is a conversion factor equal to 3.413 Btu/hr/W.

Due to measurement uncertainties, the exact amount of energy used by the electric autoboards is not known. In order to determine the range within which the actual energy use will be found, the following equation was used

$$\Delta EU = \sqrt{\left(\sqrt{3}I(PF)\right)^2(\Delta V_o)^2 + \left(\sqrt{3}V_o(PF)\right)^2(\Delta I)^2 + \left(\sqrt{3}IV_o\right)^2(\Delta PF)^2} \tag{7-8}$$

where it estimated that ΔV_o is five volts, ΔI is two amps, and ΔPF is .1.

Using Equations 7-7 and 7-8, each electric autoboard consumes approximately 48.7 ± .4 MBtu/hr. Therefore, the two electric autoboards add a total of 97.3 MBtu/hr to the cooling load.

Because this equipment adds more than 720 MBtu/hr to the heating load, it was decided that a room should be built around the autoboards to try to isolate this load. As shown in Figure 7-4, autoboards were arranged in such a way that the rear portions of the machines are enclosed in a room. Conditioned factory air is circulated through the room and the air temperature is increased. A damper is installed in the duct so the warm air can be directed outside to decrease the summer cooling load. The air enters the room at 532 °R and 90 feet/minute through a four inch by eight inch duct. The air exits at 560 °R and 500 feet/minute through a 24 by 8 inch duct. There is some additional air leakage into this room.

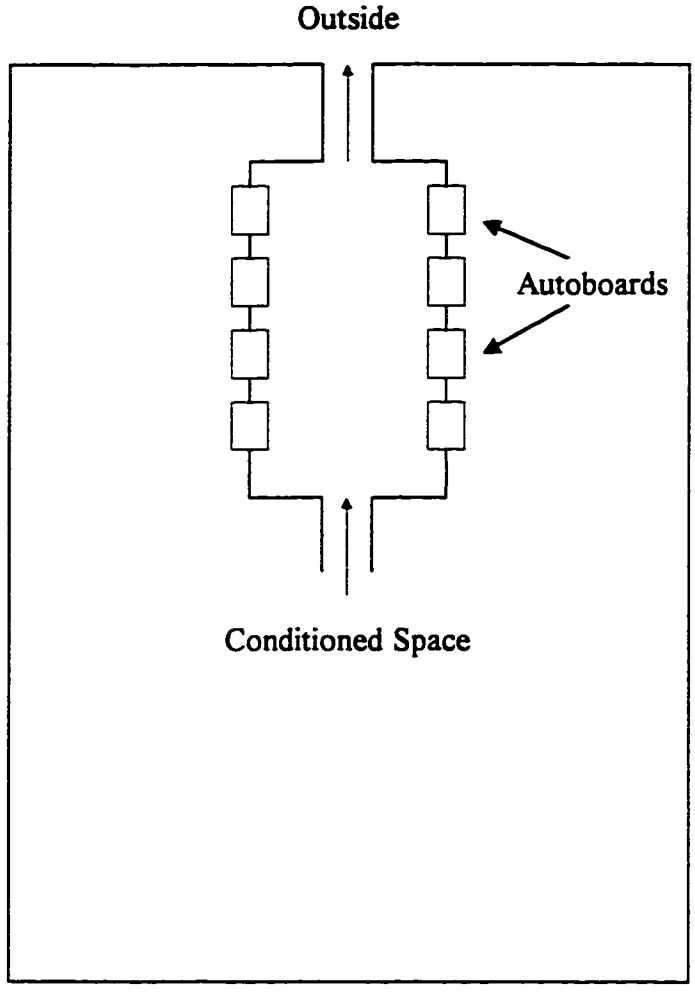

Figure 7-4. Schematic of System to Reduce Cooling Loads

The actual energy that is removed by this system can be calculated using an energy balance on the room where the back of the autoboards are located. This energy balance assumes a control volume approach, and results in Equation 7-9, which has a similar derivation to Equation 7-3

$$q = \frac{p_e A_e}{T_e \frac{R_u}{M}} C_p (T_e - T_i) V_e \tag{7-9}$$

where q is the energy transferred to the air, p_e is the absolute pressure in the duct exiting the room, A_e is the area of the duct leaving the room, T_e is the absolute temperature of the air in the duct exiting the room, R_u is the universal gas constant, M is the molecular weight of air, C_p is the specific heat of air, T_i is the absolute temperature of the air in the duct entering the room, and V_e is the velocity of the air in the duct leaving the room.

The uncertainty on the calculated heat transfer rate can be found from

$$\Delta q = \left\{ \begin{array}{l} \left(\frac{p_e C_p V_e}{\frac{R_u}{M}} \left(1 - \frac{T_i}{T_e} \right) \right)^2 (\Delta A_e)^2 + \left(\frac{p_e C_p A_e}{\frac{R_u}{M}} \left(1 - \frac{T_i}{T_e} \right) \right)^2 (\Delta V_e)^2 + \\ \left(\frac{p_e A_e C_p V_e}{\frac{R_u T_e}{M}} \right)^2 (\Delta T_i)^2 + \left(\frac{p_e A_e C_p V_e T_i}{\frac{R_u T_e^2}{M}} \right)^2 (\Delta T_e)^2 + \\ \left(\frac{V_e C_p A_e}{\frac{R_u}{M}} \left(1 - \frac{T_i}{T_e} \right) \right)^2 (\Delta p_e)^2 \end{array} \right\}^{1/2} \tag{7-10}$$

It was estimated that each linear dimension was known to ± .1 inches. This translated into a ΔA of .00007 ft^2. It is estimated that ΔV is 600 ft/hr. It was also estimated that each temperature was known to ± 5°R, and the duct pressure was measured to ±5%..

Table 7-3 shows the values used to estimate the amount of recovered energy. Note that the values for C_p, R_u, and M again come from standard tables (Moran, 1996). Using Equations 7-9 and 7-10, and the values from Table 7-3, the energy that is removed from this facility is 19 ± 5 MBtu/hr.

Table 7-3. Values Used to Estimate the Energy Removed from this Facility

Equation Variable	Value (Units)
P	2117 ($lb_f/feet^2$)
A	1.33 ($feet^2$)
V	500 (feet/minute)
C_p	.24 (Btu/lb_m-°R)
M	28.97 (lb_m/lb_{mol})
R_u	1545 (ft-lb_f/lb_{mol}-°R)
T_e	560 (°R)
T_i	532 (°R)

If it is assumed that the difference between the inlet and outlet duct temperatures are constant, the value obtained on this one day can be multiplied by the number of hours during the cooling season to determine the total energy removed by this system in a cooling season. In order to estimate the energy removed in a cooling season by this system, it is necessary to know how many hours the autoboards are in operation during the cooling season. This facility produces socks 24 hours a day, five days a week. In Iowa, it is assumed that the cooling season is from May through September. The total hours in these months are 3672. This means that the facility produces socks 2623 hours during a cooling season. Therefore, in a cooling season, this system will remove approximately 50 MMBtu of energy.

Because factory air is used as the inlet air for this system, this air will be replaced by infiltration into the factory. This replacement air will have to be conditioned. Therefore, 19 MBtu/hr will not be removed from the load. In reality, not only will the cooling load be increased by the amount of energy added by the autoboards, but an additional load will be added during the cooling season because of the need to condition the make-up air. Therefore, this system does not save as much energy as it could.

If this system were redesigned, it should be possible to remove the entire load added by the autoboards from the cooling load. This redesign would require the system to be isolated from the factory. Instead of using factory air for the inlet air to the autoboard room, outside air should be used. A damper should be installed in the duct leading out of the factory so that the warm air can be introduced into the factory in the winter. The autoboard room must also be insulated.

Conclusions

Other studies relating to reducing heating loads tend to estimate the heat recovery potential based on "rules of thumb" and information provided by manufacturers (Abou-Siedo, 1992). This study was important because it provided real data, not someone else's estimates.

It was determined that for the heat exchangers installed on the oven stacks approximately 5.5% of the energy used by the ovens was recovered. This is a very small percentage of the energy used by the ovens. A different system design would have recovered more energy. Also, proper maintenance of the heat exchanger surfaces would have increased energy savings.

Reducing heating and cooling loads can represent a significant cost savings. But, these systems must be properly designed. The system studied that was supposed to reduce the cooling load was not properly designed. In reality, this system created a larger cooling load than if the system were not in place.

When designing systems to reduce heating and cooling loads, it is important to understand what the purpose of the system is, as well as all interactions between the system and its surroundings. If this is not done, the system may not operate as expected. Facility personnel that do not fully understand the system and the interactions may purchase systems that are not only inappropriate, but may actually increase the energy costs at the facility.

The information obtained in this report is important because it provides some actual examples of systems used to reduce heating and cooling loads, actual estimates of the percentage of energy input that can be recovered from a specific heat recovery system, and

warnings that an additional load can be added to the cooling load if a system to reduce the cooling load is improperly designed.

There were three main problems associated with this part of the project. The first was even finding a system that reduces heating or cooling loads in a facility. The second problem was that information on the system to reduce the heating or cooling load and on the production equipment was lacking. The third problem was that much of the equipment from which energy could be recovered is industry specific. If a future study of projects that reduce heating or cooling loads is undertaken, it should find projects that have not been installed and follow them to completion. This would at least eliminate the lack of information on the equipment used to transfer the energy.

The following chapter contains the conclusions for this project. These conclusions include those relating to boilers and compressors, as well as reducing heating and cooling loads.

CHAPTER 8. CONCLUSIONS

This project evaluated the potential for saving energy in Iowa manufacturing facilities, focusing on compressors, boilers, and reducing heating and cooling loads. This project evaluated the theories and models that are the basis for analyzing energy conservation opportunities relating to boilers, compressors, and reducing heating and cooling loads, by collecting data at six industrial facilities and on-campus locations.

The Effect of Compressor Exit Pressure

- As predicted by theory, lowering the exit pressure from the air compressor resulted in lower power consumption. It was determined that two commonly used methods provide a good approximation of the power reduction for the studied screw compressor. The same two commonly used methods overestimated the savings for the reciprocating compressor that was studied.
- If one of the methods used to approximate the energy savings due to a decreased exit pressure was modified to account for the clearance fraction, a conservative estimate of the energy savings for the reciprocating compressor was obtained.

The Effect of Compressor Inlet Air Temperature

- It is a commonly held belief that lowering the inlet air temperature to the compressor will decrease the power consumption. Data collected for this project show that power consumption is not systematically decreased by lowering the inlet air temperature.
- It was determined that the uncertainties on the predicted power reduction are larger than the predicted power reduction.
- A study of the theory behind positive displacement compressors determined that, contrary to published information, there is no reason to expect compressor power to vary with changing compressor inlet air temperatures.
- Although not seen in previously published information, there is a theoretical reason for decreasing compressor run time with decreasing inlet air temperature. Data collected for this project show that the run time will decrease with decreasing inlet air temperatures. This will result in an energy savings.
- If the compressor is constantly operating, lowering the temperature of the intake air will result in a mass increase, not an energy savings.
- For a cycling air compressor, the same equation that is used to estimate the power savings due to decreased compressor intake temperatures can be used to conservatively predict the run time savings.

Boilers

- Published information predicts that as the combustion efficiency increases, the fuel usage will decrease. An equation that predicts the energy savings based on the current combustion efficiency and energy usage and the proposed combustion efficiency was evaluated. This was compared to the difference between the fuel usage at proposed efficiency and the fuel usage at the current efficiency. The results did not appear to compare favorably.
- This project determined that boiler fuel usage and combustion efficiency cannot be obtained within the accuracy needed. Because of measurement uncertainty, the calculated energy savings can be exceeded by the uncertainty on the energy savings.
- This project determined that in general, it is inaccurate to use combustion efficiency to approximate boiler efficiency, because boiler efficiency varies more than combustion efficiency.
- For the two watertube boilers, at a fixed steam generation rate, as boiler efficiency increased, fuel usage decreased. It is unknown at this time what caused the boiler efficiency to increase.
- Boilers are complicated systems. Because there are so many variables it is difficult to know what modifications will result in an energy savings on a particular boiler, loaded a specific way, in a certain facility.

- The only method currently known that will always result in a decreased fuel usage is to reduce the steam generation rate.

Reducing Heating and Cooling Loads

- The information obtained in this report relating to reducing heating and cooling loads is important because it provides some actual examples of systems used to reduce heating and cooling loads, actual estimates of the percentage of energy input that can be recovered from a specific heat recovery system, and warnings that additional loads can be added to the cooling load if a system to reduce the cooling load is improperly designed.
- When designing systems to reduce heating and cooling loads, it is important to understand what the purpose of the system is, as well as all interactions between the system and its surroundings. If this is not done, the system may not operate as expected.
- Facility personnel that do not fully understand the system and the interactions may purchase systems that are not only inappropriate, but may actually increase the energy costs at the facility.

Suggestions for Future Work

1. A detailed study of a single boiler that can be easily controlled should be undertaken to attempt to verify the relationships between stack temperature, excess oxygen, and combustion efficiency shown in the literature review.
2. A study should be undertaken to determine at what excess air level it becomes cost effective to tune the boiler.
3. Heat recovery strategies that may be transferable to other facilities, such as recovering heat from an oven stack, from an air compressor, or from a boiler room must be studied in more detail.

APPENDIX A. DATA COLLECTED ON 125 HORSEPOWER SCREW COMPRESSOR

Table A-1. Data Collected on 125 Horsepower Screw Compressor

Inlet Air Temperature (°R)	Exit Pressure (psig)	Pressure Ratio	Power (kW)
506	111	8.55	69.8
506	113	8.69	70.1
508	109	8.41	69.5
508	111	8.55	69.8
510	101	7.87	66.4
510	102	7.94	66.6
510	104	8.08	66.5
510	108	8.35	69.1
510	111	8.55	69.7
510	112	8.62	70.5
510	113	8.69	70.5
510	114	8.76	70.6
512	97	7.60	66.2
512	98	7.67	66.8
512	108	8.35	69.0
512	111	8.55	69.6
512	113	8.69	70.9
512	116	8.89	72.5
512	117	8.96	69.7

Table A-1. Continued

Inlet Air Temperature (°R)	Exit Pressure (psig)	Pressure Ratio	Power (kW)
512	118	9.03	72.9
512	120	9.16	73.3
512	121	9.23	74.2
514	122	9.30	73.7
514	123	9.37	74.3
515	104	8.08	66.6
515	105	8.14	67.3
515	106	8.21	68.5
515	109	8.42	68.8
515	110	8.48	70.4
515	112	8.62	70.6
515	113	8.69	70.6
515	114	8.76	70.8
515	116	8.89	71.8
515	119	9.91	73.5
515	121	9.23	73.7
515	122	9.30	73.4
515	123	9.37	74.2
515	124	9.44	74.0

Table A-1. Continued

Inlet Air Temperature (°R)	Exit Pressure (psig)	Pressure Ratio	Power (kW)
516	112	8.62	70.9
516	117	8.96	72.2
516	120	9.16	74.2
516	121	9.23	73.4
518	98	7.67	64.6
518	104	8.08	67.3
518	108	8.35	68.4
518	113	8.69	70.8
518	119	9.10	73.2
520	104	8.08	67.3
520	106	8.21	67.9
520	107	8.28	68.3
520	108	8.35	69.2
520	109	8.42	68.7
520	110	8.48	69.9
520	111	8.55	69.8
520	112	8.62	70.9
520	113	8.69	71.0
520	114	8.76	70.4

Table A-1. Continued

Inlet Air Temperature (°R)	Exit Pressure (psig)	Pressure Ratio	Power (kW)
520	115	8.82	71.2
522	104	8.01	67.7
522	112	8.62	69.3
525	98	7.67	65.6
528	101	7.87	71.2

APPENDIX B. PREDICTED AND EXPERIMENTAL POWERS FOR 125 HORSEPOWER SCREW COMPRESSOR

Table B-1. Predicted and Experimental Powers for 125 hp Screw Compressor

Exit Pressure (psia)	Measured Power (kW)	Isentropic Prediction (kW)	Graphical Prediction (kW)	"Rule of Thumb" Prediction (kW)
138.7	74.0	74.0	74.0	74.0
137.7	74.2	73.7	73.5	73.6
136.7	73.4	73.4	72.9	73.3
135.7	74.2	73.0	72.4	72.9
135.7	73.7	73.0	72.4	72.9
135.7	73.4	73.0	72.4	72.9
134.7	73.3	72.7	71.9	72.5
134.7	74.2	72.7	71.9	72.5
133.7	73.5	72.4	71.3	72.2
133.7	73.2	72.4	71.3	72.2
132.7	72.9	72.0	70.8	71.8
131.7	69.7	71.7	70.3	71.4
131.7	72.2	71.7	70.3	71.4
130.7	72.5	71.4	69.7	71.0
130.7	71.8	71.4	69.7	71.0
129.7	71.2	71.0	69.2	70.7
128.7	70.6	70.7	68.7	70.3
128.7	70.8	70.7	68.7	70.3

Table B-1. Continued

Exit Pressure (psia)	Measured Power (kW)	Isentropic Prediction (kW)	Graphical Prediction (kW)	"Rule of Thumb" Prediction (kW)
128.7	70.4	70.7	68.7	70.3
127.7	70.5	70.4	68.1	69.9
127.7	70.9	70.4	68.1	69.9
127.7	70.6	70.4	68.1	69.9
127.7	70.8	70.4	68.1	69.9
127.7	71.0	70.4	68.1	69.9
126.7	70.5	70.0	67.6	69.6
126.7	70.6	70.0	67.6	69.6
126.7	70.9	70.0	67.6	69.6
126.7	70.9	70.0	67.6	69.6
126.7	69.3	70.0	67.6	69.6
125.7	69.7	69.7	67.1	69.2
125.7	69.6	69.7	67.1	69.2
125.7	69.8	69.7	67.1	69.2
124.7	70.4	69.3	66.5	68.8
124.7	69.9	69.3	66.5	68.8
123.7	68.8	69.0	66.0	68.5
123.7	68.7	69.0	66.0	68.5

Table B-1. Continued

Exit Pressure (psia)	Measured Power (kW)	Isentropic Prediction (kW)	Graphical Prediction (kW)	"Rule of Thumb" Prediction (kW)
122.7	69.1	68.6	65.5	68.1
122.7	69.0	68.6	65.5	68.1
122.7	68.4	68.6	65.5	68.1
122.7	69.2	68.6	65.5	68.1
121.7	68.3	68.3	64.9	67.7
120.7	68.5	67.9	64.4	67.3
120.7	67.9	67.9	64.4	67.3
119.7	67.3	67.6	63.9	67.0
118.7	66.5	67.2	63.3	66.6
118.7	66.6	67.2	63.3	66.6
118.7	67.3	67.2	63.3	66.6
118.7	67.3	67.2	63.3	66.6
117.7	67.7	66.8	62.8	66.2
116.7	66.6	66.5	62.3	65.9
116.7	71.9	66.5	62.3	65.9
115.7	66.4	66.1	61.7	65.5
112.7	66.8	65.0	60.1	64.4
112.7	64.6	65.0	60.1	64.4
111.7	66.2	64.6	59.6	64.0

APPENDIX C. UNCERTAINTIES FOR ISENTROPIC PREDICTION FOR 125 HORSEPOWER SCREW COMPRESSOR

Table C-1. Uncertainties for Isentropic Prediction for 125hp Screw Compressor

Exit Pressure (psia)	Measured Power (kW)	Isentropic Prediction (kW)	- Error Band (kW)	+ Error Band (kW)
138.7	74.0	74.0	73.3	74.7
137.7	74.2	73.7	73.0	74.4
136.7	73.4	73.4	72.7	74.0
135.7	74.2	73.0	72.4	73.7
135.7	73.7	73.0	72.4	73.7
135.7	73.4	73.0	72.4	73.7
134.7	73.3	72.7	72.0	73.4
134.7	74.2	72.7	72.0	73.4
133.7	73.5	72.4	71.7	73.0
133.7	73.2	72.4	71.7	73.0
132.7	72.9	72.0	71.4	72.7
131.7	69.7	71.7	71.0	72.4
131.7	72.2	71.7	71.0	72.4
130.7	72.5	71.4	70.7	72.0
130.7	71.8	71.4	70.7	72.0
129.7	71.2	71.0	70.4	71.7
128.7	70.6	70.7	70.0	71.4
128.7	70.8	70.7	70.0	71.4
128.7	70.4	70.7	70.0	71.4

Table C-1. Continued

Exit Pressure (psia)	Measured Power (kW)	Isentropic Prediction (kW)	- Error Band (kW)	+ Error Band (kW)
127.7	70.5	70.4	69.7	71.0
127.7	70.9	70.4	69.7	71.0
127.7	70.6	70.4	69.7	71.0
127.7	70.8	70.4	69.7	71.0
127.7	71.0	70.4	69.7	71.0
126.7	70.5	70.0	69.4	70.7
126.7	70.6	70.0	69.4	70.7
126.7	70.9	70.0	69.4	70.7
126.7	70.9	70.0	69.4	70.7
126.7	69.3	70.0	69.4	70.7
125.7	69.7	69.7	69.0	70.3
125.7	69.6	69.7	69.0	70.3
125.7	69.8	69.7	69.0	70.3
124.7	70.4	69.3	68.7	70.0
124.7	69.9	69.3	68.7	70.0
123.7	68.8	69.0	68.3	69.6
123.7	68.7	69.0	68.3	69.6
122.7	69.1	68.6	68.0	69.3
122.7	69.0	68.6	68.0	69.3

Table C-1. Continued

Exit Pressure (psia)	Measured Power (kW)	Isentropic Prediction (kW)	- Error Band (kW)	+ Error Band (kW)
122.7	68.4	68.6	68.0	69.3
122.7	69.2	68.6	68.0	69.3
121.7	68.3	68.3	67.6	68.9
120.7	68.5	67.9	67.3	68.6
120.7	67.9	67.9	67.3	68.6
119.7	67.3	67.6	66.9	68.2
118.7	66.5	67.2	66.6	67.9
118.7	66.6	67.2	66.6	67.9
118.7	67.3	67.2	66.6	67.9
118.7	67.3	67.2	66.6	67.9
117.7	67.7	66.8	66.2	67.5
116.7	66.6	66.5	65.8	67.1
116.7	71.9	66.5	65.8	67.1
115.7	66.4	66.1	65.5	66.8
112.7	66.8	65.0	64.4	65.6
112.7	64.6	65.0	64.4	65.6
111.7	66.2	64.6	64.0	65.3

APPENDIX D. EQUATIONS TO CALCULATE THE PROPAGATION OF ERROR FOR EQUATIONS 4-7 AND 4-8

For Equation 4-7 the uncertainty is found from

$$\frac{\partial WR}{\partial T_o} = \left(\frac{\left(\frac{P_{exit}}{P_{inlet}}\right)^{\frac{k-1}{nk}}_{new} - 1}{\left(\frac{P_{exit}}{P_{inlet}}\right)^{\frac{k-1}{nk}}_{old} - 1} \right) \left(\frac{1}{T_I} \right)$$

$$\frac{\partial WR}{\partial T_I} = \left(\frac{\left(\frac{P_{exit}}{P_{inlet}}\right)^{\frac{k-1}{nk}}_{new} - 1}{\left(\frac{P_{exit}}{P_{inlet}}\right)^{\frac{k-1}{nk}}_{old} - 1} \right) \left[\frac{1}{T_I} - \frac{T_I - T_o}{(T_I)^2} \right]$$

$$\frac{\partial WR}{\partial P_{exit_{New}}} = \frac{(wr)\frac{k-1}{nk}\left(\frac{P_{exit}}{P_{inlet}}\right)^{\frac{k-1-nk}{nk}}_{new}}{\left[\left(\frac{P_{exit}}{P_{inlet}}\right)^{\frac{k-1}{nk}} - 1\right]_{old}}$$

$$\frac{\partial WR}{\partial P_{exit_{old}}} = \frac{(wr) * \left(\frac{\left(\frac{P_{exit}}{P_{inlet}}\right)^{\frac{k-1}{nk}}_{new} - 1}{\left(\frac{P_{exit}}{P_{inlet}}\right)^{\frac{k-1}{nk}}_{old} - 1} \right) * \left[\frac{k-1}{nk}\right]\left[\left(\frac{P_{exit}}{P_{inlet}}\right)^{\frac{k-1-nk}{nk}}\right]_{old}}{\left[\left(\frac{P_{exit}}{P_{inlet}}\right)^{\frac{k-1}{nk}} - 1\right]^2_{old}}$$

$$\frac{\partial WR}{\partial P_{in}} = \frac{(wr)\left[P_{exit_{new}}\right]^{\frac{k-1}{nk}}\left[\frac{1-k}{nk}\right]\left[P_{inlet}\right]^{\frac{1-k-nk}{nk}}}{\left[\left(\frac{P_{exit}}{P_{inlet}}\right)^{\frac{k-1}{nk}}-1\right]_{old}} + \frac{(wr)\left[\left(\frac{P_{exit}}{P_{inlet}}\right)^{\frac{k-1}{nk}}-1\right]_{new}\left(P_{exit_{old}}\right)^{\frac{k-1}{nk}}\left(P_{inlet}\right)^{\frac{1-k-nk}{nk}}}{\left[\left(\frac{P_{exit}}{P_{inlet}}\right)^{\frac{k-1}{nk}}-1\right]^2_{old}}$$

Then, the calculated value is accurate to within

$$\Delta ES_{4-7} = \left\{\begin{array}{l}\left(\frac{\partial ES}{\partial T_o}\right)^2(\Delta T_o)^2 + \left(\frac{\partial ES}{\partial T_i}\right)^2(\Delta T_i)^2 + \left(\frac{\partial ES}{\partial P_{exit_{old}}}\right)^2\left(\Delta P_{exit_{old}}\right)^2 + \\ \left(\frac{\partial ES}{\partial P_{exit_{new}}}\right)^2\left(\Delta P_{exit_{new}}\right)^2 + \left(\frac{\partial ES}{\partial P_{in}}\right)^2(\Delta P_{in})^2\end{array}\right\}^2$$

where the Δ terms under the square root represent the values being measured to $\pm\Delta$.

For Equation 4-8, the calculated value is accurate to within

$$\Delta ES_{4-8} = \sqrt{\left(\frac{1}{Power_{high}}\right)^2(\Delta Power_{low})^2 + \left(\frac{Power_{low}}{Power_{high}^2}\right)^2\left(\Delta Power_{high}\right)^2}$$

APPENDIX E. DATA COLLECTED ON THREE HORSEPOWER RECIPROCATING COMPRESSOR

Table E-1. Data Collected on Three Horsepower Reciprocating Compressor

Air Temperature (°R)	Tank Temperature (°R)	Final Tank Pressure (psig)	Time (s)	Barometric Pressure (in Hg)
558	587.3	67	168	28.94
5577	587.4	67	167	28.94
556	587.2	67	165	28.94
554	586.4	67	167	28.94
553	586.8	67	165	28.94
553	585.8	67	166	28.94
552	584.9	67	164	28.94
551	585.4	67	165	28.94
551	584.4	67	164	28.94
551	585.8	67	165	28.94
551	584.9	67	164	28.94
549	582.3	67	165	28.94
548	583.6	67	165	28.94
547	579.6	67	167	28.94
547	577.6	66	163	28.94
546	578.9	66	163	28.94
544	578.6	65	163	28.94
543	578.0	65	164	28.94

Table E-1. Continued

Air Temperature (°R)	Tank Temperature (°R)	Final Tank Pressure (psig)	Time (s)	Barometric Pressure (in Hg)
536	568.0	65	166	28.88
535	567.3	64	162	28.88
535	569.1	65	165	28.88
534	567.5	64	164	28.88
534	567.4	64	163	28.88
534	568.1	65	165	28.88
533	567.3	64	164	28.88
533	567.6	64	164	28.88
533	568.0	64	164	28.88
532	568.5	65	164	28.88
532	567.9	65	165	28.88
532	566.2	64	164	28.88
532	567.8	64	164	28.88
527	558.4	63	158	28.80
526	557.6	63	158	28.80
526	559.3	63	159	28.80
526	559.6	63	161	28.80
526	559.3	63	160	28.80

Table E-1. Continued

Air Temperature (°R)	Tank Temperature (°R)	Final Tank Pressure (psig)	Time (s)	Barometric Pressure (in Hg)
526	559.3	63	160	28.80
525	558.0	63	160	28.80
525	558.9	63	160	28.80
525	559.2	63	160	28.80
525	559.0	63	160	28.80
525	558.7	63	161	28.80
525	558.7	63	159	28.80
525	558.9	63	161	28.80
525	558.9	63	161	28.80
525	558.6	63	158	28.80
524	558.0	63	159	28.80
524	558.7	63	159	28.80
524	558.2	63	157	28.80
524	558.5	63	159	28.80
524	558.2	63	158	28.80
524	557.8	63	158	28.80
524	558.3	63	158	28.80
524	559.4	63	161	28.80

Table E-1. Continued

Air Temperature (°R)	Tank Temperature (°R)	Final Tank Pressure (psig)	Time (s)	Barometric Pressure (in Hg)
524	557.8	63	158	28.80
524	557.8	63	158	28.80
524	558.0	63	159	28.80
524	558.2	63	161	28.80
524	558.0	63	161	28.80
524	557.9	63	160	28.80

APPENDIX F. DATA COLLECTED ON 400 PSI SUPERHEATED WATERTUBE BOILER

Table F-1. Data Collected on 400 PSI Superheated Watertube Boiler

Inlet Air Temp (°R)	Stack Temp (°R)	Steam Temp (°R)	Steam Pressure (psig)	Water Flow Rate (klb/day)	Water Temp (°R)	Stack O_2 (%)	Natural Gas (MSCF/day)
836	1036	1010	375	926	696	2.83	1364
835	1033	1009	375	901	696	2.99	1335
836	1036	1008	375	923	695	2.74	1394
836	1043	1008	375	951	695	2.89	1425
837	1047	1007	375	988	696	2.59	1512
837	1040	1006	375	946	696	2.68	1457
810	1100	1005	375	986	696	2.62	1480
808	1098	1004	375	979	695	2.64	1456
816	1093	1004	375	969	695	2.65	1452
809	1081	1003	375	930	696	2.78	1369
800	1046	1002	375	780	696	3.20	1155
804	1056	1002	375	822	696	3.07	1207
808	1055	1003	375	851	697	3.12	1188
804	1049	1001	375	820	697	3.37	1145
803	1057	1000	375	865	696	3.04	1215
837	1062	1002	375	874	697	3.17	1259

Table F-1. Continued

Inlet Air Temp (°R)	Stack Temp (°R)	Steam Temp (°R)	Steam Pressure (psig)	Water Flow Rate (klb/day)	Water Temp (°R)	Stack O_2 (%)	Natural Gas (MSCF/day)
789	1040	977	321	832	696	3.76	1140
794	1043	975	300	879	696	3.11	1209
794	1058	959	316	937	696	2.90	1304
795	1048	970	320	893	697	2.99	1243
794	1033	978	320	802	696	3.28	1134
798	1042	989	370	776	696	3.44	1123
795	1060	987	346	886	696	2.92	1287

APPENDIX G. INTERACTIVE THERMODYNAMICS ROUTINE

/*boiler analysis problem-Calculating the Air-Fuel Ratio and Combustion Efficiency, etc

****

Assumptions:

1. Natural Gas is Methane-CH4
2. Assume Complete combustion
3. Assume Fuel enters at 70 F
4. Assume no auxiliary power required (no pumps, blowers, etc on boiler)

Analysis:
For combustion of Natural Gas with air

CH4 + (ath+2) * (O2 + 3.76 N2) ===> CO2 + 2 H2O +(ath+2) * 3.76 * N2+ath*O2

O2 Balance: */
// measured stack % O2 ->2.76
stop=LOOKUP(boilave,n,1)
ath = (stop*10.52)/(1-.0276*4.76)

/*
The energy balance is used to find Qdotc- heat transfer released from combustion of gasses in Btu/day */

0=Qdotc + ndotf * (hfuel + (2+ ath) * (hO2in + 3.76 * hN2in) - hCO2 - 2* hH2O - ath * hO2out - (ath+2) * 3.76 * hN2out)

//A second energy balance can be performed on the water-steam side to find Qdotws is in Btu/day

0=-Qdotws+ndotw*(hsteamout-hwaterin)

// Known and assumed quantities
Tf = 70 //F
n=1 // for first iteration

//mscf is amount of natural gas used in day, while ndot is lb_{mol}/day
mscf=LOOKUP(boilave,n,2)
ndotf = 2.79301745636*mscf

```
//feedf is feedwater flow rate in klb/day while ndotw is in lb_mol/day
feedf=LOOKUP(boilave,n,8)
ndotw=feedf*55.4938956715

// Measured Air Temperature Ta
Ta = LOOKUP(boilave,n,3)  // F

// Measured Stack Temperature Tp
Tp=LOOKUP(boilave,n,4)  // F
HHV=383030 // Btu/lb_mol (Moran, 1996)

//Tw Feedwater Temperature F
Tw=LOOKUP(boilave,n,5)

//Ts is Steam Temperature in F
Ts=LOOKUP(boilave,n,6)

//Ps is Steam Pressure
Ps=LOOKUP(boilave,n,7)
//  Obtain other data
hfuel = -32210  // Btu/lb_mol
hO2in = h_T("O2",Ta)
hN2in = h_T("N2",Ta)
hCO2 = h_T("CO2",Tp)
hH2O = h_T("H2O",Tp)
hO2out = h_T("O2",Tp)
hN2out = h_T("N2",Tp)
p = Psat_T("Water/Steam", Tw)
hwaterin=hsat_Px("Water/Steam", p, 0)
hsteamout=h_PT("Water/Steam",Ps,Ts)

// Calculate the Combustion Efficiency

ceff=100*abs(hfuel+(ath+2)*hO2in+(ath+2)*3.76*hN2in-hCO2-2*hH2O-
(ath+2)*3.76*hN2out-ath*hO2out)/HHV

// Calculate the Boiler Efficiency
beff=100*(ndotw*(hsteamout-hwaterin))/(ndotf*HHV)

// Calculate the Air Fuel Ratio

AF=(ath+2)+3.76*(ath+2)
```

APPENDIX H. ENERGY SAVINGS AND UNCERTAINTIES FOR INCREASED COMBUSTION EFFICIENCY

Table H-1 Energy Savings and Uncertainties for Increased Combustion Efficiency

$ES_{predicted}$ (cf/s)	$\Delta ES_{predicted}$ (cf/s)	$ES_{measured}$ (cf/s)	$\Delta ES_{measured}$ (cf/s)
.117	.051	.450	.183
.111	.056	.967	.183
.086	.047	-.150	.183
.037	.052	.533	.183
.014	.049	.083	.183
.062	.063	.533	.183
.043	.061	.333	.183
.046	.065	.850	.183
.036	.064	.717	.183
.185	.076	.333	.183
.126	.068	-.700	.183
.087	.068	-.717	.183
.084	.074	-.033	.183
.072	.072	-.200	.183
.384	.081	.017	.183
.301	.080	-.050	.183
.201	.082	.033	.183
.213	.083	.183	.183
.161	.081	-.100	.183

Table H-1. Continued

$ES_{predicted}$ (cf/s)	$\Delta ES_{predicted}$ (cf/s)	$ES_{measured}$ (cf/s)	$\Delta ES_{measured}$ (cf/s)
.084	.019	.404	.408
.027	.016	.105	.408
.017	.014	-.205	.408
.010	.018	.356	.408
.002	.015	-.064	.408

APPENDIX I. EQUATIONS AND COEFFICIENTS OF DETERMINATION FOR FIGURE 6-7

For a nominal flow rate of 8.25×10^5 lb/day

$$\eta_{boiler} = -.0447(NG) + 122.16$$

where η_{boiler} is in percent, NG is the natural gas usage in 10^3 ft^3/day, and the index of determination is .6763.

For a nominal flow rate of 8.75×10^5 lb/day

$$\eta_{boiler} = -.0359(NG) + 114.74$$

The index of determination for the curve fit to these data is .8616.

For a nominal flow rate of 9.25×10^5 lb/day

$$\eta_{boiler} = -.0326(NG) + 112.23$$

The index of determination for the curve fit to these data is .8816.

For a nominal flow rate of 9.75×10^5 lb/day

$$\eta_{boiler} = -.0176(NG) + 92.47$$

The index of determination for the curve fit to these data is .6838.

WORKS CITED

Abou-Siedo, Ehab I. *Energy Conservation and Heat Recovery Strategies in Iowa Industry*. M. S. Thesis, Iowa State University, 1992

Anderson, David Robert. *Improvement of Method to Calculate the Savings Associated with the Use of High Efficiency Electric Motors in Manufacturing Facilities*. M. S. Thesis, Iowa State University, 1995

Bloch, Heinz P. *A Practical Guide to Compressor Technology*. McGraw-Hill, New York: 1996.

Coerper, Phil. "Evaluating Boiler Efficiency." *Plant Engineering*. July 9, 1995, 66-68.

Dukelow, Sam G. *The Control of Boilers*. Instrument Society of America, North Carolina: 1991.

Dyer, David and Glennon Maples. *Boiler Efficiency Improvement Fourth Edition*. Boiler Efficiency Institute, Alabama: 1988.

Energy Information Administration. *Manufacturing Energy Consumption Survey Consumption of 1991*. U. S. G. P. O., Washington, D. C.: 1991.

Garcia-Borras, Thomas. *Manual for Improving Boiler and Furnace Performance*. Gulf Publishing Company, Houston: 1983.

Gibbs, Charles W. ed. *Compressed Air and Gas Data*. Ingersoll-Rand, Woodcliff Lake, NJ: 1971.

Goldstick, Robert and Albert Thumann. *Principles of Waste Heat Recovery*. The Fairmont Press, Inc., Atlanta, GA: 1986.

Iowa State University Energy Analysis and Diagnostic Center. Unpublished Data from Energy Audits between 1991-1994.

Iowa State University Energy Analysis and Diagnostic Center. Unpublished Energy Conservation Opportunity Calculation Procedures. 1994.

Kiang, Yen-Hsiung. *Waste Energy Utilization Technology*. Marcel Dekker, Inc., New York: 1981.

Kirsch, F. William, et al. *Energy Analysis And Diagnostic Centers: Five Years of Assisting Small and Medium-Size Manufacturers to Conserve Energy and Reduce Costs 1987-1992.* Philadelphia, PA: University Science Center, December 1993.

KVB, Inc. *Assessment of the Potential for Energy Conservation Through Improved Industrial Boiler Efficiency. Volume I.* Report Number PB-262 576. Washington, D.C: U. S. Department of Commerce, National Technical Information Service, January, 1977.

Landry, Russell W. et al. "Measuring Seasonal Efficiency of Space Heating Boilers." *ASHRAE Journal.* September 1993, 38+.

Landry, R. W. et al. "Field Validation of Diagnostic Techniques for Estimating Boiler Part-Load Efficiency." *ASHRAE Transactions.* 1994, 859-875.

Lipták, Béla G. *Optimization of Unit Operations: Boilers, Chemical Reactors, Chillers, Clean Rooms, Compressors, Condensers, Cooling Towers, fans, Fired Heaters, Heat Exchangers, HVAC Systems, Pumping Stations, Reboilers, Vaporizers.* Chilton Book Company, Radnor, PA: 1987.

Modera, Mark. "Jacket and Stack Losses from Multifamily Boilers." *Proceedings of the 1988 ACEEE Summer Study on Energy Efficiency in Buildings.* 1988, 2.148-2.154.

Moran, Michael J. and Howard N. Shapiro. *Fundamentals of Engineering Thermodynamics.* Third Edition. John Wiley & Sons, New York: 1996.

North American Combustion Handbook. The North American Manufacturing Co. Cleveland, Ohio: 1952.

Ottaviano, Victor B. *Energy Management.* The Fairmont Press, Incorporated, Atlanta, Georgia: July 1985.

Oviatt, Mark D. and Richard K. Miller. *Industrial and Pneumatic Systems: Noise Control and Energy Conservation.* The Fairmont Press, Inc., Atlanta: 1981.

Pichot, Pierre. *Compressor Application Engineering Volume 1: Compression Equipment.* Gulf Publishing Company, Houston: 1986.

Price, Brian C. "Know the range and Limitations of Screw Compressors." *Chemical Engineering Progress.* February 1991, 50-56.

Reiter, Sydney. *Industrial and Commercial Heat Recovery Systems.* Van Nostrand Reinhold Company, New York: 1983.

Rollins, John P. ed. *Compressed Air and Gas Handbook.* 4th ed. New York: Compressed Air and Gas Institute, 1973.

Sengupta, Subrata and Samual S. Lee. *Waste Heat Utilization and Management.* Hemisphere Publishing Corporation, Washington: 1983.

Site Energy Handbook: Volume 1: Methodology for Energy Survey and Appraisal. National Technical Information Service, October 1976.

Talbott, Edwin M. *Compressed Air Systems: A Guidebook on Energy and Cost Savings.* 2nd ed. The Fairmont Press, Linburn, GA: 1993.

Tierney, T. M. and C. J. Fishman. "Field Study of 'Real World' Gas Steam Boiler Seasonal Efficiency." *ASHRAE Transactions.* 1994, 892-896.

Utracki, Christopher. "Use Consistent Methods When Comparing Boiler Efficiencies." *Power.* December 1986, 74-74.

Woollatt, D. "Factors Affecting Reciprocating Compressor Performance." *Hydrocarbon Processing.* June 1993, 57+.

Yaverbaum, L. H. ed. Energy Savings by Increasing Boiler Efficiency. Noyes Data Corporation, Park Ridge, NJ: 1979.